UNIVERSITY OF LIVERPOOL

An efficient stochastic dynamics framework for response determination, reliability assessment, and performance based design of nonlinear structural systems

Thesis submitted in accordance
with the requirements of the University of Liverpool
for the degree of Doctor in Philosophy

by

Ioannis P. Mitseas

April, 2015

Abstract

An efficient stochastic dynamics framework for response determination, reliability assessment, and performance based design of nonlinear structural systems

by

Ioannis P. Mitseas

An approximate analytical technique for determining the survival probability and first-passage probability density function (PDF) of nonlinear multi-degree-of-freedom (MDOF) structural systems subject to an evolutionary stochastic excitation vector is developed. The proposed technique can be construed as a two-stage approach. First, relying on statistical linearization and utilizing a dimension reduction approach the nonlinear n-degree-of-freedom system is decoupled and cast into (n) effective single-degree-of-freedom (SDOF) linear time-varying (LTV) oscillators corresponding to each and every DOF of the original MDOF system. Second, utilizing the effective SDOF LTV oscillator time-varying stiffness and damping elements in conjunction with a stochastic averaging treatment of the problem, the MDOF system survival probability and first-passage PDF are efficiently determined. Applications regarding MDOF structural systems exhibiting highly nonlinear behavior subject to stochastic excitations possessing separable as well as non-separable evolutionary power spectra (EPS) are included.

Furthermore, a computationally efficient methodology for conducting fragility analysis of nonlinear/hysteretic MDOF structural systems is developed. Specifically,

fragility surfaces are estimated for nonlinear/hysteretic MDOF structural systems subject to evolutionary stochastic earthquake excitations. An approximate nonlinear stochastic dynamics formulation which consist the core of the developed methodology, allows for the efficient computation of structural system fragilities in a straightforward manner while it keeps the computational cost for the corresponding analyses at a minimum level. Nonlinear MDOF structural systems exhibiting a hysteretic restoring force-displacement Bouc-Wen feature, serve as numerical examples for demonstrating the efficiency of the proposed methodology. Comparisons with pertinent Monte Carlo simulations are included as well demonstrating the satisfactory level of the exhibited accuracy.

Appended to the above, a novel integrated approach for structural system optimal design considering life cycle cost (LCC) is developed. Specifically, a performance-based multi-objective design optimization framework for nonlinear/hysteretic MDOF structural systems subject to non-stationary stochastic excitations is formulated. The developed approach encompasses an efficient analytical nonlinear stochastic dynamics approach for the determination of the response EPS as well as the non-stationary inter-story drift ratio (IDR) amplitude PDFs, circumventing computationally intensive numerical integrations of the nonlinear equations of motion. It is notable that the proposed framework complies with the most contemporary performance-based earthquake engineering (PBEE) provisions proposed by the Pacific Earthquake Engineering Research (PEER) center. Although the herein developed framework is tailored specifically for earthquake engineering related applications, it can be readily modified to account for other hazard kinds as well. Nonlinear building structures comprising the versatile Bouc-Wen (hysteretic) model serve as numerical applications for demonstrating the efficiency of the developed methodology.

Acknowledgements

I wish to express my sincere appreciation and gratitude to my research advisors Professor *Michael Beer* and Assistant Professor *Ioannis Kougioumtzoglou*. Their wise mentorship and valuable suggestions during my studies at University of Liverpool are highly appreciated. I am especially grateful to *Ioannis Kougioumtzoglou* for his substantial supervision, friendly encouragement, and invaluable guidance. Further, the assistance of Lecturer *Edoardo Patelli* and Professor *John Mottershead* is also highly acknowledged.

I would like also to express my thanks to Senior Lecturer *Agathoklis Giaralis* and Professor *Huajiang Ouyang* for participating in my thesis committee and reviewing the manuscript.

The author feels indebted to the *University of Liverpool* for financial support over the years of his postgraduate studies. Further, the financial support from the *State Scholarships Foundation* (*IKY*) in Greece is also gratefully acknowledged.

Finally, I would like to express my gratitude to my family for their encouragement, and trust in my skills, but mostly for their unconditional love. Specifically, I dedicate this thesis to my father, *Petros Mitseas*, my first and greatest tutor in life and science; and to my mother, *Marianthi Mitsea*, for her urging me to make this thinking more colorful.

Table of contents

List of Figures

List of Tables

Chapter 1

Introduction

1.1 Motivation and objectives

In the general area of structural dynamics, an interesting and challenging branch has always been the efficient analysis of nonlinear systems subject to evolutionary excitations. Regarding the complexity that characterizes the majority of the today's engineering systems and structures, the rather simplified analysis approach that neglects any effect stemming from nonlinearities seems particularly inadequate for a realistic study of system behaviour. Although, the inclusion of nonlinear effects leads to an increasing of the complexity of the problem, a possible disregard can have considerably adverse consequences on the quality and the accuracy of the system analysis. Specifically, in the field of structural engineering, it is common for structural systems to be subjected to extreme seismic ground motion excitations. Therefore large system responses may reasonably occur. Clearly, in the earthquake engineering field structural systems become nonlinear and inelastic, exhibiting restoring forces that depend on the response history. This kind of behaviour is described in the literature by the term hysteresis. In this setting, the notion of conducting a realistic structural system analysis is weaved with the necessity of employing a nonlinear dynamics analysis extended to the challenging class of hysteretic systems. Available techniques oriented to earthquake engineering applications can be found in Iwan (1974).

Aseismic code provisions promote the utilization of inelastic design in conjunction with equivalent linear dynamic behaviour due to their simplicity and precedent. However in cases of designing complex structural systems of critical importance or including non conventional means of protection against seismic hazard the code regulations prescribe

nonlinear dynamic response history analysis to be performed. A degree of empiricism is inherent in the initial approach while the consideration of nonlinearity on the latter case increases the complexity of the problem as well as the associated computational cost which stems from the numerical integration of the governing nonlinear equations of motion. This interesting complementarity reveals the overriding need of conducting reliable structural system analyses considering the presence of nonlinearities under an integrated and efficient context.

Over the last decades particular interest has arisen for considering also stochasticity in problems related to the nonlinear system response determination. One major reason for this interest stems from the fact that seismic excitations are usually so complex that they can only be described in a stochastic sense (e.g., Spanos, 1976). In this regard, a reasonably fair treatment for problems related to the above kind, passes indispensably from the area of nonlinear stochastic dynamics. In conceptual agreement with the necessity of considering stochasticity in the formulation of problems related to structural system analysis and design, performance-based engineering (PBE) frameworks (e.g., Cornell and Krawinkler, 2000; Ellingwood, 2001; Porter, 2003; Mohle and Deierlein, 2004; Der Kiureghian, 2005; Ciampoli and Petrini, 2012; Barbato and Petrini, 2013) were recently emerged by the structural engineering community. In general, PBE frameworks aim at facilitating risk-based decision making via performance assessment and design methods that properly account for the presence of uncertainties. Typically, a general probabilistic framework for PBE analysis involves a number of analysis components such as: (i) stochastic hazard analysis; (ii) stochastic structural/damage analysis; and (iii) stochastic loss analysis reflecting the effect of the underlying uncertainties on a quantifiable decision variable.

Normally, performing nonlinear stochastic dynamic analysis includes the numerical integration of the governing nonlinear equations of motion, whereas the input seismic excitations are represented by real recorded or synthetic earthquake time-histories. Over the past few decades, a number of methods for nonlinear stochastic dynamic analysis have been developed. Monte Carlo simulation (MCS) (e.g., Rubinstein, 1981; Spanos and

Zeldin, 1998; Schueller and Spanos, 2000; Proppe et al., 2003; Gamerman, 2006; Rubinstein and Kroese, 2008; Rubino and Tuffin, 2009) stands as the most potent method for conducting nonlinear stochastic dynamic analysis. Despite its wide applicability, it remains particularly cumbersome due to its significant associated computational cost. More recently, advanced simulation methods using variance-reduction techniques have been emerged. Among them, one can find i) importance sampling (e.g., Melchers, 1989; Song, 1997), ii) latin hypercube sampling (e.g., McKay et al., 1979; Florian, 1992), iii) adaptive sampling (e.g., Bucher, 1988; Mori and Ellingwood, 1993), iv) descriptive sampling (e.g., Saliby, 1990), v) line sampling (e.g., Koutsourelakis et al., 2004), vi) antithetic variates (e.g., Fishman and Huang, 1983), vii) directional simulation (e.g., Nie and Ellingwood, 2004; Nie and Ellingwood, 2005) and viii) subset simulation (e.g., Au and Beck, 2001b). The above MCS-based approaches are characterized by a significant computational advantage comparing to the conventional MCS method, however they still require a significant number of nonlinear dynamic analyses.

As an alternative during the same decades, random variable-based methods have been developed as well. In general, the above methods include the adoption of one or more limit-state functions involving a number of random variables. The first- and second-order reliability methods (FORM and SORM respectively), are usually employed for this class of problems. Some recent accounts of these methods can be found in Ditlevsen and Madsen (1996). It is noteworthy that these methods can also be used to nonlinear stochastic dynamic problems (e.g., Li and Der Kiureghian, 1995; Zhang and Der Kiureghian, 1997; Der Kiureghian, 2000; Franchin, 2004; Koo et al., 2005; Barbato and Conte, 2006; Jensen and Capul, 2006). Note in passing that the associated computational cost remains considerably high also in this case, rendered even prohibitive for cases where complex nonlinear large-scale MDOF structural systems are considered.

Clearly, the field of nonlinear stochastic dynamics is weaved with significant computational demands, thus it is an ideal area for exploiting the considerable abilities of nonlinear stochastic dynamics/random vibration based techniques. In this setting, analytical/approximate methods for determining the response statistics of simple linear

and nonlinear structural models under stochastic excitation have been proposed in the literature over the last decades (e.g., Nigam, 1983; Lin and Cai, 1995; Roberts and Spanos, 2003; Lutes and Sarkani, 2004). These include methods using perturbation, statistical linearization, Fokker-Planck equation, stochastic averaging and moment closure. It is noteworthy that among the above methods the statistical linearization method is the one that is characterized by the greater versatility and applicability. Regarding the other methods it should be noted that these are largely restricted to specialized nonlinear systems or forms of the excitation, and thus particularly cumbersome to apply in structural engineering problems of the common practice. Incorporation of stochastic approaches of the above kind in the analysis and design of structural systems can be found in (e.g., Crandall, 1958; Crandall, 1963; Crandall and Mark, 1963; Soong, 1973, Newland, 1993; Soong and Grigoriu, 1993, Preumont, 1994; Elishakoff, 1999; Roberts and Spanos, 2003; Lutes and Sarkani, 2004; Li and Chen, 2009).

To this end a significant part of this dissertation is concerned with the utilization of nonlinear stochastic dynamics/random vibration based techniques to the study of problems considering nonlinear dynamic MDOF structural systems of the hysteretic kind subject to stochastic excitations of the evolutionary kind. In this regard, several novel methods were developed for proposing efficient solutions to important structural engineering problems related to the exposure of structures to seismic hazard. Among them the efficient determination of the first-passage problem, namely the determination of the probability the response of the nonlinear MDOF system reaches a predetermined barrier level for the first time, can be found. Further, a novel methodology for determining the seismic fragilities regarding realistic hysteretic multi-story building structures under non-stationary stochastic excitations is proposed. An analysis/design framework regarding structural system's robustness which allows for the simultaneous treatment of different performance features defined in the joint time-frequency domain is also part of this thesis. Finally a novel efficient integrated approach for dealing with the performance-based earthquake engineering (PBEE) problem in one of the most

demanding formulations has been developed. In the section that follows the organization of this thesis is given explicitly.

1.2 Organization of the thesis

The thesis comprises eight chapters followed by the list of cited references. Excluding the first chapter, which plays an introductory role, and the final one, which contains the concluding remarks, each of the remaining chapters are self-contained and include a separate introductory section followed by the pertinent theoretical background and integrated by sections presenting numerical results, as well as verification by digital simulations in cases it is deemed appropriate.

Chapter 1 provides an introduction to the thesis and outlines the motivation and the objectives of the current research effort. A brief requisite review of the methods for conducting nonlinear stochastic dynamic analysis with emphasis to the ones that have been applied to the field of structural dynamics is also included. Furthermore, the contents of the thesis are briefly outlined.

Chapter 2 contains a presentation of the seismic excitation models that utilized throughout this thesis for the stochastic representation of the seismic action. Phenomenological stochastic seismic excitation models of both separable and non-separable kind as well as a more sophisticated stochastic seismological model that is commonly applied in the earthquake engineering field are included.

In Chapter 3 an alternative analytical/approximate method to the type of nonlinear stochastic dynamic analysis is presented. Specifically, relying firstly on an evolutionary spectral matrix analysis approach and on statistical linearization second order response statistics of a MDOF nonlinear system subject to a stochastic excitation vector with an evolutionary broad-band power spectrum matrix are derived. Further, a system dimension reduction/decoupling approach is introduced by determining an effective auxiliary LTV SDOF system corresponding to each degree of freedom. Subsequently, relying on a stochastic averaging treatment the time-varying response amplitude PDFs of the

corresponding LTV SDOF systems are efficiently determined. Note that the approach can handle readily stochastic excitations of arbitrary non-separable EPS forms that exhibit strong variability in both the intensity and the frequency content.

In chapter 4 an approximate analytical technique for determining the survival probability and first-passage PDF of nonlinear MDOF structural systems subject to a non-stationary stochastic excitation vector is developed. The proposed technique can be construed as a two-stage approach. First, relying on statistical linearization and utilizing a dimension reduction approach the nonlinear n-degree-of-freedom system is decoupled and cast into (n) effective SDOF LTV oscillators corresponding to each and every DOF of the original MDOF system. Second, utilizing the effective SDOF LTV oscillator time-varying stiffness and damping elements in conjunction with a stochastic averaging treatment of the problem, the non-stationary marginal, transition, joint response amplitude PDFs as well as the MDOF system survival probability and first-passage PDF are determined. Overall, the developed technique appears to be efficient and versatile since it can handle readily, at a low computational cost, a wide range of nonlinear/hysteretic behaviors as well as various stochastic excitation forms, even of the fully non-stationary in time and frequency kind. A 3-DOF structural system exhibiting hysteresis following the Bouc-Wen model is included in the numerical examples section. Comparisons with pertinent Monte Carlo simulations demonstrate the reliability of the technique.

In chapter 5 a novel methodology for determining the seismic fragility of nonlinear MDOF structural systems is developed based on an efficient approximate stochastic dynamics technique. Specifically, fragility surfaces are determined for nonlinear/hysteretic MDOF structural systems subject to earthquake excitations compatible with a specific stochastic seismological model of the sophisticated type. Note that the employed intensity measure (IM) comprises two parameters, namely the earthquake moment magnitude (M_m) and the epicentral distance (r); that is, the distance from the system site to the epicentre of the earthquake**.** Further, based on the concepts of stochastic averaging and of statistical linearization the response amplitude envelope is

modelled as a one-dimensional Markov process. Further, relying on the Fokker-Planck (F-P) equation and on the associated first-order stochastic differential equation the response amplitude envelope PDFs are obtained efficiently without resorting to numerical integration of the nonlinear equations of motion. This attribute is of particular importance since the computational cost of the corresponding analyzes is significantly limited. Further, a direct transformation of the response amplitude envelope PDF yields the non-stationary IDR amplitude envelope PDF. Then, considering the IDR as the selected engineering demand parameter (EDP) and appropriately defined damage states structural system related fragility surfaces are determined at a low computational cost. Building structures serve as numerical examples for demonstrating the efficiency and robustness of the proposed methodology. Moreover, appropriate Monte Carlo analyses are conducted to determine the accuracy of the approach.

Chapter 6 includes an efficient robust design optimization (RDO) framework for linear MDOF structural systems subject to evolutionary stochastic earthquake excitations. A significant feature of the developed RDO framework relates to the consideration of both inter-story drift and absolute floor acceleration second order statistics as performance measures. Further, an efficient frequency domain approach is utilized for determining the system response EPS matrix circumventing computationally intensive Monte Carlo simulations. Furthermore, the optimization problem is solved by employing a Genetic Algorithm based approach. An illustrative numerical example is included to demonstrate the efficiency and robustness of the proposed framework.

In chapter 7 a novel and comprehensive approach for structural system optimal stochastic design considering LCC is developed. Specifically, a performance-based multi-objective design optimization framework for nonlinear/hysteretic MDOF structural systems subject to evolutionary stochastic excitations is formulated. Although the developed PBE framework is tailored specifically for earthquake engineering related applications in general agreement with the PBEE framework proposed by the PEER center, it can be readily modified to account for other hazard kinds as well. The core of the developed framework is the efficient approximate dimension reduction/decoupling

technique based on the concepts of statistical linearization and of stochastic averaging for determining the non-stationary system response amplitude PDFs; thus, computationally intensive Monte Carlo simulations are circumvented. Next, the convolution between the derived closed-form expressions for the non-stationary IDR amplitude PDFs with the appropriately defined damage measures, leads to the computation of the system related fragility curves corresponding to every DOF. Then a weighted integral of the fragility curves over the derivative of the hazard rate function provides the annual rates of the seismic demand exceeding specified levels of damage which in turn can be expressed in design life rates. Upon obtaining the design life rates, the computation of the expected value of the LCC due to seismic hazard can be done in a straightforward manner and at a considerable low computational cost. Further, in the developed LCC formulation the expected value of the seismic losses serves as the decision variable (DV), whereas the coherent attribute of considering every DOF's behavior leads to better account for the system overall performance in the formulation of the optimization problem. Finally, the structural system stochastic design optimization problem is formulated as a multi-objective one to be solved by a Genetic Algorithm based approach. Certain remarks regarding the formulation of the problem, involve the concept of implementing appropriate stochastic constraints for avoiding "moving resonance" phenomena. A reinforced concrete building structure comprising the versatile Bouc-Wen (hysteretic) model serves as a numerical example for demonstrating the efficiency of the proposed methodology.

Concluding remarks along with suggestions for future work are provided in chapter 8. Further, Appendix A briefly reviews an efficient random field simulation method used in various applications in this thesis for simulating time-histories as samples of an underlying stochastic process characterized by a given power spectrum. Finally, a list of cited references is provided while a list of the author’s publications follows.

Chapter 2

Stochastic representation of the seismic action

2.1 Models of the seismic excitation

In the field of structural engineering, performing nonlinear dynamic analysis presupposes the definition of the seismic excitation in the form of acceleration time-histories. Commonly, these belong to the following three broad categories

- realizations of a stochastic process
- real recorded seismic accelerograms
- accelerograms from stochastic seismological models

Note in passing that throughout this thesis acceleration time-histories generated from the first as well as the third category have been utilized.

2.2 Stochastic process modeling

A sustained challenge for the seismological society has always been the definition of realistic models for the seismic action. The observed statistical stability regarding the frequency content of real ground motions records under similar conditions led to the consideration of accelerograms as realizations of random processes. In this setting, several stochastic models of varying complexity have been proposed over the last decades.

2.2.1 Phenomenological seismic stationary models

Given an earthquake occurs, the seismic wave produced by the seismic source is a time process. Actually, the shape of the seismic wave through its propagation in the earth media will undergo complex changes (Li and Chen, 2009). In applications related to earthquake engineering, one of the most widely used stationary seismic models is the one of Kanai-Tajimi (K-T) (Kanai, 1957). Based on empirical data the K-T model take into account the dependence of the power spectrum $S(\omega)$ on local soil conditions and the corresponding dominant frequency. Real earthquake records show that the time history of the seismic motion accelerations usually includes three stages of vibrations: the initial, the strong, and the attenuating stages. Clearly, the ground motion is a typical non-stationary process and the assumption of stationarity cannot capture its modulation in time. In cases where a stationary seismic model is adopted, it is assumed that this only reflects the strong stage of the ground motion.

The seismic motion on the surface can be seen as a filtered white noise. In this setting, if the ground motion on the bedrock is assumed as a zero mean white-noise process with amplitude S_0, and the soil surface is simulated as a linear single-degree-of-freedom (SDOF) system, then the proposed stationary power spectrum (PS) for the K-T model is given as

$$S_{KT}(\omega) = S_0 \frac{{\omega_g}^4 + 4(\xi_g)^2 {\omega_g}^2 \omega^2}{({\omega_g}^2 - \omega^2)^2 + 4{\xi_g}^2 {\omega_g}^2 \omega^2} \tag{2.1}$$

where ξ_g and ω_g are the damping factor of the soil and the fundamental natural frequency, respectively. Note that for the specific case of a zero-mean, stationary Gaussian process the complete definition of the stochastic process can be done once its power spectrum is specified. Meanwhile, the K-T model was found to exaggerate inappropriately at the low frequency content of the ground motions. To overcome this shortcoming, Clough and Penzien (1993) modified it appropriately by incorporating a second-order high-pass filter to eliminate the presence of low-frequency content allowed

by the K-T form. The Clough-Penzien (C-P) spectrum model is assumed to have the following form

$$S_{CP}(\omega) = S_0 \frac{(\omega/\omega_f)^4}{(1-(\omega/\omega_f)^2)^2 + 4\xi_f{}^2(\omega/\omega_f)^2} \frac{\omega_g{}^4 + 4(\xi_g)^2\omega_g{}^2\omega^2}{(\omega_g{}^2-\omega^2)^2 + 4\xi_g{}^2\omega_g{}^2\omega^2} \quad (2.2)$$

where ξ_f and ω_f are parameters describing the Clough-Penzien filter (Clough and Penzien, 1993). For the parameters values $\xi_g = 0.7$, $\omega_g = 2$ rad/ s, $\xi_f = 0.6$, $\omega_f = 12.5$ rad/s and input white noise intensity $S_0 = 0.5692$ m^2/s^3 and $S_0 = 1.0000$ m^2/s^3 the resulting power spectra are shown in Fig.(2.1).

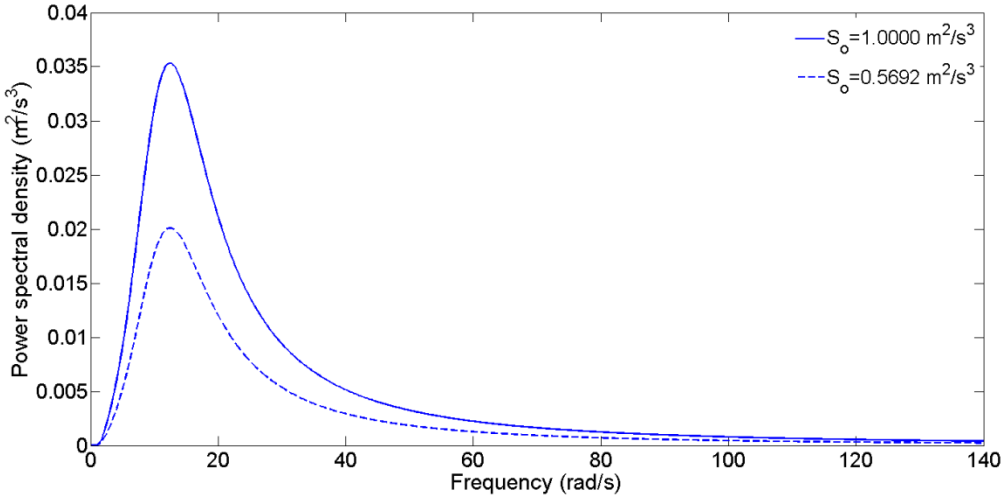

Figure 2.1. Clough-Penzien power spectra for various levels of the amplitude of the bedrock excitation spectrum S_0.

Next, the spectral representation method of Shinozuka and Deodatis (1991) can be employed to generate PS compatible excitation realizations; see also Appendix A. Fig.(2.2) shows typical realizations of the ground acceleration stochastic process for the two considered cases of different amplitude S_0.

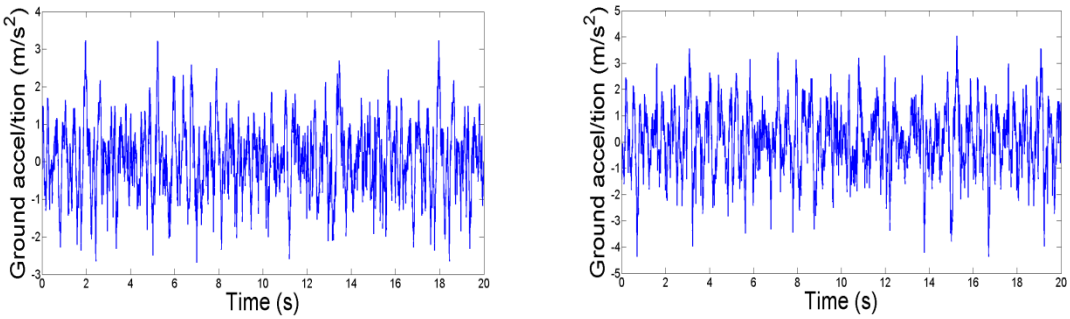

Figure 2.2. Typical realizations of the ground acceleration stationary stochastic process based on the C-P spectrum model for various levels of the amplitude S_0.

2.2.2 Phenomenological seismic non-stationary models: separable and non-separable form

Dealing with the non-stationarity of the ground motion, the necessity to capture the rising and decaying sections of the seismic motion led to the introduction of time-modulated non-stationary stochastic processes of the form

$$X_{NS}(t) = g(t)X_S(t) \tag{2.3}$$

where $X_S(t)$ stands for a stationary process and $g(t)$ is a deterministic time function. Regarding the modulated time envelope function many different forms have been proposed (Amin and Ang, 1968; Clough and Penzien, 1993; Mitseas et al, 2014b). Throughout this thesis whenever a separable non-stationary seismic model is adopted, the time-modulating envelope function is assumed to have the following form

$$g(t) = k\left(e^{-b_1 t} - e^{-b_2 t}\right), \tag{2.4}$$

where b_1 and b_2 are parameters of the envelope function; and k is a normalization constant so that $g(t)_{max} = 1$. Then, the excitation evolutionary power spectrum (EPS) can be defined as a product of the deterministic function $g(t)$ and the stationary PS $S_{CP}(\omega)$. In this setting the EPS $S_{\ddot{\alpha}_g}(\omega, t)$ takes the following separable form

$$S_{\ddot{\alpha}_g}(\omega, t) = |g(t)|^2 S_{CP}(\omega), \tag{2.5}$$

Considering the following values $b_1 = 0.1$ and $b_2 = 0.3$ for the envelope function the resulting EPS for the case of input white noise intensity $S_0 = 0.5692\ m^2/s^3$ is given in Fig.(2.3)

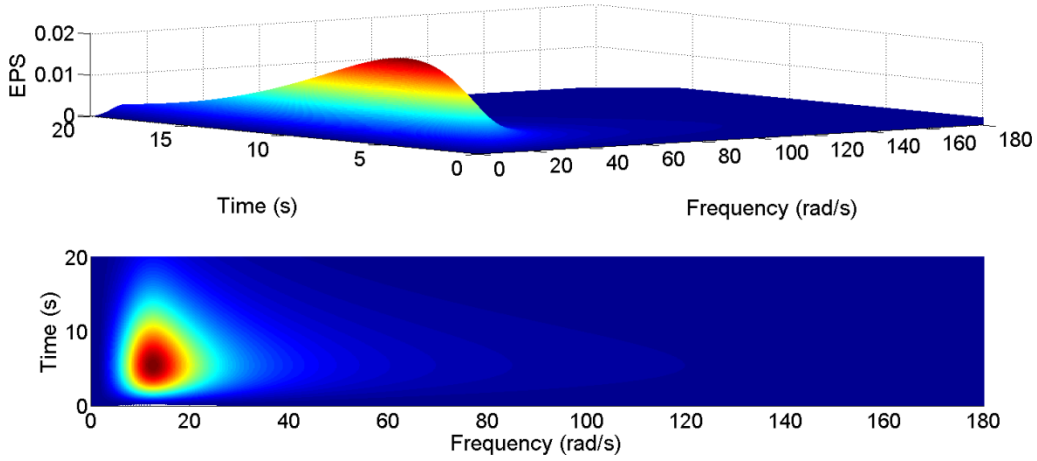

Figure 2.3. Clough-Penzien evolutionary power spectrum $S_{\ddot{\alpha}_g}(\omega, t)$.

Further, excitation realizations compatible with the EPS of Eq.(2.5) are generated based on the spectral representation technique (e.g. Shinozuka and Deodatis 1991). In Fig.(2.4), typical realizations of the ground acceleration non-stationary stochastic process are depicted for different values of amplitude S_0.

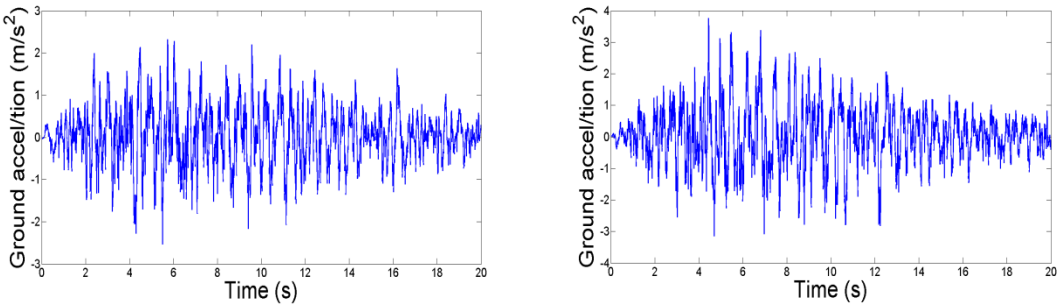

Figure 2.4. Typical realizations of the ground acceleration non-stationary stochastic process for various levels of the amplitude S_0.

Furthermore, evolutionary stochastic excitation models of the non-separable form have been introduced as well. Clearly, excitations acting upon structural systems such as wind, wave, and seismic loads commonly exhibit strong variability in both the intensity and the frequency content. However, over the last decades the study of the available recorded ground motion data was mainly focused on the frequency content of the ground motion in terms of the modulation in time of the ground motion and to a less degree to the evolution in time of the frequency content. One of the main characteristics of the seismic shaking that of the decreasing of the dominant frequency with respect to time (e.g., Liu, 1970; Spanos and Solomos, 1983) is comprised by the non-separable EPS

$$S_{\ddot{\alpha}_g}(\omega, t) = S_0 \left(\frac{\omega}{15\pi}\right)^2 e^{-bt} t^2 e^{-\left(\frac{\omega}{15\pi}\right)^2 t}, \tag{2.6}$$

where S_0 stands for the amplitude of the bedrock excitation spectrum and b is a parameter of the model. Note in passing that the calibration of such non-separable models that take into account this frequency-content time dependence versus statistical data has proven to be a rather difficult task. Notable contributions towards this direction can be found in (e.g., Conte and Peng, 1997; Lungu and Giaralis, 2013). In Fig.(2.5) the non-separable EPS $S_{\ddot{\alpha}_g}(\omega, t)$ is given for the case of $S_0 = 10\ m^2/s^3$ and $b = 0.2$.

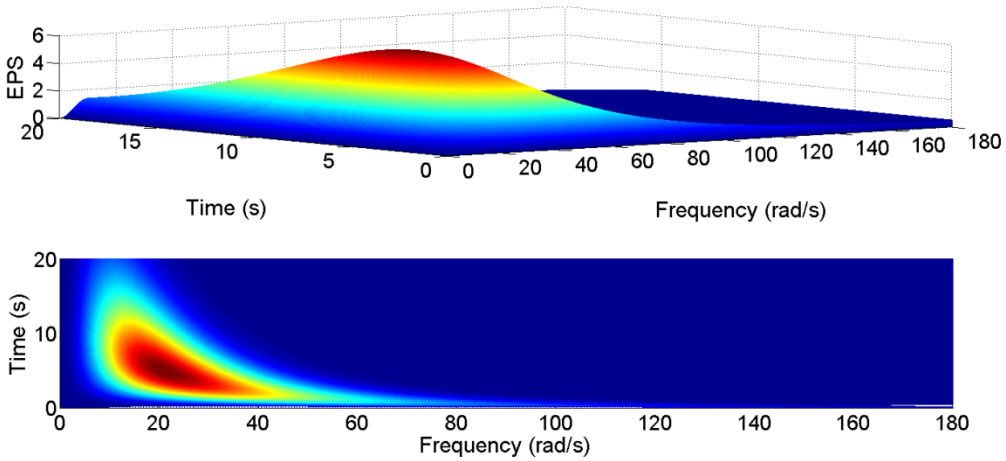

Figure 2.5. Non-separable excitation evolutionary power spectrum $S_{\ddot{\alpha}_g}(\omega, t)$.

2.3 Stochastic seismological model

In this section the most important elements of the stochastic seismological model developed in Boore (2003) are presented. This seismological model is characterized primarily by the radiation spectrum $Y(f; M_m, r)$ and the envelope function $e(t; M_m, r)$, where f denotes the frequency expressed in Hz.

2.3.1 Radiation spectrum determination

The radiation spectrum $Y(f; M_m, r)$ of the ground motion at a site can be construed as the composition of several contributions from various factors such as the earthquake source (E), the path (P), the site (G), and the type of motion (I); this is expressed as

$$Y(f; M_m, r) = E(f, M_o)\, P(f, r)\, G(f)\, I(f) \tag{2.7}$$

where the equivalent two point-source spectrum developed by Atkinson and Silva (2000) is adopted for the source E in the form

$$E(f, M_m) = C\, M_o \left[\frac{1-\varepsilon}{1+(f/f_a)^2} + \frac{\varepsilon}{1+(f/f_b)^2}\right]. \tag{2.8}$$

In Eq.(2.8), the symbol M_o stands for the seismic moment (in dyn-cm), given by (e.g., Kanamori, 1977; Hanks and Kanamori, 1979)

$$M_o = 10^{1.5(M_m+10.7)} \tag{2.9}$$

Clearly the seismic moment M_o and the moment magnitude M_m are related via a unique mapping. Further, the constant C is given by the relationship

$$C = \frac{R_{\Phi} V F}{4\pi R_o \rho_s {\beta_s}^3} \tag{2.10}$$

where R_{Φ} is the average radiation pattern, V is a coefficient to account for the partition of waves into two horizontal components, F is the free surface amplification; β_s and ρ_s are the shear-wave velocity and density in the vicinity of the seismic source; and R_o is a

reference distance. Next, the lower and upper corner frequencies f_a and f_b in Eq.(2.8) are given by the relationships $\log_{10} f_a = 2.181 - 0.496 M_m$ and $\log_{10} f_b = 2.410 - 0.408 M_m$ (in Hz), respectively. The weighting parameter ε is described by the expression $\log_{10} \varepsilon = 0.605 - 0.255 M_m$. Further, the path component of the process that affects the radiation spectrum of ground motion at a particular site is given by

$$P(f, r) = \frac{1}{R} \exp\left(-\pi f R / Q(f) \beta_s\right), \tag{2.11}$$

where $R = \sqrt{h^2 + r^2}$ is the radial distance from the earthquake source to the site, with h representing a moment dependent, nominal pseudo-depth (in km), given by the expression $\log_{10} h = 0.15 M_m - 0.05$. The employed regional quality factor Q(f) is given by

$$Q(f) = 680\, f^{0.38}, \tag{2.12}$$

whereas the modification of seismic waves by local site conditions is considered through the expression

$$G(f) = \exp(-\pi k_o f)\, A_m, \tag{2.13}$$

where $k_o = 0.015$; and A_m is a near-surface amplification factor described via empirical curves for generic rock sites (e.g., Boore and Joyner, 1997). As a simplification it is usually assumed that A_m is equal to a constant value (e.g., Au and Beck, 2003). Next, considering the acceleration as the utilized type of ground motion yields $n = 2$, and the filter I(f) takes the form

$$I(f) = (2\pi f)^2. \tag{2.14}$$

In Fig.(2.6) the radiation spectra for various values of moment magnitude M_m and a constant value of the epicentral distance r equal to 30km are plotted. Regarding the parameters of the seismological model the following values are considered herein: $R_\Phi = 0.55$, $V = 1/\sqrt{2}$, $F = 4$, $\beta_s = 3.5 \text{km/s}$ and $\rho_s = 2.8 \text{g/cm}^3$, $R_o = 1 \text{km}$, and $A_m = 2.5$. Note in passing that in the following the radiation spectra are expressed in terms of angular frequency ω; thus, the radiation spectrum takes the form $Y(\omega; M_m, r)$.

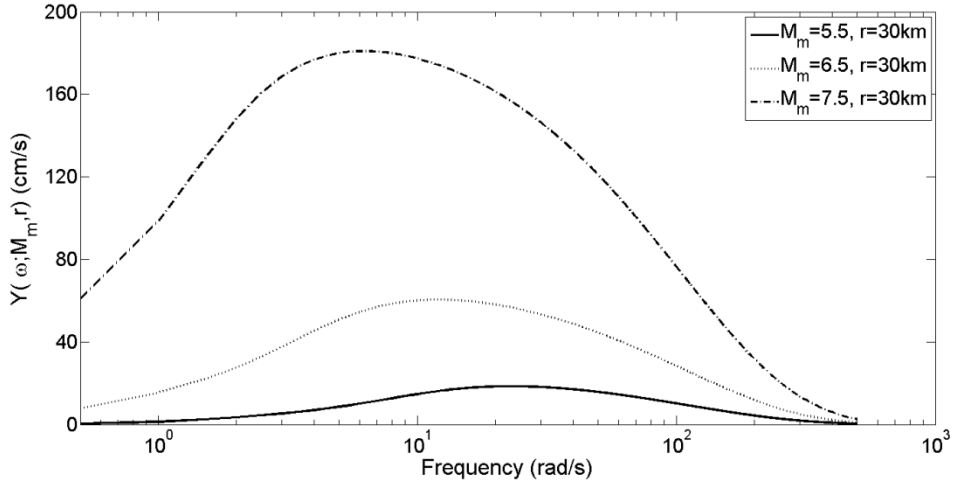

Figure 2.6. Radiation spectrum $\mathrm{Y}(\omega; \mathrm{M_m}, \mathrm{r})$ for various $\mathrm{M_m}$ and $\mathrm{r} = 30\mathrm{km}$.

2.3.2 Time-envelope function determination

The envelope function $\mathrm{e}(\mathrm{t}; \mathrm{M_m}, \mathrm{r})$ for the earthquake excitations is given by

$$\mathrm{e}(\mathrm{t}; \mathrm{M_m}, \mathrm{r}) = \alpha(\mathrm{t}/\mathrm{t_n})^{\,\mathrm{b}} \exp\big(-c(t/\mathrm{t_n})\big), \tag{2.15}$$

where

$$\mathrm{b} = -\lambda \ln(\eta)/[1 + \lambda(\ln(\lambda) - 1)], \tag{2.16}$$

$$\mathrm{c} = \mathrm{b}/\lambda, \tag{2.17}$$

$$\alpha = [\exp(1)/\lambda]^{\,\mathrm{b}}, \tag{2.18}$$

and

$$\mathrm{t_n} = 0.1\mathrm{R} + 1/\mathrm{f_a}. \tag{2.19}$$

In Eq.(2.16) λ and η take the values 0.2 and 0.05 respectively; and $\mathrm{t_n}$ is related to the duration of the envelope function (Boore, 1983). In Fig.(2.7) envelope functions for various values of $\mathrm{M_m}$ and a constant value of the epicentral distance $\mathrm{r} = 30$ km are plotted.

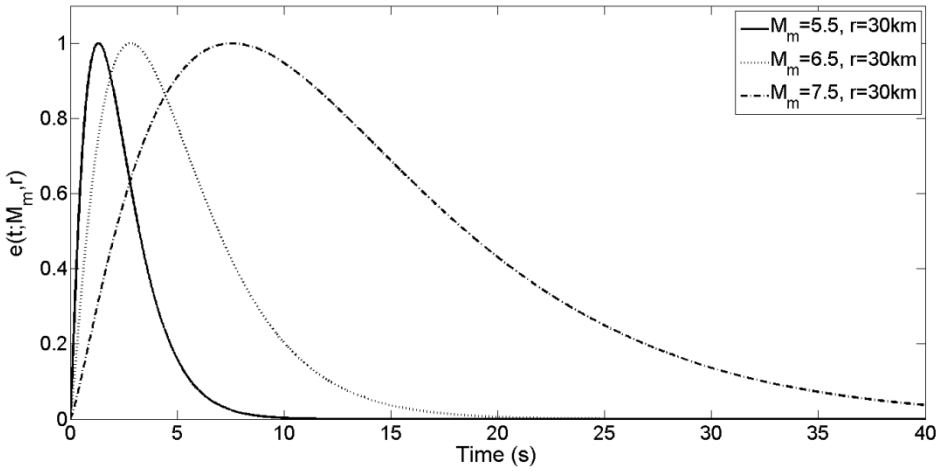

Figure 2.7. Envelope function $e(t; M_m, r)$ for various M_m values and $r = 30\text{km}$.

Further, seismic ground acceleration realizations at a site with moment magnitude M_m and epicentral distance r can be readily generated through the utilization of the derived EPS by multiplying the radiation spectrum $Y(\omega; M_m, r)$ with the envelope function $e(t; M_m, r)$; i.e.,

$$S_{\ddot{\alpha}_g}(\omega, t) = |e(t; M_m, r)|^2 Y(\omega; M_m, r). \tag{2.20}$$

Next, the spectral representation method of Shinozuka and Deodatis (1991) can be employed to generate EPS compatible excitation realizations. Figs.(2.8-2.10) show typical realizations of the ground acceleration stochastic process as well as the associated EPS for site and earthquake conditions depicted in Figs. (2.6-2.7).

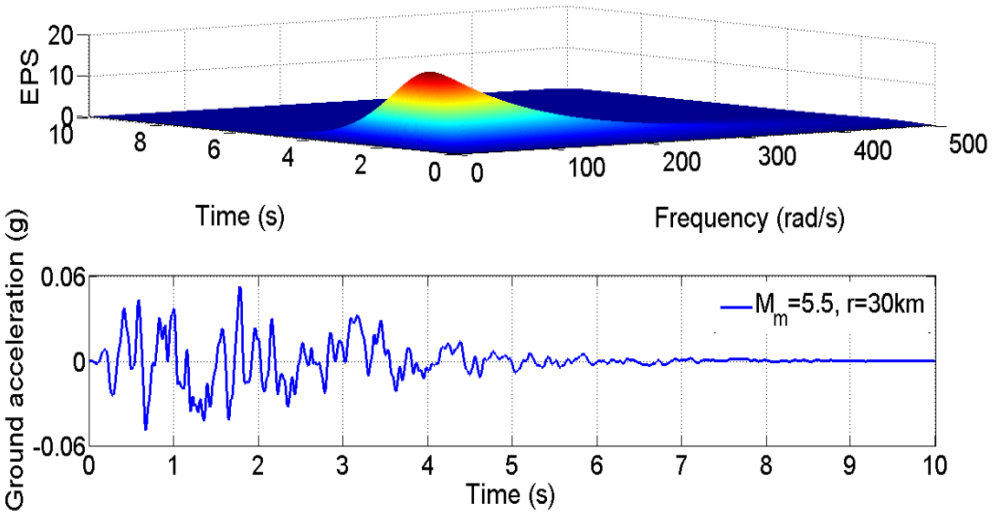

Figure 2.8. EPS and sample ground motion for $M_m = 5.5$ and $r = 30$km

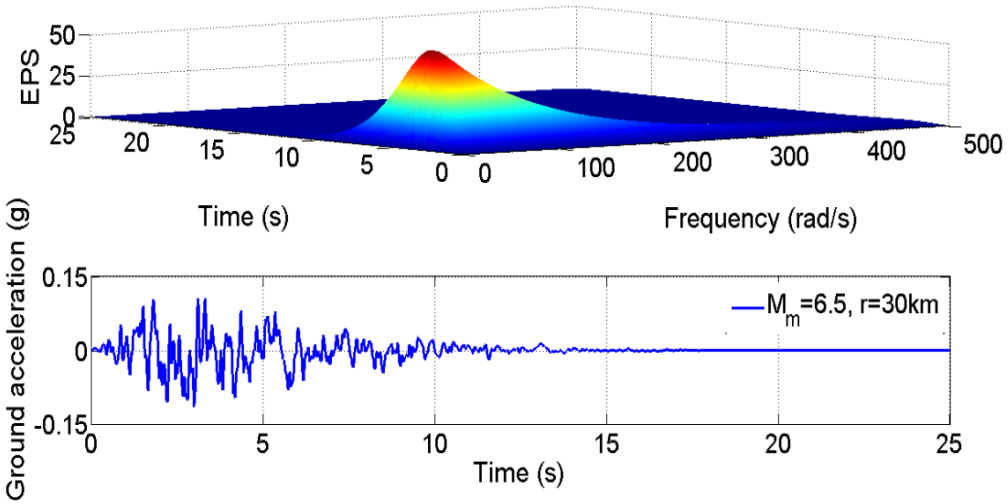

Figure 2.9. EPS and sample ground motion for $M_m = 6.5$ and $r = 30$km.

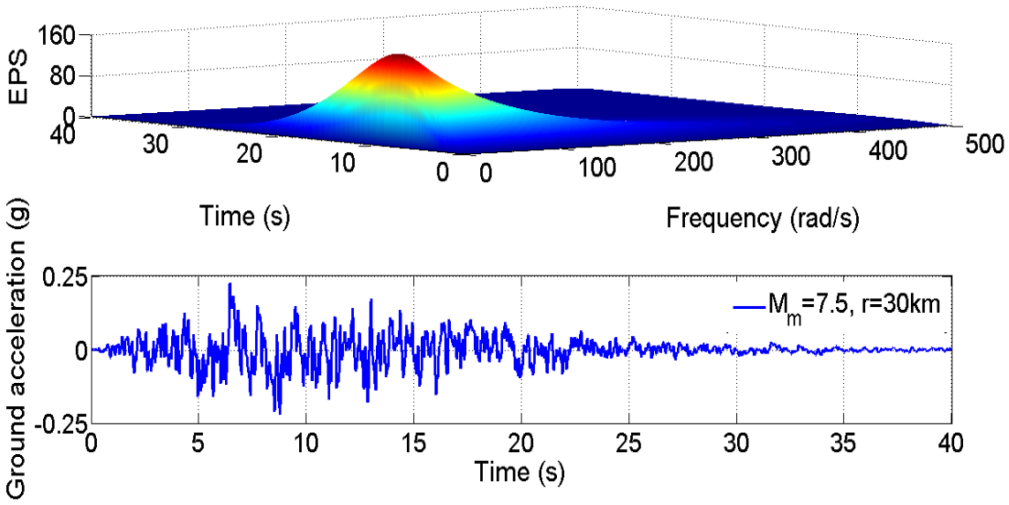

Figure 2.10. EPS and sample ground motion for $M_m = 7.5$ and $r = 30km$

Chapter 3

An alternative analytical/approximate method to the type of nonlinear stochastic dynamic analysis

3.1. Preliminary remarks

In this section, a recently developed approximate dimension reduction/decoupling technique (Kougioumtzoglou and Spanos, 2013) for determining the non-stationary response amplitude probability density function (PDF) of a nonlinear MDOF system subject to evolutionary stochastic excitation is presented; see also Spanos and Lutes (1980).

3.2. Statistical linearization approximation

Consider an n-degree-of-freedom nonlinear structural system governed by the equation

$$\mathbf{M}\ddot{\mathbf{x}} + \mathbf{C}\dot{\mathbf{x}} + \mathbf{K}\mathbf{x} + \mathbf{g}(\mathbf{x}, \dot{\mathbf{x}}, t) = \mathbf{F}(t), \tag{3.1}$$

where $\ddot{\mathbf{x}}$ denotes the response acceleration vector, $\dot{\mathbf{x}}$ is the response velocity vector, $\mathbf{x}$ is the response displacement vector; $\mathbf{M}$, $\mathbf{C}$ and $\mathbf{K}$ denote the $(n \times n)$ mass, damping and stiffness matrices, respectively; $\mathbf{g}(\mathbf{x}, \dot{\mathbf{x}}, t)$ is an arbitrary nonlinear $(n \times 1)$ vector function of the variables $\mathbf{x}$, $\dot{\mathbf{x}}$ and t. $\mathbf{F}(t)^T = (f_1(t), f_2(t), \dots, f_n(t))$ is a $(n \times 1)$ zero mean, non-stationary stochastic excitation vector process defined as $\mathbf{F}(t) = \boldsymbol{\gamma}\boldsymbol{\Gamma}\alpha(t)$, where $\boldsymbol{\gamma}^T = (\gamma_1, \gamma_2, \dots, \gamma_n)$ is an arbitrary $(n \times 1)$ vector of constant weighting coefficients, $\boldsymbol{\Gamma}$ is the unit column vector, and $\alpha(t)$ is a non-stationary process with an EPS $S_\alpha(\omega, t)$. In this regard, $\mathbf{F}(t)$ possesses the EPS matrix

$$\mathbf{S_F}(\boldsymbol{\omega}, \mathbf{t}) = \begin{bmatrix} \gamma_1{}^2 S_\alpha(\omega, t) & 0 & \cdots & 0 \\ 0 & \gamma_2{}^2 S_\alpha(\omega, t) & \cdots & 0 \\ \vdots & \ddots & \cdots & \vdots \\ 0 & 0 & \cdots & \gamma_n{}^2 S_\alpha(\omega, t) \end{bmatrix}. \quad (3.2)$$

The diagonality which characterizes the EPS matrix of the excitation process stems from the assumption of lumped masses regarding the system under consideration (e.g., Roberts and Spanos, 2003). Further, the non-stationary stochastic excitation process is regarded to be a filtered stationary stochastic process according to the concept proposed by Priestley (1965); see also Dahlhaus (1997). The excitation EPS matrix of Eq.(3.2) takes the form

$$\mathbf{S_F}(\omega, t) = \mathbf{A}(\omega, t)\mathbf{S_{\tilde{F}}}(\omega)\mathbf{A}(\omega, t)^{\mathbf{T}*}, \quad (3.3)$$

where the superscripts (T) and (*) denote matrix transposition and complex conjugation, respectively; $\mathbf{A}(\omega, t)$ is the modulating matrix which serves as a time-variant filter; and $\mathbf{S_{\tilde{F}}}(\omega)$ is the power spectrum matrix corresponding to the stationary stochastic vector process $\tilde{\mathbf{F}}(t)$. Note that both separable and non-separable EPS can be defined considering Eq.(3.3). In this manner, excitations exhibiting variability in both the intensity and the frequency content can be modelled. Focusing next on the frequency domain, the response determination problem is defined as seeking the corresponding system response EPS matrix of the form

$$\mathbf{S_x}(\omega, t) = \begin{bmatrix} S_{x_1x_1}(\omega, t) & S_{x_1x_2}(\omega, t) & \cdots & S_{x_1x_n}(\omega, t) \\ S_{x_2x_1}(\omega, t) & S_{x_2x_2}(\omega, t) & \cdots & \vdots \\ \vdots & \ddots & \cdots & S_{x_{n-1}x_n}(\omega, t) \\ S_{x_nx_1}(\omega, t) & \cdots & S_{x_nx_{n-1}}(\omega, t) & S_{x_nx_n}(\omega, t) \end{bmatrix}. \quad (3.4)$$

According to the statistical linearization method (e.g., Soong and Grigoriu, 1993; Crandall, 2000; Roberts and Spanos, 2003; Li and Chen, 2009), a linearized version of Eq.(3.1) takes the form

$$\mathbf{M}\ddot{\mathbf{y}} + \left(\mathbf{C} + \mathbf{C_{eq}}\right)\dot{\mathbf{y}} + \left(\mathbf{K} + \mathbf{K_{eq}}\right)\mathbf{y} = \mathbf{F}(t). \quad (3.5)$$

The $\mathbf{C_{eq}}$ and $\mathbf{K_{eq}}$ are deterministic matrices that are to be determined through the minimization of the expected value of the difference between Eqs.(3.1) and (3.5) in a least square sense. The difference ε may be written as

$$\varepsilon = \mathbf{M}\ddot{\mathbf{x}} + \mathbf{C}\dot{\mathbf{x}} + \mathbf{K}\mathbf{x} + \mathbf{g}(\mathbf{x}, \dot{\mathbf{x}}, \mathrm{t}) - \mathbf{M}\ddot{\mathbf{y}} - \left(\mathbf{C} + \mathbf{C_{eq}}\right)\dot{\mathbf{y}} - \left(\mathbf{K} + \mathbf{K_{eq}}\right)\mathbf{y} \tag{3.6}$$

Furthermore, it is also assumed that the statistics and especially the variances of the process **x** and **y** are equal (Roberts and Spanos, 2003; Crandall 2001). Next, adopting the standard assumption that the response processes are Gaussian and considering the above minimization criterion, the time-dependent elements of the equivalent linear matrices $\mathbf{C_{eq}}$ and $\mathbf{K_{eq}}$ are given by the expressions

$$\mathrm{c}_{\mathrm{i,j}}^{\mathrm{eq}} = \mathrm{E}\left\{\frac{\partial \mathrm{g}(\mathbf{y}, \dot{\mathbf{y}}, \mathrm{t})_{\mathrm{i}}}{\partial \dot{\mathrm{y}}_{\mathrm{j}}}\right\}, \tag{3.7}$$

and

$$\mathrm{k}_{\mathrm{i,j}}^{\mathrm{eq}} = \mathrm{E}\left\{\frac{\partial \mathrm{g}(\mathbf{y}, \dot{\mathbf{y}}, \mathrm{t})_{\mathrm{i}}}{\partial \mathrm{y}_{\mathrm{j}}}\right\}. \tag{3.8}$$

Further, for a linear MDOF system subject to evolutionary stochastic excitation a matrix input-output spectral relationship of the form

$$\mathbf{S_y}(\omega, \mathrm{t}) = \mathbf{H_{gen}}(\omega, \mathrm{t})\mathbf{S_{\bar{F}}}(\omega)\mathbf{H_{gen}^{T^*}}(\omega, \mathrm{t}), \tag{3.9}$$

can be derived (e.g., Roberts and Spanos, 2003; Li and Chen, 2009), where

$$\mathbf{H_{gen}}(\omega, \mathrm{t}) = \int_0^{\mathrm{t}} \mathbf{h}(\mathrm{t} - \tau)\, \mathbf{A}(\omega, \tau)\mathrm{e}^{-\mathrm{i}\omega(\mathrm{t}-\tau)}\mathrm{d}\tau. \tag{3.10}$$

In Eq.(3.10) $\mathbf{h}(\mathrm{t})$ denotes the impulse response function matrix. Furthermore, the time dependent cross–variance of the response can be evaluated by the expression

$$\mathrm{E}\left[\mathrm{y_i y_j}\right] = \int_{-\infty}^{\infty} \mathrm{S}_{\mathrm{y_i y_j}}(\omega, \mathrm{t})\, \mathrm{d}\omega. \tag{3.11}$$

It can be readily seen that Eqs.(3.7-3.11) constitute a coupled nonlinear system of algebraic equations to be solved numerically for the system response covariance matrix.

Analytical expressions (e.g., Li and Chen, 2009) for the impulse response function handling cases where the excitation process is of the non-stationary kind could have been utilized; leading to the computation of the convolution integral of Eq.(3.10). However, omitting the convolution of the impulse response function matrix with the modulating matrix can lead to substantial reduction of computational effort, especially for the case of MDOF systems (e.g., Kougioumtzoglou and Spanos, 2013; Mitseas et al., 2014c). In this manner, Eq.(3.10) takes the form

$$\mathbf{H_{gen}}(\omega, t) = \mathbf{H}(\omega)\mathbf{A}(\omega, t), \tag{3.12}$$

where $\mathbf{H}(\omega)$ is the frequency response function (FRF) matrix defined as

$$\mathbf{H}(\omega) = \left(-\omega^2\mathbf{M} + i\omega(\mathbf{C} + \mathbf{C_{eq}}) + (\mathbf{K} + \mathbf{K_{eq}})\right)^{-1}. \tag{3.13}$$

Consequently, taking into account Eqs.(3.3) and (3.12), Eq. (3.9) becomes

$$\mathbf{S_y}(\omega, t) = \mathbf{H}(\omega)\mathbf{S_F}(\omega, t)\mathbf{H^{T*}}(\omega). \tag{3.14}$$

Further, Eq.(3.14) is a straightforward generalization of the celebrated spectral relationship based on stationarity and on the Wiener-Khinchin theorem. Thus, the above expression can be regarded as a quasi-stationary approximate relationship which, in general, yields satisfactory accuracy in cases of relatively stiff systems (e.g., Hammond, 1968,1973; Jangid and Datta, 1999). Note in passing that the spectral input-output relationship of Eq.(3.14) is exact for the case of stationary processes (e.g., Soon and Grigoriu, 1993; Roberts and Spanos, 2003; Li and Chen, 2009). Further, adopting the aforementioned quasi-stationary approach, it can be readily seen that for the i-th degree of freedom, using Eq.(3.2), Eq.(3.11) and Eq.(3.14) yields

$$E[y_i^2(t)] = \int_{-\infty}^{\infty} (|H_{i1}(\omega)|^2\gamma_1^2 + \cdots + |H_{in}(\omega)|^2\gamma_n^2)\, S_\alpha(\omega, t)d\omega, \tag{3.15}$$

and

$$E\left[\dot{y}_i^2(t)\right] = \int_{-\infty}^{\infty} \omega^2(|H_{i1}(\omega)|^2\gamma_1^2 + \cdots + |H_{in}(\omega)|^2\gamma_n^2)\, S_\alpha(\omega, t)d\omega. \tag{3.16}$$

Eqs.(3.15) and (3.16) hold true in the approximate quasi-stationary sense delineated earlier. Clearly, Eq.(3.14) constitutes an approximate formula for determining the MDOF system response EPS matrix at a low computational cost; thus, circumventing computationally intensive Monte Carlo simulations.

3.3. Dimension reduction and effective SDOF time-variant oscillator

Following next the system dimension reduction/decoupling approach developed in Kougioumtzoglou and Spanos (2013), an auxiliary effective SDOF LTV system corresponding to the i-th degree of freedom can be defined as

$$\ddot{y}_i + \beta_{aux,i}(t)\dot{y}_i + \omega_{aux,i}^2(t)y_i = f_i(t), \tag{3.17}$$

where the time-varying equivalent stiffness and damping elements of the effective LTV system can be determined by equating the variances of the response displacement and velocity expressed utilizing the quasi-stationary FRF of Eq.(3.17) with the corresponding ones determined via Eqs.(3.15-3.16); this yields

$$E[{y_i}^2(t)] = \int_{-\infty}^{\infty} \left(\frac{1}{(\omega_{aux,i}^2(t) - \omega^2)^2 + (\beta_{aux,i}(t)\omega)^2} \right) {\gamma_i}^2 S_\alpha(\omega, t)d\omega, \tag{3.18}$$

and

$$E\left[{\dot{y}_i}^2(t)\right] = \int_{-\infty}^{\infty} \omega^2 \left(\frac{1}{(\omega_{aux,i}^2(t) - \omega^2)^2 + (\beta_{aux,i}(t)\omega)^2} \right) {\gamma_i}^2 S_\alpha(\omega, t)d\omega. \tag{3.19}$$

Clearly, Eqs.(3.18) and (3.19) in conjunction with Eqs.(3.15) and (3.16) constitute a nonlinear system of two algebraic equations to be solved for the evaluation of the LTV system time-varying equivalent stiffness $\omega_{aux,i}^2(t)$ and damping $\beta_{aux,i}(t)$ coefficients.

3.4. Stochastic averaging treatment

Next, a stochastic averaging technique (e.g., Spanos and Lutes, 1980; Kougioumtzoglou and Spanos, 2013) is applied for casting the second-order stochastic differential equation (SDE) of Eq.(3.1) into a first-order SDE governing the evolution in time of the response amplitude $\alpha_i(t)$. In this regard, and based primarily on the assumption of light damping, it can be argued that the response $y_i(t)$ of the effective LTV system of Eq.(3.17) exhibits a pseudo-harmonic behavior described by the equations

$$y_i(t) = \alpha_i(t)\cos\left(\omega_{aux,i}(t)t + \varphi_i(t)\right), \tag{3.20}$$

and

$$\dot{y}_i(t) = -\omega_{aux,i}(t)\alpha_i(t)\sin\Big(\omega_{aux,i}(t)t + \varphi_i(t)\Big). \tag{3.21}$$

In Eq.(3.20) the response amplitude $\alpha_i(t)$ is a slowly varying function with respect to time defined as

$$\alpha_i{}^2(t) = y_i^2(t) + \left(\frac{\dot{y}_i(t)}{\omega_{aux,i}(t)}\right)^2, \tag{3.22}$$

whereas $\varphi_i(t)$ stands for the phase of the response $y_i(t)$. Further, relying on a combination of deterministic and stochastic averaging (e.g., Kougioumtzoglou and Spanos, 2013) a first-order SDE governing each and every degree-of-freedom response amplitude process $\alpha_i(t)$ takes the form

$$\dot{\alpha}_i(t) = -\frac{1}{2}\beta_{aux,i}(t)\alpha_i(t) + \frac{\pi S_F\big(\omega_{aux,i}(t),t\big)}{2\alpha_i(t)\omega_{aux,i}^2(t)} + \frac{\sqrt{\pi S_F\big(\omega_{aux,i}(t),t\big)}}{\omega_{aux,i}(t)}\,\eta(t). \tag{3.23}$$

In Eq.(3.23), $\eta(t)$ stands for a stationary, zero mean and delta correlated Gaussian white noise process of unit intensity, i.e., $E\big(\eta(t)\big) = 0$; and $E(\eta(t)\eta(t+\tau)) = \delta(\tau)$, with $\delta(\tau)$ being the Dirac delta function. Note that the response amplitude $\alpha_i(t)$ is considered to be a Markovian process. Further, associated with the above SDE (Eq.(3.23)) is the Fokker-

Planck partial differential equation governing the evolution of the non-stationary response amplitude PDF $p(\alpha_i, t)$ corresponding to the i-th degree of freedom; that is,

$$\frac{\partial}{\partial t}p(\alpha_i, t) = -\frac{\partial}{\partial \alpha_i}\left[\left(-\frac{1}{2}\beta_{aux,i}(t)\alpha_i + \frac{\pi S_f(\omega_{aux,i}(t), t)}{2\alpha_i \omega_{aux,i}^2(t)}\right)p(\alpha_i, t)\right]$$

$$+\frac{1}{2}\frac{\partial^2}{\partial {\alpha_i}^2}\left[\left(\frac{\pi S_f(\omega_{aux,i}(t), t)}{\omega_{aux,i}^2(t)}\right)p(\alpha_i, t)\right]. \quad (3.24)$$

Next, the system non-stationary response amplitude α_i is assumed to follow a time-dependent Rayleigh distribution of the form (e.g., Spanos, 1978; Spanos and Solomos, 1983; Kougioumtzoglou and Spanos, 2013)

$$p(\alpha_i, t) = \frac{\alpha_i}{c_i(t)}\exp\left(-\frac{{\alpha_i}^2}{2c_i(t)}\right). \quad (3.25)$$

where $c_i(t)$ accounts for the non-stationary response variance of the LTV system of Eq.(3.16). Substituting Eq.(3.24) into the F-P Eq.(3.23), yields a first-order ODE of the form

$$\dot{c}_i(t) = -\beta_{aux,i}(t)c_i(t) + \frac{\pi S_f\left(\omega_{aux,i}(t), t\right)}{\omega_{aux,i}^2(t)}, \quad (3.26)$$

to be solved via standard numerical integration schemes such as the Runge-Kutta; Overall, it can be readily seen that the presented approximate analytical technique not only determines the original MDOF system response amplitude PDF $p(\alpha_i, t)$ for each and every DOF in an efficient manner by circumventing computationally demanding Monte Carlo simulations, but also decouples the original system providing with effective time-varying stiffness and damping elements corresponding to the i-th DOF.

Chapter 4

Survival probability and first-passage PDF determination of nonlinear MDOF systems subject to evolutionary stochastic excitations

4.1 Preliminary remarks

Excitations acting upon structural systems such as wind, wave, and seismic loads commonly exhibit evolutionary features. For instance, structural systems in seismic prone areas are subject to stochastic excitations that exhibit strong variability in both the intensity and the frequency content. This fact necessitates the representation of this class of structural loads by non-stationary stochastic processes. Further, structural systems under severe excitations can exhibit significant nonlinear behavior of the hysteretic kind. Thus, of particular interest to the structural dynamics community is the development of techniques for determining the response and assessing the reliability of nonlinear/hysteretic systems subject to evolutionary stochastic excitations (e.g., Soon and Grigoriu, 1993; Roberts and Spanos, 2003; Li and Chen, 2009).

Further, in engineering dynamics, the evaluation of the probability that the system response stays within prescribed limits for a specified time interval is advantageous for reliability based system design applications. In this regard, the first-passage problem, that is, the determination of the above time-variant probability known as survival probability, has been a persistent challenge in the field of stochastic dynamics for many decades.

In general, although the SDOF oscillator has been used extensively to model a wide range of systems of engineering interest, in many cases the complexity of the system and/or the requirement for enhanced accuracy necessitate modeling of the system as a

MDOF one. In this regard, note that for the first-passage problem, analytical exact solutions have not been possible even for the case of a SDOF linear oscillator under stationary excitation. Clearly, the level of difficulty rises as the number of DOF increases, or complex nonlinear behaviors are considered.

Monte Carlo simulation techniques are among the most potent tools for assessing the reliability of a system (e.g. Schueller et al., 2004). Nevertheless, there are cases where the computational cost of these techniques can be prohibitive, especially when large-scale complex systems are considered; thus, rendering the development of alternative efficient approximate analytical/numerical techniques for addressing the first-passage problem necessary. Indicatively, one of the early approaches, restricted to linear systems, relies on the knowledge of the mean up-crossing rates and on Poisson distribution based approximations (e.g., Corotis et al., 1972; Vanmarcke, 1975; Barbato and Conte, 2001). Further attempts to address the first-passage problem range from analytical ones (e.g., Kovaleva, 2009) to numerical ones (e.g., Solomos and Spanos, 1983). Furthermore, techniques based on the concepts of the numerical path integral (e.g., Iourtchenko et al., 2006; Naess et al., 2011; Kougioumtzoglou and Spanos, 2013; Kougioumtzoglou and Spanos, 2014), of the probability density evolution (e.g., Li and Chen, 2009), or of stochastic averaging/linearization (e.g. Spanos and Kougioumtzoglou, 2014) constitute some of the more recent approaches.

In this chapter, an approximate analytical technique for determining the survival probability and first-passage PDF of nonlinear MDOF structural systems subject to an evolutionary stochastic excitation vector is developed. The proposed technique can be construed as a two-stage approach. First, relying on statistical linearization and utilizing a dimension reduction approach the nonlinear n-degree-of-freedom system is decoupled and cast into (n) effective SDOF LTV oscillators corresponding to each and every DOF of the original MDOF system. Second, utilizing the effective SDOF LTV oscillator time-varying stiffness and damping elements in conjunction with a stochastic averaging treatment of the problem, the MDOF system survival probability and first-passage PDF are determined at a low computational cost.

The remainder of this chapter is organized as follows: In section 4.2 the mathematical formulation of the problem is given. Specifically, in section 4.2.1 the statistical linearization based dimension reduction approach delineated in chapter 2 is appropriate modified to facilitate the first stage of the developed technique. Next, in section 4.2.2 it is shown that the nonlinear MDOF system non-stationary marginal, transition and the joint response amplitude PDFs can be approximated by closed-form expressions. Further, section 4.3 provides analytical closed-form expressions for the time-dependent survival probability of the nonlinear MDOF structural system as well as for the corresponding first-passage PDF. In section 4.4, illustrative examples comprising a 3-DOF structural system exhibiting Bouc-Wen hysteresis and subject to evolutionary stochastic earthquake excitations are considered. Pertinent MCS data demonstrate the reliability of the proposed technique.

4.2 Mathematical formulation

In this section, the mathematical formulation of the approximate analytical technique for determining the survival probability and first-passage PDF of nonlinear MDOF structural systems subject to an evolutionary stochastic excitation vector is presented.

4.2.1 Statistical linearization based dimension reduction approach

An n-degree-of-freedom nonlinear structural system governed by the Eq.(3.1) is considered herein. It is noteworthy that the first stage of the proposed technique lies on the utilization of the approximate dimension reduction/decoupling approach analytically presented in chapter 3. Note in passing that instead of the frequency domain Wiener-Khinchin relationship of Eq.(3.9), a state-variable formulation can be adopted yielding a system of differential equations of the Lyapunov kind (e.g., Gajic and Qureshi, 1995; Roberts and Spanos, 2003) for the system response covariance matrix. Nevertheless, although a pre-filtering treatment can be applied for considering non-stationary stochastic excitation processes of the separable kind (Roberts and Spanos, 2003), excitations

possessing a non-separable EPS (e.g. realistic cases of earthquake excitations) cannot be accounted for, at least in a straightforward manner.

Further, associated with the SDE of Eq.(3.23) is the Fokker-Planck (F-P) partial differential equation governing the response amplitude transition PDF of the Markovian process α_i; that is,

$$\frac{\partial}{\partial t}p(\alpha_{i,2}, t_2|\alpha_{i,1}, t_1) = -\frac{\partial}{\partial \alpha_i}\left[\left(-\frac{1}{2}\beta_{aux,i}(t)\alpha_i + \frac{\pi S_F(\omega_{aux,i}(t), t)}{2\alpha_i \omega_{aux,i}^2(t)}\right)p(\alpha_{i,2}, t_2|\alpha_{i,1}, t_1)\right]$$

$$+\frac{1}{2}\frac{\partial^2}{\partial {\alpha_i}^2}\left[\left(\frac{\pi S_F(\omega_{aux,i}(t), t)}{\omega_{aux,i}^2(t)}\right)p(\alpha_{i,2}, t_2|\alpha_{i,1}, t_1)\right]. \quad (4.1)$$

Specifically, considering the case $p(\alpha_{i,2}, t_2|\alpha_{i,1} = 0, t_1 = 0) = p(\alpha_i, t)$, the marginal system response amplitude PDF has been shown to follow the time-dependent Rayleigh distribution of the form of Eq.(3.25).

4.2.2 Transition and Joint Nonlinear System Response PDFs

Taking into account that no change of state can occur if the transition time is zero i.e., $p(\alpha_{i,2}, t_1|\alpha_{i,1}, t_1) = \delta(\alpha_{i,2} - \alpha_{i,1})$ and following a similar analysis as the one in Spanos and Solomos (1983), the transition response amplitude PDF $p(\alpha_{i,2}, t_2|\alpha_{i,1}, t_1)$ for the i-th degree-of-freedom of the original MDOF system is assumed to be of the form

$$p(\alpha_{i,2}, t_2|\alpha_{i,1}, t_1) = \frac{\alpha_{i,2}}{c_i(t_1, t_2)}\exp\left(-\frac{\alpha_{i,2}^2 + {h_i}^2(t_1, t_2)}{2c_i(t_1, t_2)}\right)I_0\left(\frac{\alpha_{i,2}h_i(t_1, t_2)}{c_i(t_1, t_2)}\right), \quad (4.2)$$

where $c_i(t_1, t_2)$ and $h_i(t_1, t_2)$ are functions to be determined and I_0 represents the modified Bessel function of the first kind and of zero order. Next,substituting Eq.(4.2) into the F-P Eq.(4.1) and manipulating (see also Spanos and Solomos, 1983; Solomos and Spanos, 1983; Spanos and Kougioumtzoglou, 2014) yields the linear first-order ODEs

$$\frac{dc_i(t_1, t_2)}{dt_2} + \beta_{aux,i}(c_i(t_1, t_2))c_i(t_1, t_2) - \frac{\pi S_F(\omega_{aux,i}(c_i(t_1, t_2)), t_2)}{\omega_{aux,i}^2(c_i(t_1, t_2))} = 0, \quad (4.3)$$

and

$$\frac{dh_i(t_1,t_2)}{dt_2}+\frac{1}{2}\beta_{aux,i}\big(h_i(t_1,t_2)\big)h_i(t_1,t_2)=0. \tag{4.4}$$

Relying on the assumption that the equivalent damping and stiffness coefficients of the effective LTV system follow a slowly varying with respect to time behavior, the following approximations over a small time interval $[t_{i,j-1},t_{i,j}]$ are introduced; i.e., $\beta_{aux,i}(t)=\beta_{aux,i}(t_{i,j-1})$ and $\omega_{aux,i}(t)=\omega_{aux,i}(t_{i,j-1})$ for $t\in[t_{i,j-1},t_{i,j}]$. Next, based on the slowly varying with time behavior of the EPS, $S_F(\omega,t)$ is also treated as a constant over the interval $[t_{i,j-1},t_{i,j}]$. Further, based on the above assumptions, introducing the variable $\tau_{i,j}=t_{i,j}-t_{i,j-1}$, and applying a first-order Taylor expansion around point $\tau_{i,j}=0$, Eqs.(4.3-4.4) become

$$c_i(t_{i,j-1},t_{i,j})=\frac{\pi S_F\big(\omega_{aux,i}(t_{i,j-1}),t_{i,j-1}\big)}{\omega_{aux,i}^2(t_{i,j-1})}\tau_{i,j}, \tag{4.5}$$

and

$$h_i(t_{i,j-1},t_{i,j})=\alpha_{i,j-1}\sqrt{1-\beta_{aux,i}(t_{i,j-1})\tau_{i,j}}. \tag{4.6}$$

Furthermore, considering Eqs.(3.26) and (4.5) and applying a first-order Taylor expansion for the response variance $c_i(t)$ around point $t=t_{i,j-1}$ yields

$$c_i(t_{i,j-1},t_{i,j})=c_i(t_{i,j})-c_i(t_{i,j-1})\big(1-\beta_{aux,i}(t_{i,j-1})\tau_{i,j}\big). \tag{4.7}$$

Relying next on the Markovian assumption for the process α_i, the joint-response amplitude PDF $p(\alpha_{i,j-1},t_{j-1};\alpha_{i,j},t_j)$ is given by

$$p(\alpha_{i,j-1},t_{j-1};\alpha_{i,j},t_j)=p(\alpha_{i,j-1},t_{j-1})p(\alpha_{i,j},t_j|\alpha_{i,j-1},t_{j-1}). \tag{4.8}$$

Utilizing Eqs.(3.25) and (4.2), Eq.(4.8) becomes

$$p(\alpha_{i,j-1},t_{j-1};\alpha_{i,j},t_j)=\frac{\alpha_{i,j-1}\alpha_{i,j}}{c_i(t_{j-1})c_i(t_{j-1},t_j)}\times$$

$$\exp\left(-\frac{\alpha_{i,j}^2 c_i(t_{j-1}) + \alpha_{i,j-1}^2 c_i(t_{j-1},t_j) + {h_i}^2(t_{j-1},t_j)c_i(t_{j-1})}{2c_i(t_{j-1})c_i(t_{j-1},t_j)}\right)\ldots$$

$$I_0\left(\frac{\alpha_{i,j}h_i(t_{j-1},t_j)}{c_i(t_{j-1},t_j)}\right). \tag{4.9}$$

Further, setting

$$r_{i,j}^2 = \frac{c_i(t_{i,j-1})}{c_i(t_{i,j})}(1-\beta_{aux,i}(t_{i,j-1})\tau_{i,j}), \tag{4.10}$$

Eq.(4.7) yields

$$c_i(t_{i,j-1},t_{i,j}) = c_i(t_{i,j})(1-r_{i,j}^2). \tag{4.11}$$

Next, considering Eqs.(4.5-4.6) and Eqs.(4.10-4.11), the joint response amplitude PDF $p(\alpha_{i,j-1},t_{i,j-1};\alpha_{i,j},t_{i,j})$ of Eq.(4.9) is given in the form

$$p(\alpha_{i,j-1},t_{i,j-1};\alpha_{i,j},t_{i,j}) = \frac{\alpha_{i,j-1}\alpha_{i,j}}{c_i(t_{i,j-1})c_i(t_{i,j})(1-r_{i,j}^2)}\ldots$$

$$\exp\left(-\frac{\alpha_{i,j}^2 c_i(t_{i,j-1}) + \alpha_{i,j-1}^2 c_i(t_{i,j})}{2c_i(t_{i,j-1})c_i(t_{i,j})(1-r_{i,j}^2)}\right) I_0\left(\frac{\alpha_{i,j}\alpha_{i,j-1}r_{i,j}}{\sqrt{c_i(t_{i,j-1})c_i(t_{i,j})}(1-r_{i,j}^2)}\right). \tag{4.12}$$

4.3 Nonlinear MDOF system reliability assessment

In this section the approximate analytical technique developed in Spanos and Kougioumtzoglou (2014) for nonlinear SDOF survival probability determination is generalized herein to account for MDOF systems by utilizing the statistical linearization based dimension reduction approach.

In this regard, the survival probability P_i^B is defined as the probability that the system response amplitude α_i stays below a prescribed barrier B over the time interval $[0,T]$,

given that $\alpha_i(t=0) < B$. Further, the first-passage PDF $p_i^B(T)$ and the survival probability P_i^B are related according to the expression

$$p_i^B(T) = -\frac{dP_i^B(T)}{dT}. \tag{4.13}$$

Next, adopting the discretization scheme employed in Solomos and Spanos (1983) yields intervals of the form

$$[t_{i,j-1}, t_{i,j}], \quad j = 1,2,\dots,m, \quad t_{i,0} = 0, \quad t_{i,m} = T, \quad t_{i,j} - t_{i,j-1} = \frac{T_{aux,i}(t_{i,j-1})}{2}, \tag{4.14}$$

where the response amplitude α_i is assumed to be constant over $[t_{i,j-1}, t_{i,j}]$ due to its slowly varying in time behavior. In Eq.(4.14) $T_{aux,i}$ represents the effective LTV system equivalent natural period given by

$$T_{aux,i}(t) = \frac{2\pi}{\omega_{aux,i}(t)}. \tag{4.15}$$

Note in passing that a smaller time interval can be chosen if higher accuracy is required. In this regard, the survival probability P_i^B is assumed to have a constant value over the same time interval as well. Obviously, the survival probability is given by

$$P_i^B(T) = \prod_{j=1}^{m} [1 - F_{i,j}^B], \tag{4.16}$$

where $F_{i,j}^B$ is defined as the probability that the response amplitude α_i will exceed the prescribed barrier B over the time interval $[t_{i,j-1}, t_{i,j}]$, given that no crossings have occurred prior to time $t_{i,j-1}$. Next, invoking the Markovian property of the response amplitude α_i, one gets

$$F_{i,j}^B = \frac{\text{Prob}[\alpha_i(t_{i,j}) \geq B \cap \alpha_i(t_{i,j-1}) < B]}{\text{Prob}[\alpha_i(t_{i,j-1}) < B]} = \frac{H_{i,j-1,j}^B}{H_{i,j-1}^B}, \tag{4.17}$$

where $\cap$ denotes the intersection symbol. Utilizing Eq.(3.25) $H_{i,j-1}^B$ can be determined analytically in a straightforward manner; that is,

$$H_{i,j-1}^{B} = \int_{0}^{B} p\left(\alpha_{i,j-1}, t_{i,j-1}\right) d\alpha_{i,j-1} = 1 - \exp\left(-\frac{B^2}{2c_i(t_{i,j-1})}\right), \tag{4.18}$$

whereas $H_{i,j-1,j}^{B}$ is defined as a double integral of the form

$$H_{i,j-1,j}^{B} = \int_{B}^{\infty} d\alpha_{i,j} \int_{0}^{B} p\left(\alpha_{i,j-1}, t_{i,j-1}; \alpha_{i,j}, t_{i,j}\right) d\alpha_{i,j-1}. \tag{4.19}$$

Further, taking into account Eq.(4.12) and expanding the Bessel function $I_0(x)$ in the form (e.g., Abramowitz and Stegun, 1970)

$$I_0(x) = \sum_{k=0}^{\infty} \frac{(x/2)^{2k}}{k!\,\Gamma(\kappa + 1)}, \tag{4.20}$$

analytical treatment of the involved integrals is possible yielding

$$H_{i,j-1,j}^{B} = A_{i,0} + \sum_{n=1}^{N} A_{i,n}, \tag{4.21}$$

where

$$A_{i,0} = \exp\left(\frac{-B^2}{2c_i\left(t_{i,j}\right)\left(1 - r_{i,j}^2\right)}\right)\left(1 - \exp\left(\frac{-B^2}{2c_i\left(t_{i,j-1}\right)\left(1 - r_{i,j}^2\right)}\right)\right)\left(1 - r_{i,j}^2\right), \tag{4.22}$$

and

$$A_{i,n} = \frac{r_{i,j}^{2n}}{\left(c_i\left(t_{i,j-1}\right)c_i\left(t_{i,j}\right)\right)^{n+1}\left(1 - r_{i,j}^2\right)^{2n+1}\prod_{n=1}^{N}(2n)^2} L_{i,n}, \tag{4.23}$$

with

$$L_{i,n} = 4^n c_i(t_{i,j-1})^{n+1} c_i(t_{i,j})(1-r_{i,j}^2)^{n+2}\left(\Gamma_i\left[1+n, \frac{B^2}{2c_i(t_{i,j-1})(1-r_{i,j}^2)}\right]\right.$$
$$\left. - \Gamma_i[1+n,0]\right)\left(-\left(c_i(t_{i,j})(1-r_{i,j}^2)\right)^n \Gamma_i[1+n]\right.$$
$$+\left(\frac{B^2}{c_i(t_{i,j})(1-r_{i,j}^2)}\right)^{-n}\left(\Gamma_i[1+n]\right.$$
$$\left.\left. - \Gamma_i\left[1+n, \frac{B^2}{2c_i(t_{i,j})(1-r_{i,j}^2)}\right]\right)B^{2n}\right). \qquad (4.24)$$

In Eq.(4.24) $\Gamma_i[\gamma, z]$ represents the incomplete Gamma function defined as $\Gamma_i[\gamma, z] = \int_z^\infty t^{\gamma-1}e^{-t}dt$.

Concisely, the developed technique comprises the following steps:

i. Determination of the MDOF system non-stationary response covariance matrix (Eqs.(3.11) and (3.14)) via a statistical linearization treatment of the problem.

ii. Determination of the equivalent linear time-varying elements $\beta_{aux,i}(t)$ and $\omega_{aux,i}(t)$ by solving the system of algebraic equations (Eqs.(3.18-3.19)).

iii. Determination of $c_i(t)$ via numerically integrating the first-order ODE Eq.(3.26).

iv. Determination of the equivalent natural period $T_{aux,i}(t)$ (Eq.(4.15)) and discretization of the time domain via Eq.(4.14).

v. Determination of the parameters $H_{i,j-1}^B$ and $H_{i,j-1,j}^B$ via Eqs.(4.18) and (4.19).

vi. Determination of the survival probability $P_i^B(T)$ via Eq.(4.16) and of the corresponding first-passage PDF $p_i^B(T)$ via Eq.(4.13).

4.4 Numerical applications

4.4.1 MDOF Bouc-Wen hysteretic building structure

In this section, a nonlinear three-degree-of-freedom structural system following the Bouc-Wen hysteretic model (e.g., Wen, 1980; Ikhouane and Rodellar, 2007) subject to evolutionary stochastic earthquake excitation is considered to demonstrate the reliability of the technique. A side view of the MDOF building structure can be seen in Fig.(4.1).

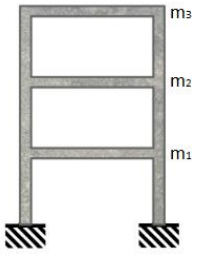

Figure 4.1. Hysteretic three-DOF structural system.

The survival probabilities and the first-passage PDFs obtained via the developed approximate technique are compared with survival probability and first-passage PDF estimates obtained via pertinent Monte Carlo simulations (10,000 realizations). The Monte Carlo simulations were conducted by utilizing a spectral representation methodology; additional details can be found in Shinozuka and Deodatis (1991).

Further, a standard fourth-order Runge-Kutta numerical integration scheme is employed for solving the nonlinear system differential equation of motion (Eq.(3.1)), whereas the barrier level B is expressed as a fraction λ of the maximum over time and over DOF value of the non-stationary response displacement standard deviation., i.e. $B = \lambda \max_{i \text{ and } t}(\sqrt{c_i(t)})$. Considering inter-story drifts y_i as well as the additional states z_i introduced by the Bouc-Wen model, the 3-DOF nonlinear structural system is governed by Eq.(3.1) where

$$\mathbf{y}^{\mathrm{T}} = (\mathrm{y}_1\ \mathrm{y}_2\ \mathrm{y}_3\ \mathrm{z}_1\ \mathrm{z}_2\ \mathrm{z}_3), \tag{4.25}$$

$$\mathbf{M} = \begin{bmatrix} \mathbf{M_{11}} & \mathbf{M_{12}} \\ \mathbf{M_{21}} & \mathbf{M_{22}} \end{bmatrix}, \tag{4.26}$$

where

$$\mathbf{M_{11}} = \begin{bmatrix} \mathrm{m}_1 & 0 & 0 \\ \mathrm{m}_2 & \mathrm{m}_2 & 0 \\ \mathrm{m}_3 & \mathrm{m}_3 & \mathrm{m}_3 \end{bmatrix}, \tag{4.27}$$

and

$$\mathbf{M_{12}} = \mathbf{M_{21}} = \mathbf{M_{22}} = \begin{bmatrix} 0 & 0 & 0 \\ 0 & 0 & 0 \\ 0 & 0 & 0 \end{bmatrix}. \tag{4.28}$$

Further,

$$\mathbf{K} = \begin{bmatrix} \mathbf{K_{11}} & \mathbf{K_{12}} \\ \mathbf{K_{21}} & \mathbf{K_{22}} \end{bmatrix}, \tag{4.29}$$

where

$$\mathbf{K_{11}} = \begin{bmatrix} \mathrm{ak}_1 & -\mathrm{ak}_2 & 0 \\ 0 & \mathrm{ak}_2 & -\mathrm{ak}_3 \\ 0 & 0 & \mathrm{ak}_3 \end{bmatrix}, \tag{4.30}$$

$$\mathbf{K_{12}} = \begin{bmatrix} (1-\mathrm{a})\mathrm{k}_1 & -(1-\mathrm{a})\mathrm{k}_2 & 0 \\ 0 & (1-\mathrm{a})\mathrm{k}_2 & -(1-\mathrm{a})\mathrm{k}_3 \\ 0 & 0 & (1-\mathrm{a})\mathrm{k}_3 \end{bmatrix} \tag{4.31}$$

and

$$\mathbf{K_{21}} = \mathbf{K_{22}} = \begin{bmatrix} 0 & 0 & 0 \\ 0 & 0 & 0 \\ 0 & 0 & 0 \end{bmatrix}. \tag{4.32}$$

In Eqs.(4.30-4.31) a stands for the rigidity ratio which can be viewed as a form of post-yield to pre-yield stiffness ratio ($\mathrm{a} = 1$ corresponds to the linear system). Further, the

damping matrix of the structural system $\mathbf{C}$ is assumed to be proportional to the stiffness matrix; that is,

$$\mathbf{C} = \begin{bmatrix} \mathbf{C_{11}} & \mathbf{C_{12}} \\ \mathbf{C_{21}} & \mathbf{C_{22}} \end{bmatrix}, \tag{4.33}$$

where

$$\mathbf{C_{11}} = c_0 \cdot \mathbf{K_{11}}, \tag{4.34}$$

$$\mathbf{C_{12}} = \mathbf{C_{21}} = \begin{bmatrix} 0 & 0 & 0 \\ 0 & 0 & 0 \\ 0 & 0 & 0 \end{bmatrix}, \tag{4.35}$$

and

$$\mathbf{C_{22}} = \begin{bmatrix} 1 & 0 & 0 \\ 0 & 1 & 0 \\ 0 & 0 & 1 \end{bmatrix}. \tag{4.36}$$

In Eq.(4.34) c_0 is taken equal to 0.2×10^{-2}. For the specific example $\boldsymbol{\gamma} = [m_i]$, and the loading vector becomes

$$\mathbf{F}(t)^T = (f_1(t)\ f_2(t)\ f_3(t)\ 0\ 0\ 0). \tag{4.37}$$

Further,

$$\mathbf{g}(\mathbf{y}, \dot{\mathbf{y}}, t)^{\mathbf{T}} = \big(0\ 0\ 0\ -g_1(\dot{y}_1, z_1, t)\ -g_2(\dot{y}_2, z_2, t)\ -g_3(\dot{y}_3, z_3, t)\big). \tag{4.38}$$

In the Bouc-Wen model the additional state z_i is associated with the displacement y_i via the equation

$$\dot{z}_i = g_i(\dot{y}_i, z_i, t), \tag{4.39}$$

where

$$g_i(\dot{y}_i, z_i, t) = -\gamma|\dot{y}_i|z_i|z_i|^{n-1} - \beta\dot{y}_i|z_i|^n + A\dot{y}_i. \tag{4.40}$$

The parameters γ, β, A and n are capable of representing a wide range of hysteresis loops (e.g., Wen, 1980; Song and Der Kiureghian, 2006; Ikhouane and Rodellar, 2007). In this example the values $a = 0.15$, $\beta = \gamma = 0.5$, $n = 1$ and $A = 1$ are considered. The

equivalent linear matrices take the form (e.g., Soong and Grigoriu, 1993; Roberts and Spanos, 2003; Li and Chen, 2009)

$$\mathbf{C_{eq}} = \begin{bmatrix} \mathbf{C_{eq11}} & \mathbf{C_{eq12}} \\ \mathbf{C_{eq21}} & \mathbf{C_{eq22}} \end{bmatrix}, \tag{4.41}$$

where

$$\mathbf{C_{eq11}} = \mathbf{C_{eq12}} = \mathbf{C_{eq22}} = \begin{bmatrix} 0 & 0 & 0 \\ 0 & 0 & 0 \\ 0 & 0 & 0 \end{bmatrix}, \tag{4.42}$$

and

$$\mathbf{C_{eq21}} = \begin{bmatrix} c_{eq1} & 0 & 0 \\ 0 & c_{eq2} & 0 \\ 0 & 0 & c_{eq3} \end{bmatrix}. \tag{4.43}$$

Further,

$$\mathbf{K_{eq}} = \begin{bmatrix} \mathbf{K_{eq11}} & \mathbf{K_{eq12}} \\ \mathbf{K_{eq21}} & \mathbf{K_{eq22}} \end{bmatrix}, \tag{4.44}$$

where

$$\mathbf{K_{eq11}} = \mathbf{K_{eq12}} = \mathbf{K_{eq21}} = \begin{bmatrix} 0 & 0 & 0 \\ 0 & 0 & 0 \\ 0 & 0 & 0 \end{bmatrix}, \tag{4.45}$$

and

$$\mathbf{K_{eq22}} = \begin{bmatrix} k_{eq1} & 0 & 0 \\ 0 & k_{eq2} & 0 \\ 0 & 0 & k_{eq3} \end{bmatrix}. \tag{4.46}$$

The elements c_{eq_i} and k_{eq_i}in Eqs.(4.43) and (4.46) are given by the expressions

$$c_{eq_i} = \sqrt{\frac{2}{\pi}}\left[\gamma \frac{E(\dot{y}_i z_i)}{\sqrt{E(\dot{y}_i{}^2)}} + \beta\sqrt{E(z_i{}^2)}\right] - A, \tag{4.47}$$

and

$$k_{eq_i} = \sqrt{\frac{2}{\pi}}\left[\gamma\sqrt{E(\dot{y}_i{}^2)} + \beta\frac{E(\dot{y}_i z_i)}{\sqrt{E(z_i{}^2)}}\right], \tag{4.48}$$

respectively.

An interesting development can be found in Song and Der Kiureghian (2006) where a flexible model of the Bouc–Wen class is proposed for use in nonlinear random vibration analysis by the equivalent linearization method. The model is characterized by the ability to describe highly asymmetric hysteresis loops in a straightforward manner. In this setting, closed-form expressions are derived also in this case for the coefficients of the equivalent linear system in terms of the second moments of the response quantities.

4.4.2 Hysteretic 3-DOF structural system under evolutionary stochastic excitation of the separable form

In this example, the excitation EPS $S_{\ddot{\alpha}_g}(\omega, t)$ takes the form of Eq.(2.5) where $S_{CP}(\omega)$ represents the widely used in earthquake engineering applications Clough-Penzien power spectrum (e.g., Clough and Penzien, 1993) and $g(t)$ denotes the time-modulating envelope function given in Eq.(2.4). The parameters values used are $S_0 = 20\ m^2/s^3$, $\xi_g = 0.7$, $\omega_g = 2\ rad/s$, $\xi_f = 0.6$, $\omega_f = 12.5\ rad/s$, $b_1 = 0.1$ and $b_2 = 0.3$. The total duration of the excitation is 20 seconds. Further, the hysteretic 3-DOF structural system has the following properties $m_1 = 2.0615 \times 10^5$ kg, $m_2 = 2.0559 \times 10^5$ kg, $m_3 = 2.0261 \times 10^5$ kg, $k_1 = 3.9668 \times 10^8$ N/m, $k_2 = 3.5007 \times 10^8$ N/m and $k_3 = 2.6927 \times 10^8$ N/m.

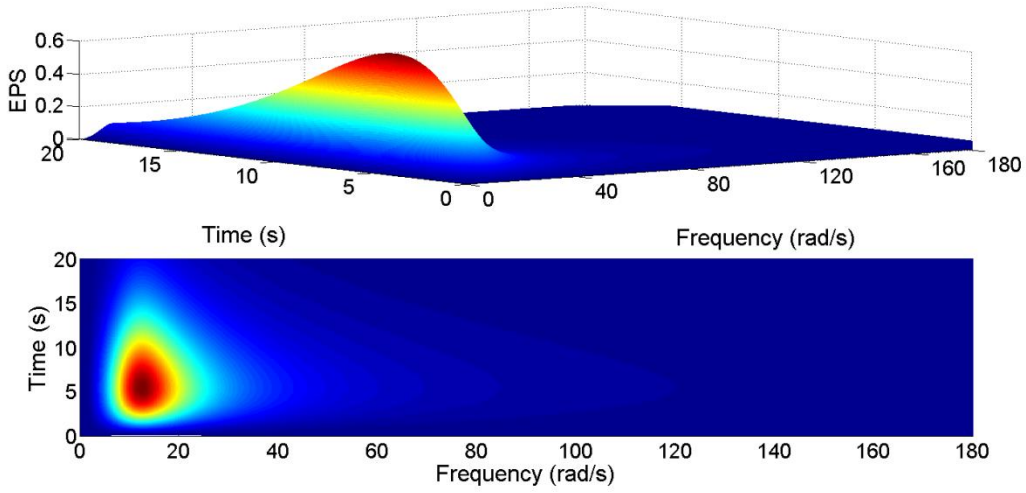

Figure 4.2. Non-stationary separable excitation power spectrum $S_{\ddot{\alpha}_g}(\omega, t)$.

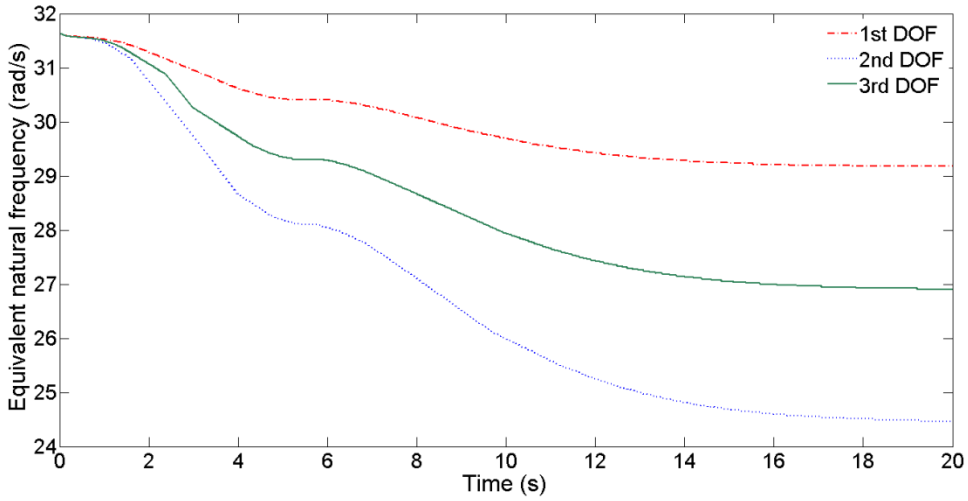

Figure 4.3. Time-varying equivalent natural frequency $\omega_{aux,i}(t)$ of the effective LTV system.

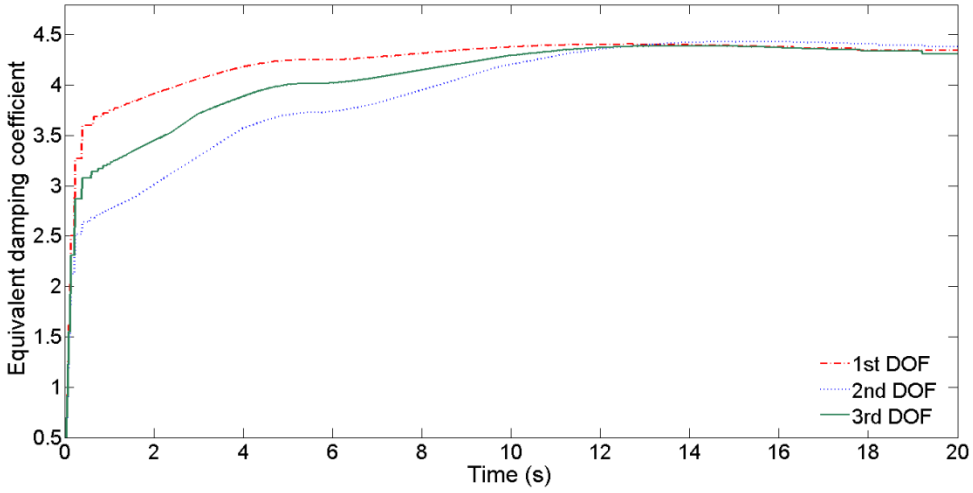

Figure 4.4. Time-varying equivalent damping coefficient $\beta_{aux,i}(t)$ of the effective LTV system.

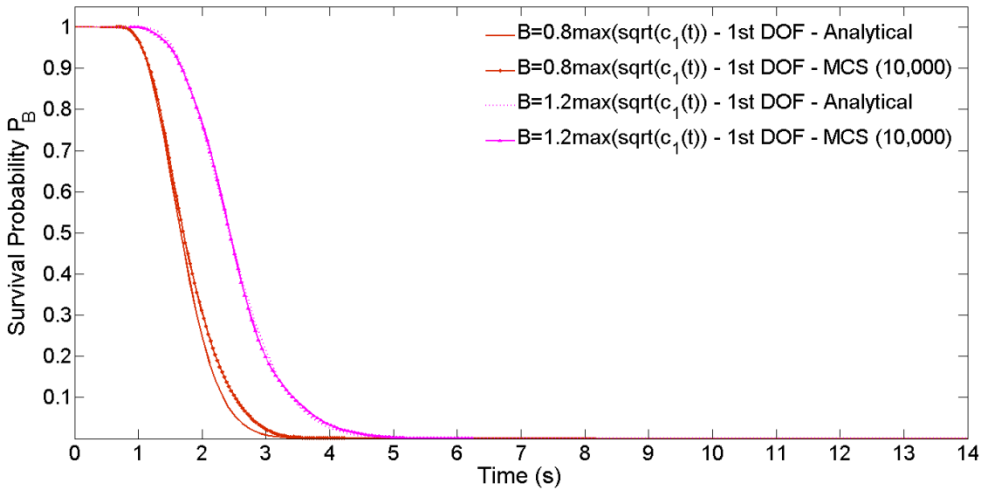

Figure 4.5. Survival probability for various values of the parameter λ for the first DOF; comparisons with MCS (10,000 realizations).

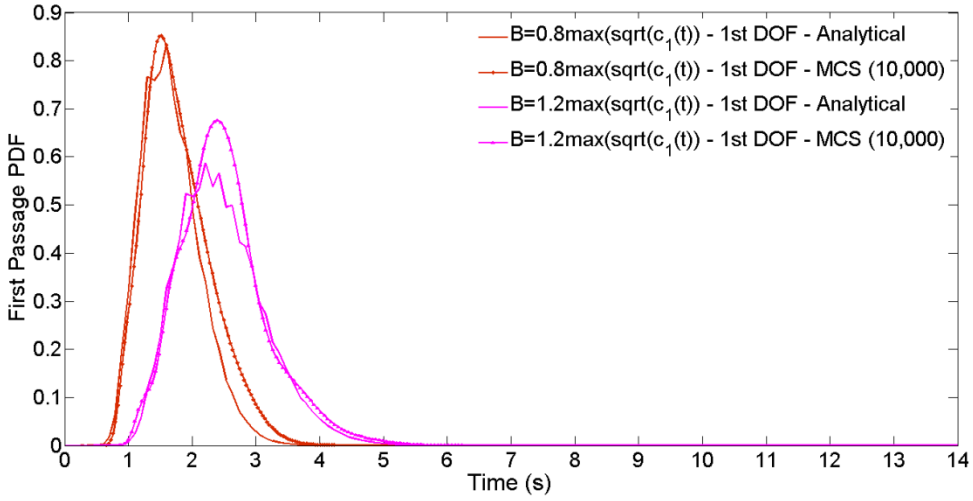

Figure 4.6. First-passage PDF for various values of the parameter λ for the first DOF; comparisons with MCS (10,000 realizations).

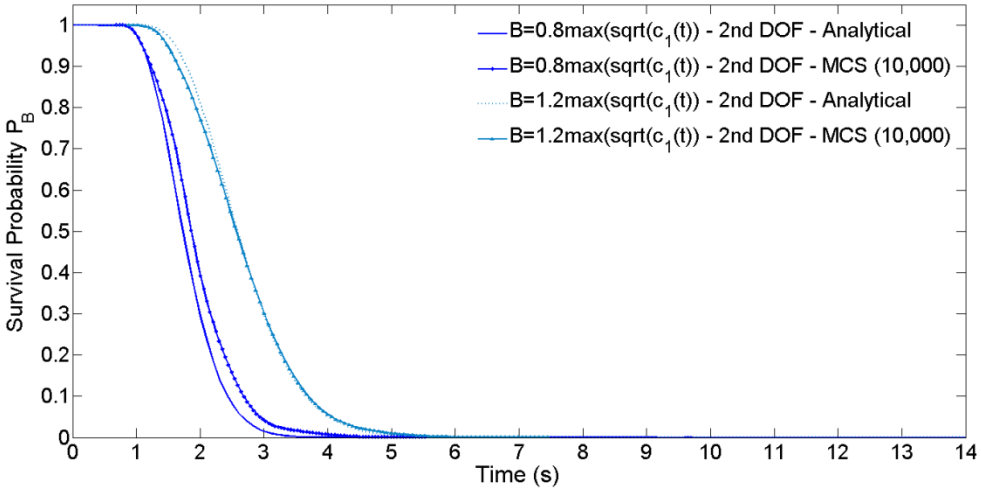

Figure 4.7. Survival probability for various values of the parameter λ for the second DOF; comparisons with MCS (10,000 realizations).

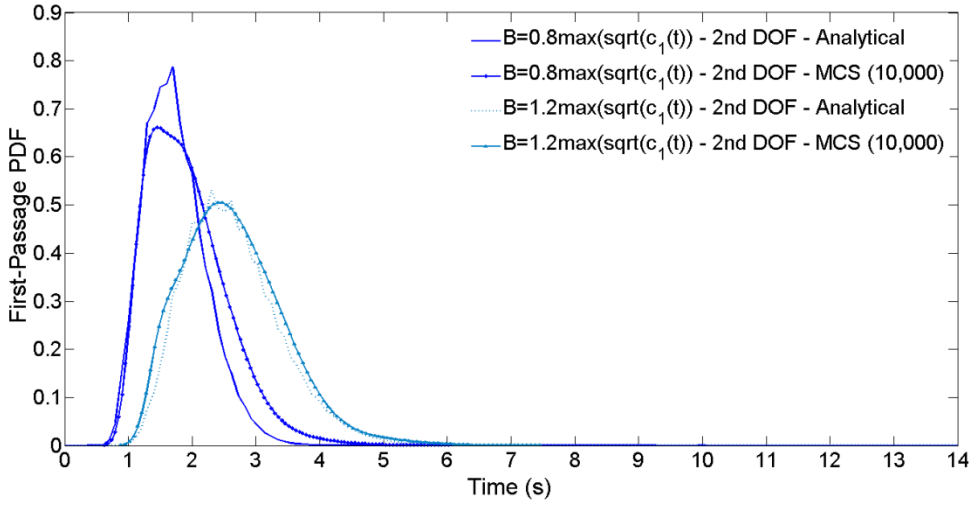

Figure 4.8. First-passage PDF for various values of the parameter λ for the second DOF; comparisons with MCS (10,000 realizations).

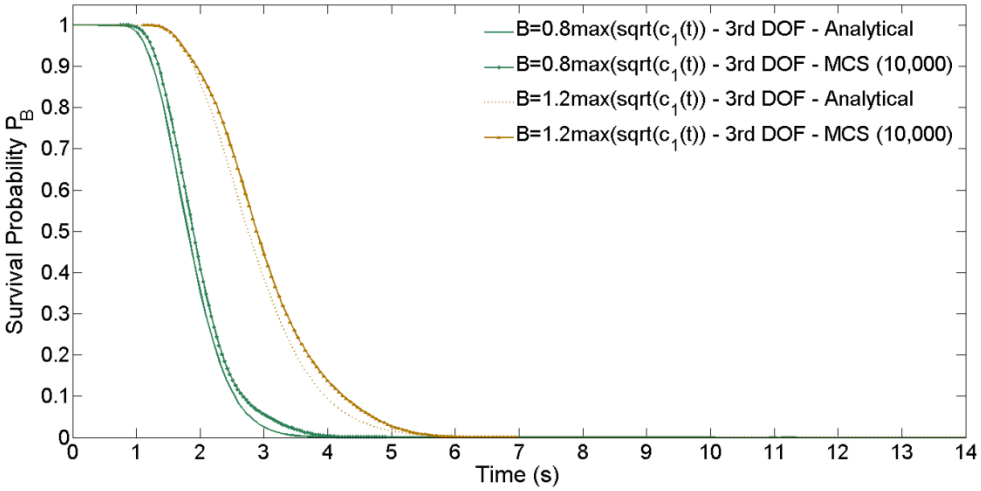

Figure 4.9. Survival probability for various values of the parameter λ for the third DOF; comparisons with MCS (10,000 realizations).

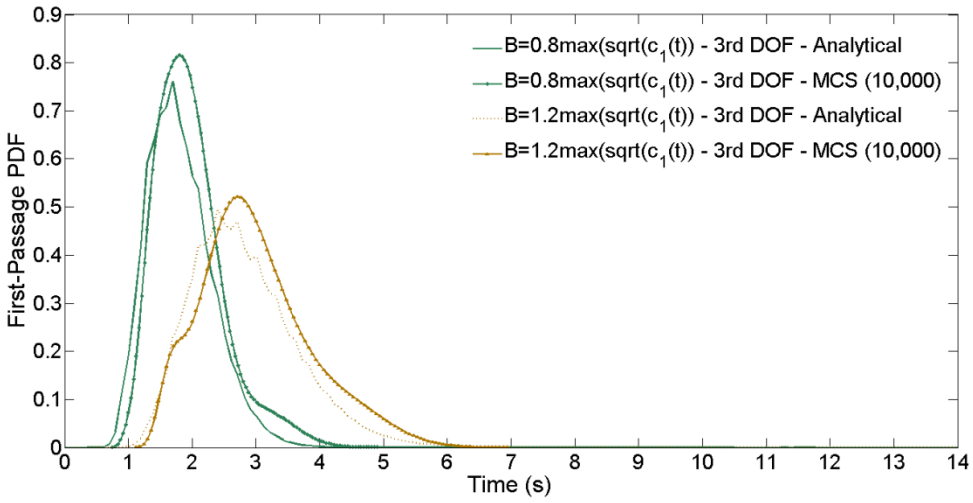

Figure 4.10. First-passage PDF for various values of the parameter λ for the third DOF; comparisons with MCS (10,000 realizations).

In Figs.(4.3) and (4.4) the equivalent time-varying natural frequency $\omega_{aux,i}(t)$ and the damping element $\beta_{aux,i}(t)$ corresponding to each DOF are plotted, respectively. Note that the hysteretic behavior of the structural system is captured by the decreasing with time trend of the stiffness element, as well as the increasing with time trend of the damping element. Further, in Figs.(4.5) and (4.6) the survival probabilities $P_i^B(T)$ and the corresponding first-passage PDFs $p_i^B(T)$ for the first DOF of the hysteretic MDOF structural system are plotted for various barrier levels, respectively. The value $N = 30$ is chosen regarding the number of terms to be included in Eq.(4.21). Comparisons between the analytical approximate technique and MCS data (10,000 realizations) demonstrate a satisfactory degree of agreement. Note that the irregular/non-smooth shape of the approximate technique based first-passage PDFs is due to the differentiation of the survival probability (Eq.(4.13)). In this regard, the survival probability Eq.(4.16) is assumed to have constant values over the time intervals $[t_{i,j-1}, t_{i,j}]$ resulting in a non-smooth representation. Obviously, the level of non-smoothness increases when differentiation takes place. Furthermore, in Figs. (4.7), (4.8), (4.9) and (4.10) the survival probabilities $P_i^B(T)$ as well as the associated first-passage PDFs $p_i^B(T)$ corresponding to

the second and third DOF of the system are plotted for various barrier levels. Comparisons with MCS demonstrate a satisfactory degree of accuracy for these cases as well.

4.4.3 Hysteretic 3-DOF structural system under evolutionary stochastic excitation of the non-separable form

The excitation EPS $S_{\ddot{\alpha}_g}(\omega, t)$ is assumed to have the non-separable form given in Eq.(2.6) where S_0 and b are taken to be equal to $10\ m^2/s^3$ and 0.5 respectively. This spectrum comprises some of the main characteristics of seismic shaking, such as decreasing of the dominant frequency with respect to time (e.g., Liu, 1970; Spanos and Solomos, 1983). Further, the hysteretic 3-DOF structural system parameters take the values $m_1 = 1.0240 \times 10^5$ kg, $m_2 = 1.0225 \times 10^5$ kg, $m_3 = 1.0105 \times 10^5$ kg, $k_1 = 5.6889 \times 10^7 N/m$, $k_2 = 5.6889 \times 10^7 N/m$ and $k_3 = 4.3945 \times 10^7 N/m$.

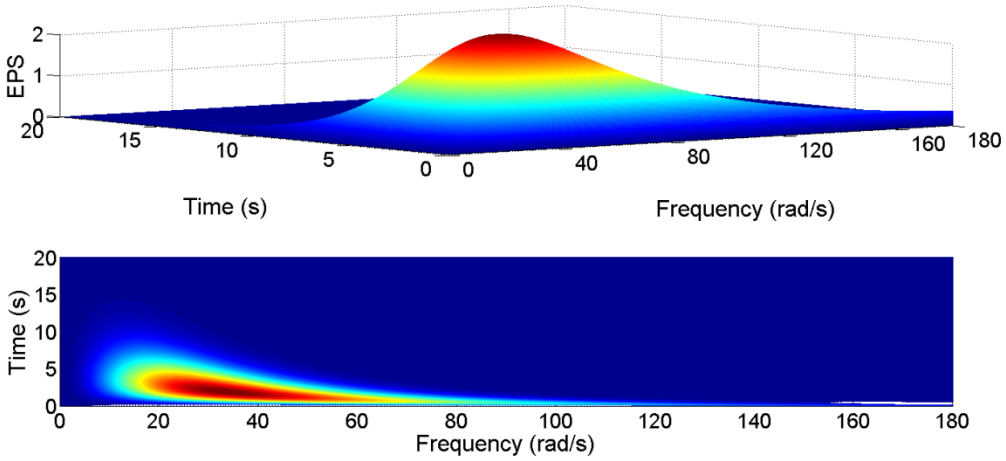

Figure 4.11. Non-separable excitation evolutionary power spectrum $S_{\ddot{\alpha}_g}(\omega, t)$.

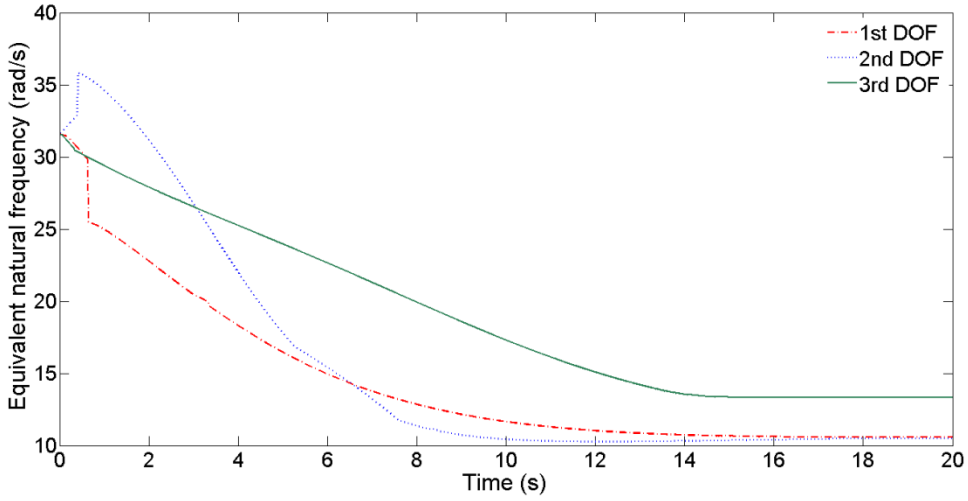

Figure 4.12. Time-varying equivalent natural frequency $\omega_{aux,i}(t)$ of the effective LTV system.

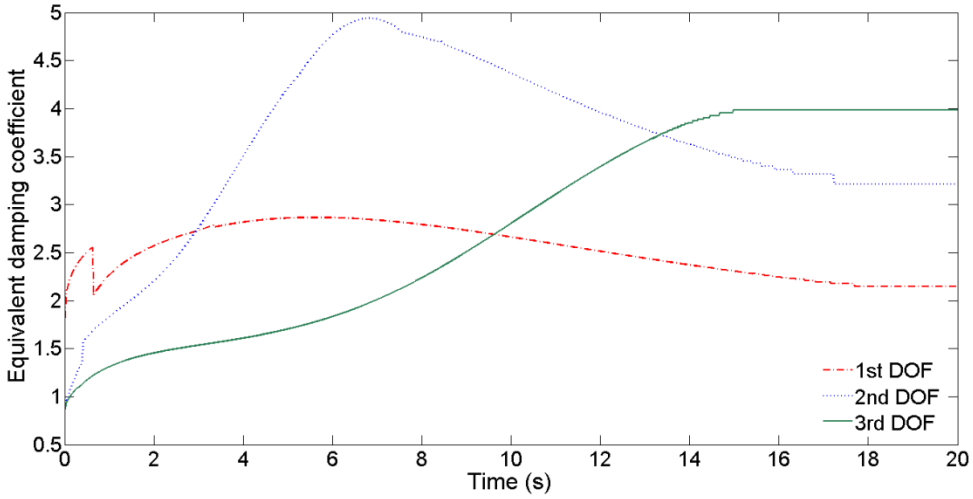

Figure 4.13. Time-varying equivalent damping coefficient $\beta_{aux,i}(t)$ of the effective LTV system.

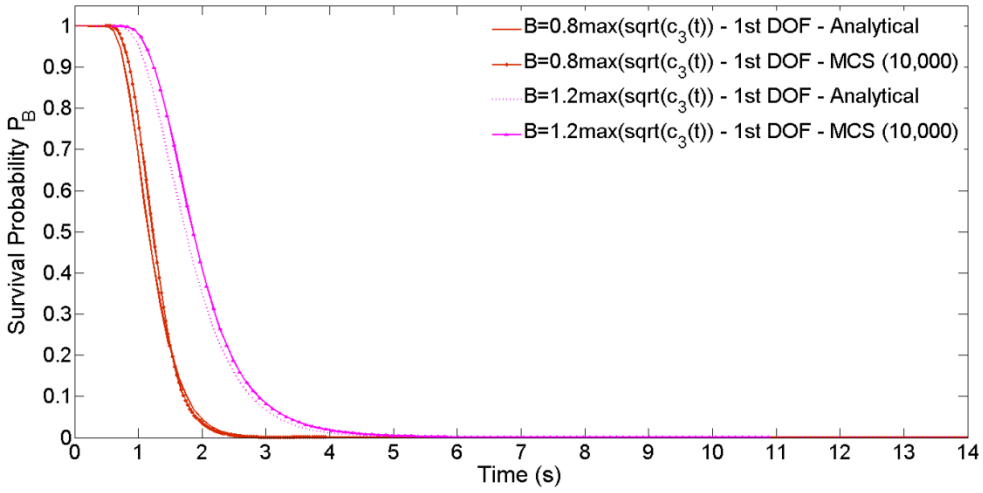

Figure 4.14. Survival probability for various values of the parameter λ for the first DOF; comparisons with MCS (10,000 realizations).

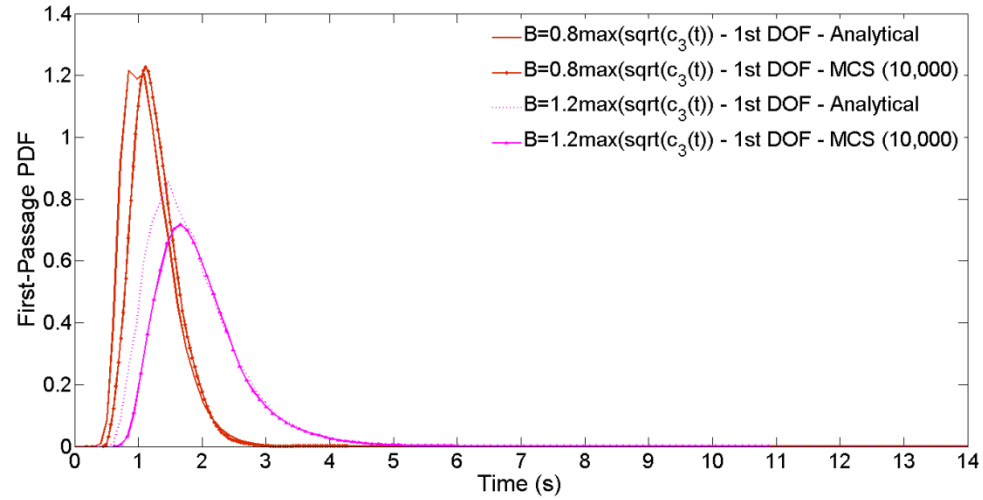

Figure 4.15. First-passage PDF for various values of the parameter λ for the first DOF; comparisons with MCS (10,000 realizations).

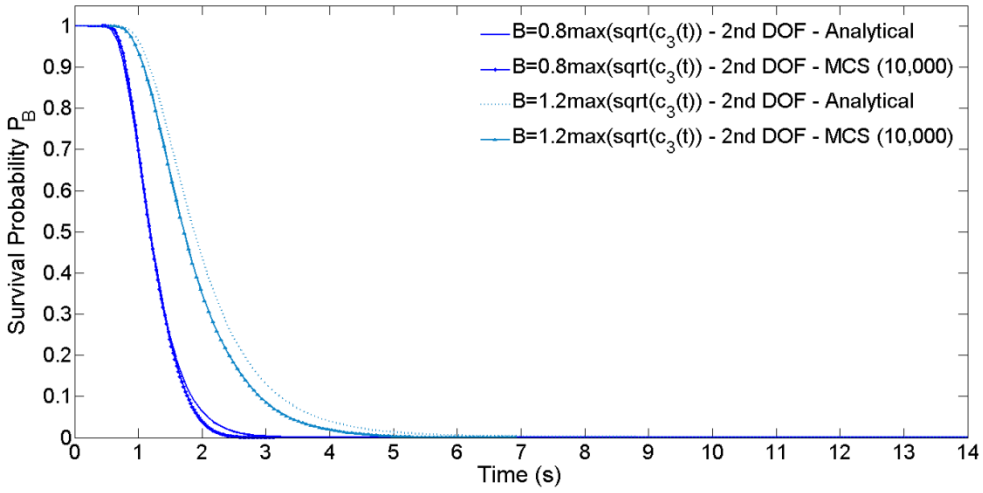

Figure 4.16. Survival probability for various values of the parameter λ for the second DOF; comparisons with MCS (10,000 realizations).

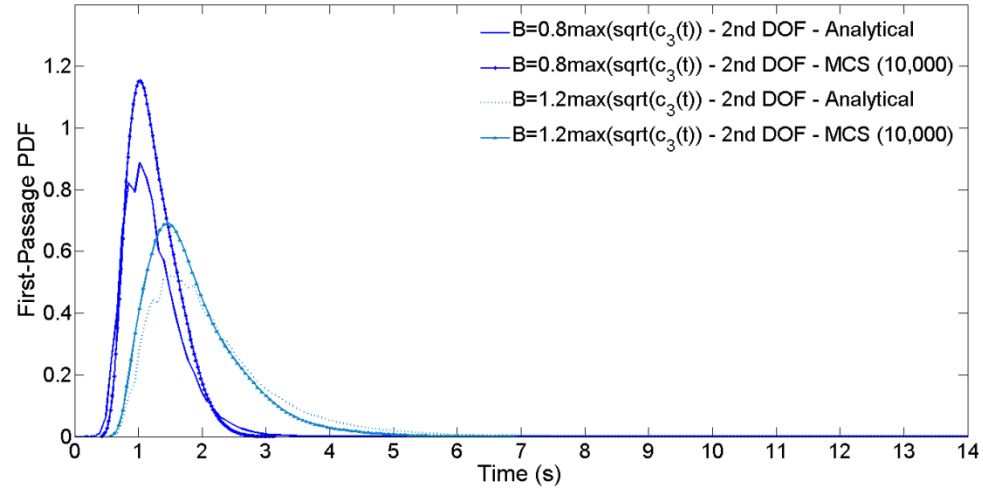

Figure 4.17. First-passage PDF for various values of the parameter λ for the second DOF; comparisons with MCS (10,000 realizations).

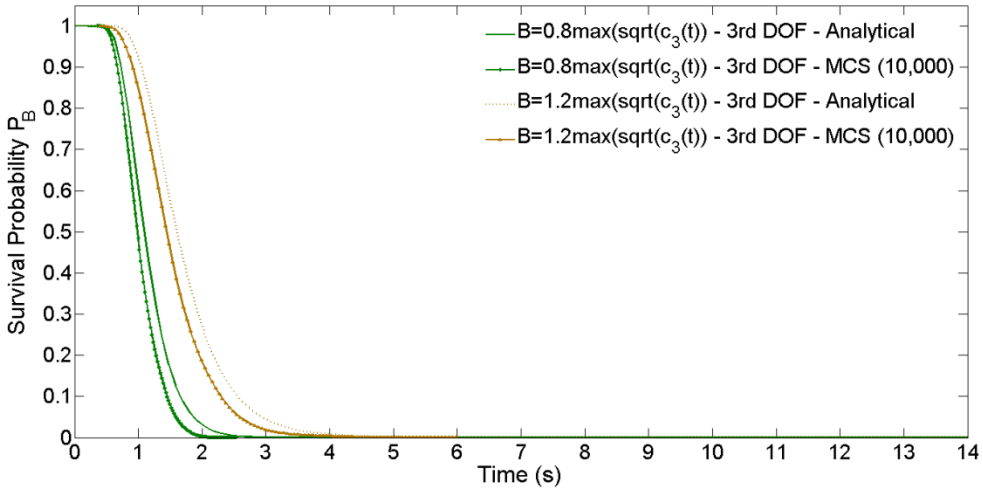

Figure 4.18. Survival probability for various values of the parameter λ for the third DOF; comparisons with MCS (10,000 realizations).

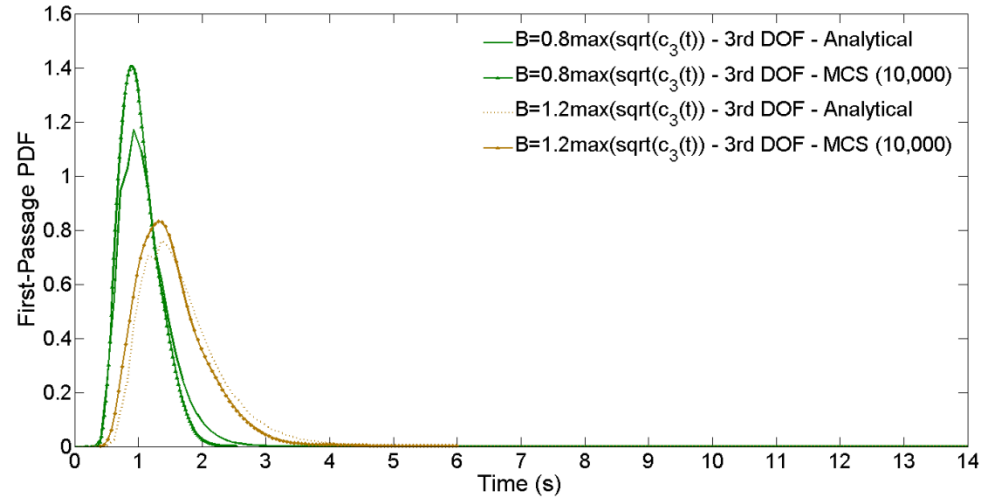

Figure 4.19. First-passage PDF for various values of the parameter λ for the third DOF; comparisons with MCS (10,000 realizations).

In Figs.(4.12) and (4.13) the equivalent time-varying natural frequency $\omega_{aux,i}(t)$ and damping $\beta_{aux,i}(t)$ elements corresponding to each DOF are plotted, respectively. Underlying the analytical approximate approach is the ability to capture the time

evolution as well as the essential characteristics of the frequency content of the nonlinear structural system response. Note that the ability of the technique to provide with time-varying natural frequencies $\omega_{aux,i}(t)$ can be of particular importance if seen in conjunction with recent theoretical developments regarding the concept of the mean instantaneous frequency (MIF) (e.g., Qian, 2002; Kijewski-Correa and Kareem, 2006; Spanos et al., 2007). In this regard, $\omega_{aux,i}(t)$ together with the MIF of the seismic excitation can be potentially employed for evaluating the effects of temporal non-stationarity in the frequency content of the seismic excitation on the structural system response as well as for tracking moving resonance phenomena (e.g., Beck and Papadimitriou, 1993; Tubaldi and Kougioumtzoglou, 2014). Further, in Figs.(4.14) and (4.15) the survival probabilities $P_i^B(T)$ and the corresponding first-passage PDFs $p_i^B(T)$ for the first DOF of the hysteretic MDOF structural system are plotted for various barrier levels, respectively; comparisons with MCS (10,000 realizations) demonstrate a satisfactory degree of accuracy. Considering Figs.(4.16), (4.17), (4.18) and (4.19) which correspond to the second and third DOF, the same conclusion regarding the accuracy of the approach can be drawn.

Chapter 5

Efficient fragility analysis within a PBEE framework for nonlinear MDOF structural systems

5.1 Preliminary remarks

Structural systems are often subjected to earthquake excitations that exhibit evolutionary characteristics such as strong variability in both the intensity and the frequency content. This fact necessitates the representation of this class of loads by non-stationary stochastic processes (e.g., Soong and Grigoriu, 1993; Roberts and Spanos, 2003; Li and Chen, 2009; Spanos and Kougioumtzoglou 2012). Further, structural systems can behave in a nonlinear/hysteretic manner with restoring forces depending on the time history of the response when subjected to severe excitations such as earthquakes (e.g., Mayergoyz, 2003; Ikhouane and Rodellar, 2007). Thus, a sustained challenge in the area of earthquake engineering has been the efficient response analysis of nonlinear/hysteretic structures under evolutionary stochastic excitations.

In general, PBEE serves as a potent framework for facilitating seismic risk decision-making for engineering structures, while properly accounting for the underlying uncertainties. In this regard, the Pacific Earthquake Engineering Research (PEER) Center proposed a general probabilistic framework for PBEE analysis (e.g., Der Kiureghian, 2005), which involves a number of analysis components such as: (i) stochastic hazard analysis; (ii) stochastic structural/damage analysis; and (iii) stochastic loss analysis reflecting the effect of the underlying uncertainties on a quantifiable decision variable, commonly expressed in economic terms. In the ensuing analysis focus is placed on component (ii) that constitutes the most computationally demanding one.

Over the last few decades, several approaches have been developed for performing fragility analysis and for generating the corresponding homonymous curves; i.e. probabilities of exceeding specified damage states (DS) given an intensity measure (IM) value (e.g., Hwang and Jaw, 1990; Hwang and Huo, 1994; Porter et al., 2007). Indicatively, a limited number of nonlinear time-history analyses with prescribed IM level compatible scaled real earthquake records (e.g., Vamvatsikos and Cornell, 2002) are typically employed in conjunction with a statistical analysis of the response statistics. Alternatively, in cases where an appropriate stochastic model exists for the excitation (e.g., evolutionary power spectrum), standard, or efficient Monte Carlo simulation (MCS) based methodologies such as importance/line sampling, and subset simulation (e.g., Hammersley and Handscomb, 1964; Au and Beck, 2003; Schueller et al., 2004) can be utilized. Clearly, in the former case the accuracy of the results is undermined by the limited number of samples, whereas in the latter case the computational cost involved can be significantly high, or even prohibitive.

In this regard, it can be argued that there is a need for developing approximate analytical and/or numerical techniques for determining efficiently the response and the related fragilities of nonlinear structural systems subject to evolutionary stochastic excitations. Nevertheless, although there is a considerable body in the literature referring to the development of such stochastic response determination techniques (e.g. Roberts and Spanos, 2003; Lutes and Sarkani, 2004; Li and Chen, 2009) there are limited results related to utilizing such techniques for efficient fragility analysis applications. An interesting contribution in this regard is the work by Der Kiureghian and Fujimura (2009) where an efficient tail-equivalent linearization based approach was applied for fragility analysis of a nonlinear building structure (see also Fujimura and Der Kiureghian, 2007). Further, Kafali and Grigoriu (2007) performed structural system fragility analysis utilizing the crossing theory for the cases of linear and nonlinear oscillators, whereas Tubaldi et al. (2014) employed a combination of analytical and simulation techniques to assess fragilities for adjacent steel buildings connected by linear and nonlinear viscous dampers.

The fragility analysis methodology developed herein differs, as compared with a typically applied fragility analysis implementation, in the following three aspects: (i) the ground motion is modeled as a stochastic process rather than a suite of scaled real earthquake records; (ii) instead of the commonly employed scalar IMs of the peak ground acceleration (PGA) or spectral acceleration, a vector-valued IM consisting of two parameters (e.g., Baker and Cornell, 2005), namely the earthquake moment magnitude $\mathrm{M_m}$ and the epicentral distance r (i.e. the distance from the epicentre to system site), is adopted herein; (iii) a recently developed efficient approximate analytical stochastic dynamics technique is utilized for determining the system fragilities; thus, circumventing computationally demanding MCS. The proposed methodology is characterized by a number of attributes that can be construed as significant advantages. Specifically, the challenge of selecting and scaling earthquake records is conveniently avoided; note in passing that the above issue remains highly controversial in the relevant literature (e.g., Luco and Bazzuro, 2007; Der Kiureghian and Fujimura, 2009; Grigoriu, 2011, Giaralis and Vamvatsikos, 2014). Further, due to the nature of the adopted IM, depicting system fragilities versus the employed IM leads to producing fragility surfaces instead of the usual two-dimensional fragility curves. Clearly, the fragility surfaces provide with enhanced information and with a more comprehensive perspective of the system fragilities for various levels of damage (see also Kafali and Grigoriu, 2007; Koutsourelakis, 2010).

In this chapter a novel methodology for conducting efficient fragility analysis of nonlinear/hysteretic multi-degree-of-freedom (MDOF) structural systems subject to evolutionary stochastic earthquake excitations is formulated. First, an appropriate seismological model is used for describing the probability law of ground motion for various values of $\mathrm{M_m}$ and r. Next, a recently developed efficient approximate dimension reduction/decoupling technique based on the concepts of statistical linearization and of stochastic averaging for determining the non-stationary system response statistics is employed; thus, computationally demanding Monte Carlo simulations are circumvented. Further, approximate closed-form expressions are derived for the non-stationary response

amplitude PDFs of the IDRs corresponding to each and every DOF. In this regard, considering appropriately defined levels of damage structural system related fragilities are determined at a low computational cost. Overall, the proposed framework appears to be highly efficient for performing fragility analysis, reducing significantly the computational burden for this task.

Following the introductory section, in section 5.2 the mathematical formulation as well as the efficient fragility analysis framework are delineated whereas in section 5.3 illustrative examples comprising the versatile Bouc-Wen (hysteretic) model are considered for demonstrating the efficiency of the proposed approach. Comparisons with pertinent MCS are included as well indicating a satisfactory level of accuracy exhibited by the proposed technique.

5.2 Mathematical formulation

5.2.1 Statistical linearization based dimension reduction approach

Consider an n-degree-of-freedom nonlinear structural system governed by the Eq.(3.1) where $\ddot{\mathbf{y}}, \dot{\mathbf{y}}$ and $\mathbf{y}$ denote the response acceleration, velocity and displacement vectors, respectively, defined in relative coordinates; namely that the vector $\mathbf{y}$ contains the inter-story drifts. Focusing next on the joint time-frequency domain and following the approximate/analytical statistical linearization based dimension reduction/decoupling approach delineated in chapter 3 the determination of the effective auxiliary LTV SDOF time-dependent parameter $c_i(t)$ is efficiently achieved via the corresponding first-order ODE of Eq.(3.26) at a low computational cost (e.g., Spanos and Lutes, 1980; Kougioumtzoglou and Spanos, 2009; Kougioumtzoglou, 2013). Note in passing that in the herein analysis, the EPS excitation $S_{\ddot{\alpha}_g}(\omega, t)$ is assumed to have the form given in Eq.(2.20).

5.2.2 Efficient fragility analysis framework

Clearly, the development of a fragility analysis methodology involves the definition of suitable levels of damage that are correlated with the structural performance. Typically, the DS for reliability analysis purposes are defined in terms of the overall inelastic deformation or the maximum inter-story drift of the structural system (e.g., Ellingwood, 2001). In the ensuing analysis, DS are defined through the inter-story drift ratio (IDR), i.e. the difference of the horizontal displacements between two successive stories, normalized by the inter-story height h. In this setting, IDRs act as the engineering demand parameters (EDPs) for monitoring the structural performance. Note in passing that the IDR constitutes one of the most reliable measures of structural damage due to its close relationship to plastic rotation demands for individual beam-column connection assemblies.

Next, considering the IDR amplitude $\theta_i(t) = \alpha_i(t)/h$, a direct transformation (e.g., Ang and Tang, 2007) of the response amplitude PDF $p(\alpha_i, t)$ (see Eq.(3.25)) yields the non-stationary IDR amplitude PDF in the form

$$p(\theta_i, t) = h^2 \frac{\theta_i}{c_i(t)} \exp\left(-\frac{h^2 {\theta_i}^2}{2c_i(t)}\right). \tag{5.1}$$

Further, of particular interest from a reliability assessment perspective is the time instant where the IDR amplitude reaches its most critical value, i.e. $p_{cr}(\theta_i) = p(\theta_i, t = t_{cr})$. In the following, this is assumed to be the time when $c_i(t)$ reaches its peak value, and thus, the PDF of Eq.(5.1) takes its most broad-band form yielding higher failure probabilities. In this regard, the non-stationary IDR amplitude PDF $p(\theta_i, t)$ can be directly related to the considered DS leading to the efficient estimation of structural system fragilities. Specifically, the structural system fragility P_i defined as the probability of exceeding a specific level of damage δ_{ds} conditioned upon the earthquake moment magnitude M_m and the epicentral distance r, is expressed as

$$P_i[\theta_i(t) \geq \delta_{ds} = \delta | \, IM(M_m, r)] = 1 - \int_0^{\delta} p_{cr}(\theta_i | \, IM(M_m, r)) \, d\theta \tag{5.2}$$

Considering Eq.(5.1), and integrating analytically Eq.(5.2) yields

$$P_i[\theta_i(t) \geq \delta_{ds} = \delta | \, IM(M_m, r)] = \exp\left(-\frac{h^2\delta^2}{2c_i(t)}\right). \tag{5.3}$$

In this setting, structural system fragilities for various DS can be readily computed rendering the proposed methodology highly efficient computationally.

Note that the above determined seismic fragility of Eq.(5.3) should not be confused with the first-passage kind failure probability, which is uniquely defined by satisfying a failure criterion for the first time. In fact, several approximate analytical and/or numerical techniques have been developed over the past few decades for addressing the first-passage problem in stochastic dynamics with varying degrees of success (e.g., Vanmarcke, 1975; Solomos and Spanos, 1983; Au and Beck, 2001; Barbato and Conte, 2001; Naess et al., 2011; Kougioumtzoglou and Spanos, 2013b; Kougioumtzoglou and Spanos, 2014; Spanos and Kougioumtzoglou, 2014; Mitseas et al., 2014b). However, it can argued that for the herein considered structural systems the drift ratio amplitude may cross a prescribed damage level several times during an earthquake event without leading to total collapse of the structure; thus, rendering, perhaps, the fragility definition of Eq.(5.3) more relevant. The first-passage kind failure definition may, perhaps, be appropriate for the most severe damage state or for brittle masonry structures, where potential exceedance may lead to total collapse. In the herein proposed methodology, only failure definitions of the form of Eq.(5.3) are considered, whereas incorporation of first-passage kind failure criteria is identified as a topic of potential future work.

Concisely, the proposed fragility methodology comprises the following components:

i. Determination of the earthquake excitation stochastic process EPS via Eq.(2.20) for specific values of moment magnitude M_m and of epicentral distance r.

ii. Determination of the MDOF system non-stationary response variances (Eqs.(3.15-3.16)) via an evolutionary spectral matrix analysis approach and a statistical linearization treatment of the problem.

iii. Determination of the equivalent linear time-varying elements $\beta_{aux,i}(t)$ and $\omega_{aux,i}(t)$ by solving the two-by-two system of algebraic equations (Eqs.(3.18-3.19)).

iv. Determination of $c_i(t)$ via numerically integrating the first-order ODE Eq.(3.26).

v. Structural system fragilities determination for various levels of damage conditioned upon the moment magnitude M_m and the epicentral distance r via Eq.(5.3).

Note that the proposed methodology can be readily adapted to account for alternative other stochastic seismological models as well (e.g., Rezaeian and Der Kiureghian 2008).

5.3 Numerical applications

In this section, a nonlinear three-degree-of-freedom structural system following the Bouc-Wen hysteretic model (e.g., Wen, 1980; Ikhouane and Rodellar, 2007) is considered for demonstrating the efficiency and reliability of the proposed methodology.

5.3.1 MDOF Bouc-Wen hysteretic building structure

A three-DOF lumped parameter model is considered for representing a three-story reinforced concrete building whose floors are assumed to be rigid with a constant height equal to 3m, whereas the masses of its plates are constant for all floors with a value $m_{plate} = 3.5 \times 10^4$kg. Further, a Young's modulus of $E = 30 \times 10^9$Pa and mass density of $\rho = 2{,}5 \times 10^3 \text{kg/m}^3$ are considered. Columns' square cross-section dimensions for a given floor are assumed to be equal and thus, the vector of the considered design variables $\mathbf{d}$ has one component for every story, i.e. the width of the cross-section. A side view of the 3-DOF building structure is shown in Fig.(5.1).

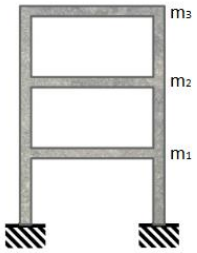

Figure 5.1. Nonlinear 3-DOF structural system.

Considering inter-story drifts y_i as well as the additional states z_i introduced by the Bouc-Wen model, the 3-DOF nonlinear structural system is governed by Eq.(3.1) where

$$\mathbf{y}^{\mathrm{T}} = (y_1\ y_2\ y_3\ z_1\ z_2\ z_3). \tag{5.4}$$

The Bouc-Wen formulation related to MDOF systems unfolded in Eqs.(4.26-4.48) is adopted herein. Considering the parameters of the model the following values are employed: $\beta = \gamma = 0.5,\ n = 1,\ c_o = 2 \times 10^{-2}$, and $A = 1$. In order to estimate the accuracy of the developed methodology structural systems characterized by different level of nonlinearity are considered; the rigidity ratio a is taken equal to 0.15 and 0.25 for the case studies I and II, respectively.

5.3.2 Fragility surfaces considering a hysteretic MDOF building structure (case study I)

In this study, as well as in various PBEE studies, discrete DS are considered (e.g, Tubaldi et al., 2014). The DOF that possesses the most critical non-stationary IDR amplitude PDF $p(\theta_i, t)$ according to the definition given in section 5.2.2 serves as the global EDP while the employed relationship between the EDP and the DS is based on the work by Ghobarah (2004) related to ductile reinforced concrete (RC) moment resisting frames (see Table. 5.1).

Damage States	δ_{ds} (%)
(I)-Moderate	$0.4 \leq \delta_{ds}$
(II)-Heavy	$1.0 \leq \delta_{ds}$
(III)-Major	$1.8 \leq \delta_{ds}$
(IV)-Destroyed	$3.0 \leq \delta_{ds}$

Table 5.1: Damage states (DS) and the associated inter-story drift ratio limits (δ_{ds}).

Further, the seismic fragility surfaces that serve as a quantitative measure of the structural system vulnerability are evaluated for the considered damage levels following the methodology presented in section 5.2.2. The seismic fragilities are efficiently determined by simply integrating the critical non-stationary response IDR amplitude PDF $p_{cr}(\theta_i)$ of the DOF that exhibits the maximum $c_i(t = t_{cr})$ value; see Eq.(5.2). Notably, the fragility surfaces for various damage levels are determined at a minimum computational cost via Eq.(5.3).

Next, approximate technique based fragility estimates are compared with pertinent Monte Carlo simulation based estimates utilizing 5,000 realizations. Specifically, excitation realizations compatible with the EPS of Eq.(2.20) are generated based on the spectral representation technique (e.g. Shinozuka and Deodatis 1991). Next, the nonlinear equation of motion (Eq.(3.1)) is numerically integrated via a standard fourth order Runge-Kutta scheme, and finally, system response statistics as well as structural system fragilities are obtained based on the ensemble of the response realizations. In Figs.(5.2-5.9), the fragility surfaces determined via the approximate nonlinear stochastic dynamics technique are compared with corresponding MCS data for a given design vector $\mathbf{d} = [0.30\ 0.25\ 0.20]^T$ (in m). Specifically, in Figs.(5.2) and (5.3) the fragility surfaces corresponding to damage state (I) "Moderate" are plotted based on the approximate technique and on MCS, respectively. Similarly, Figs.(5.4-5.5) correspond to damage state (II) "Heavy", Figs.(5.6-5.7) correspond to damage state (III) "Major", and Figs.(5.8-5.9) correspond to damage state (IV) "Destroyed".

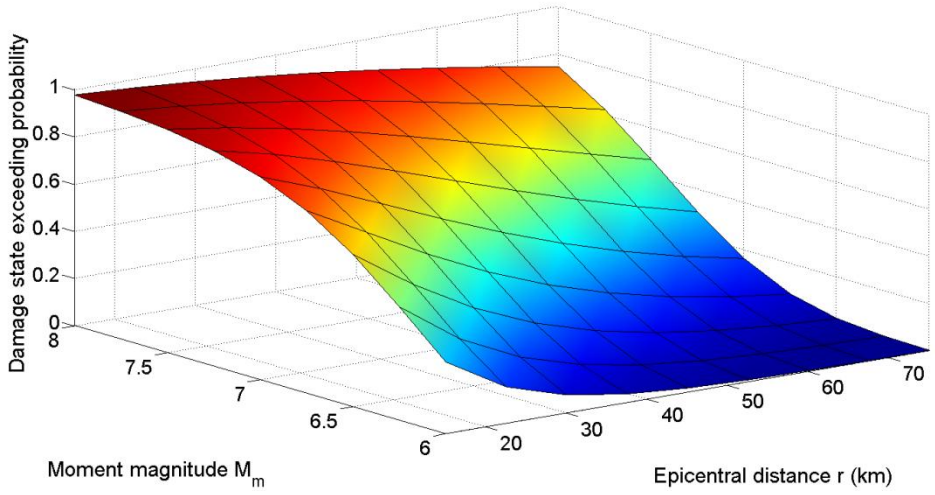

Figure 5.2. Fragility surface of a 3-DOF Bouc-Wen hysteretic system (a = 0.15) via the proposed approximate methodology for damage state (I) "Moderate".

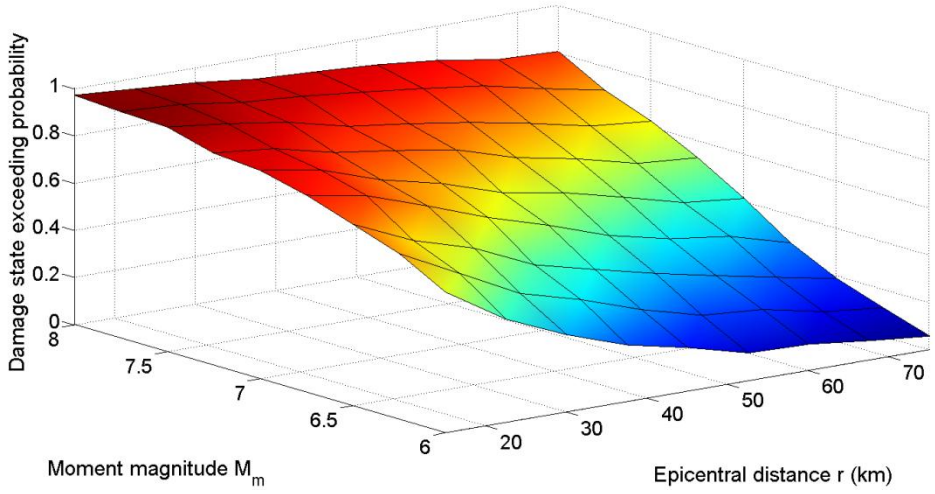

Figure 5.3. Fragility surface of a 3-DOF Bouc-Wen hysteretic system (a = 0.15) via MCS (5,000 realizations) for damage state (I) "Moderate".

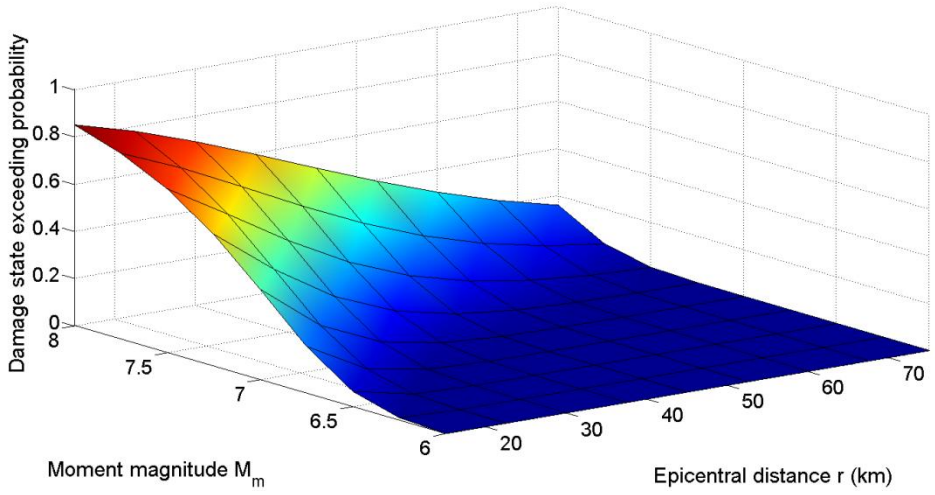

Figure 5.4. Fragility surface of a 3-DOF Bouc-Wen hysteretic system (a = 0.15) via the proposed approximate methodology for damage state (II) "Heavy".

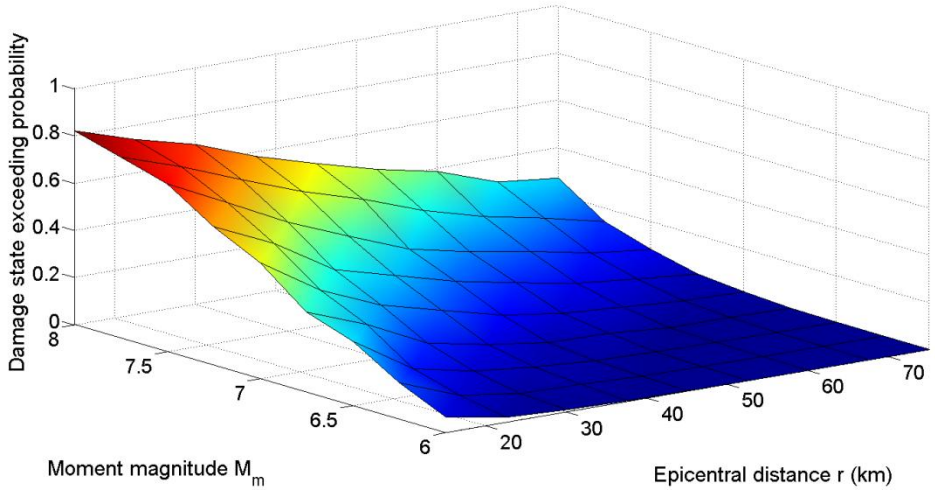

Figure 5.5. Fragility surface of a 3-DOF Bouc-Wen hysteretic system (a = 0.15) via MCS (5,000 realizations) for damage state (II) "Heavy".

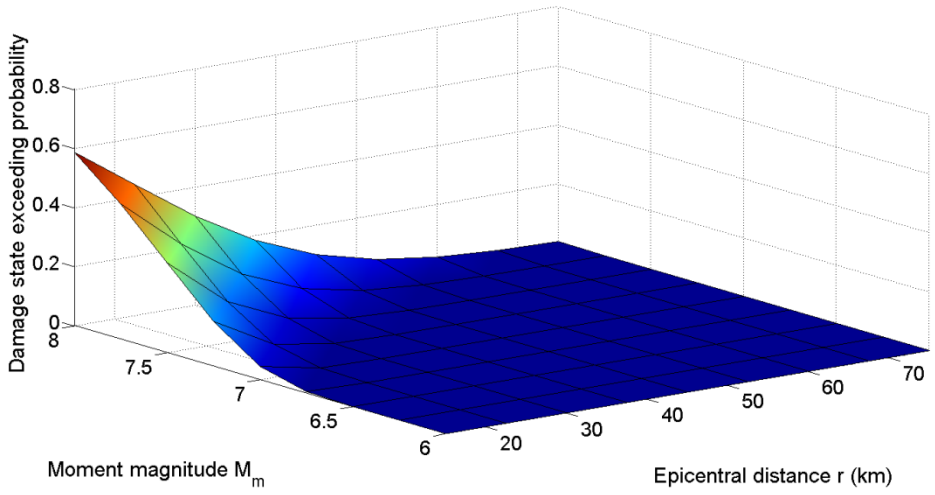

Figure 5.6. Fragility surface of a 3-DOF Bouc-Wen hysteretic system (a = 0.15) via the proposed approximate methodology for damage state (III) "Major".

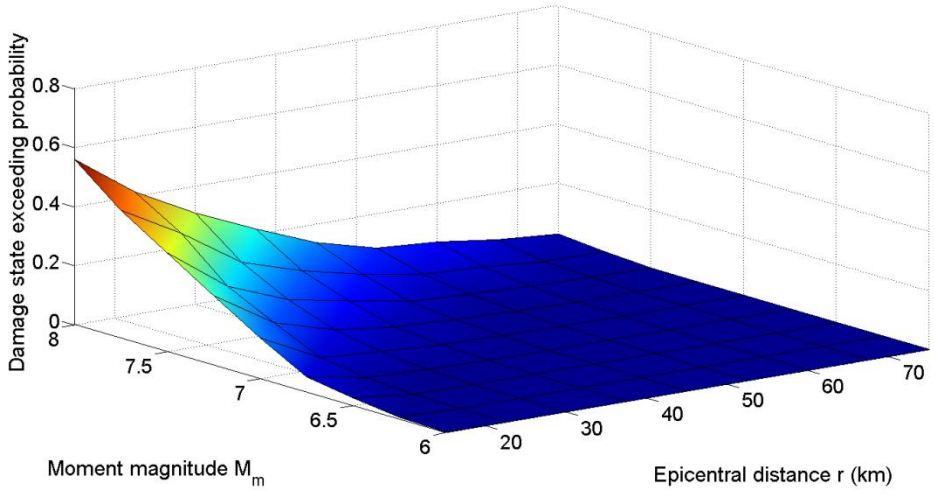

Figure 5.7. Fragility surface of a 3-DOF Bouc-Wen hysteretic system (a = 0.15) via MCS (5,000 realizations) for damage state (III) "Major".

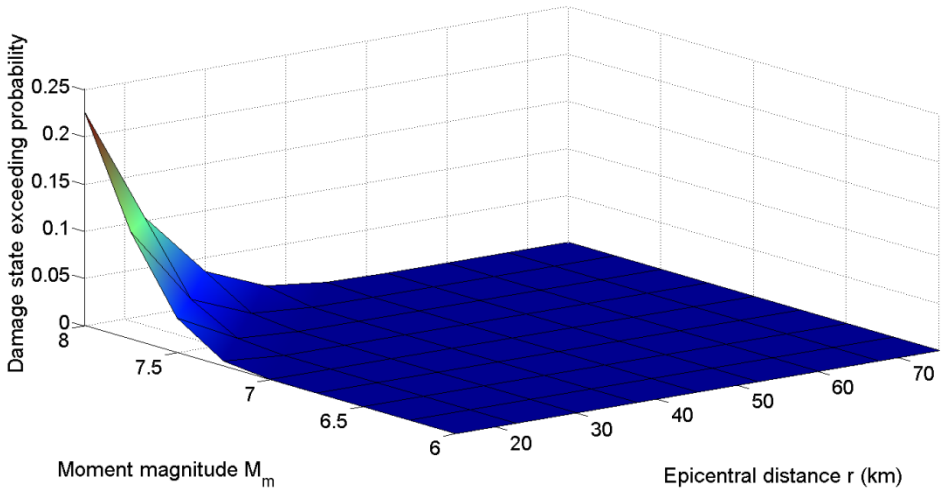

Figure 5.8. Fragility surface of a 3-DOF Bouc-Wen hysteretic system (a = 0.15) via the proposed approximate methodology for damage state (IV) “Destroyed”.

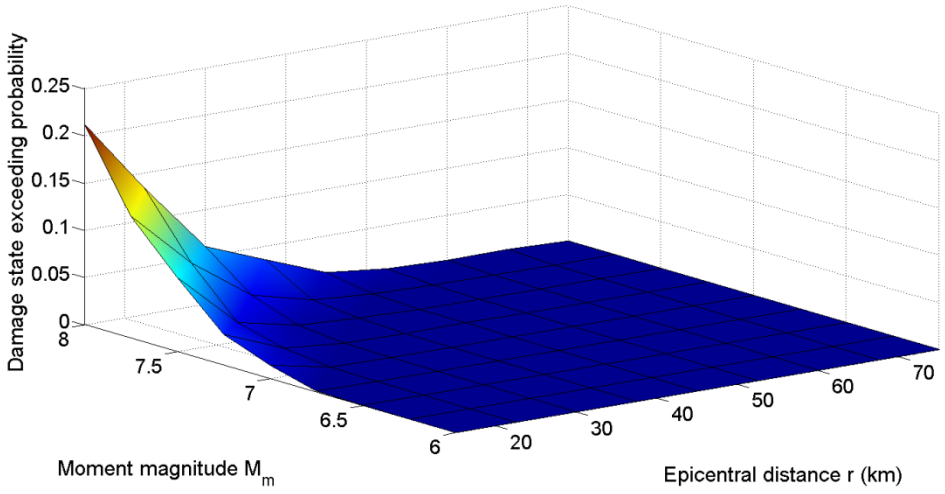

Figure 5.9. Fragility surface of a 3-DOF Bouc-Wen hysteretic system (a = 0.15) via MCS (5,000 realizations) for damage state (IV) defined as "Destroyed".

Further, in Fig.(5.10) computed fragilities of the considered 3-DOF Bouc-Wen hysteretic system for a constant value of epicentral distance $r = 15km$ are presented. Analytical/approximate as well as MCS data (5,000 realizations) are given for every considered damage state. In this setting fragilities for the case of treating the moment magnitude as a constant parameter are given as well in Fig.(5.11).

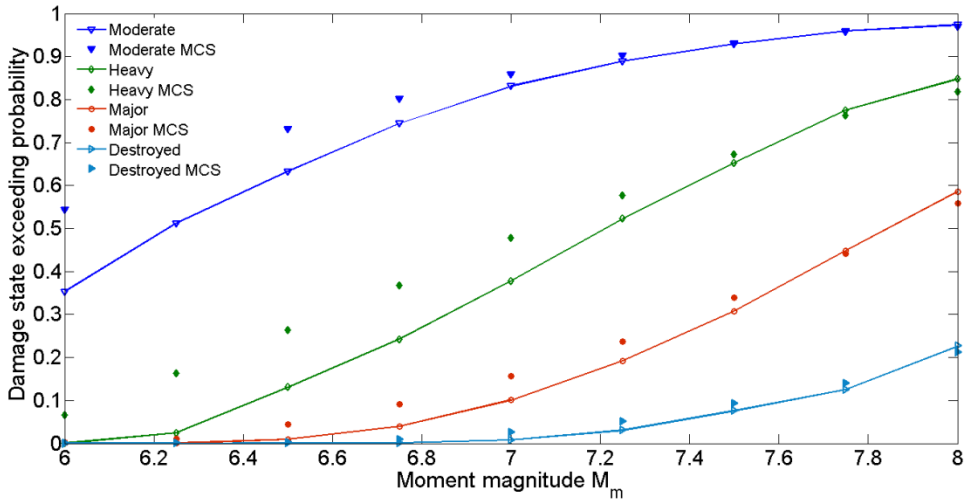

Figure 5.10. Fragility curves of a 3-DOF Bouc-Wen hysteretic system (a = 0.15) for a constant value of epicentral distance $r = 15km$. Analytical/approximate as well as MCS data (5,000 realizations) are presented for every considered damage state.

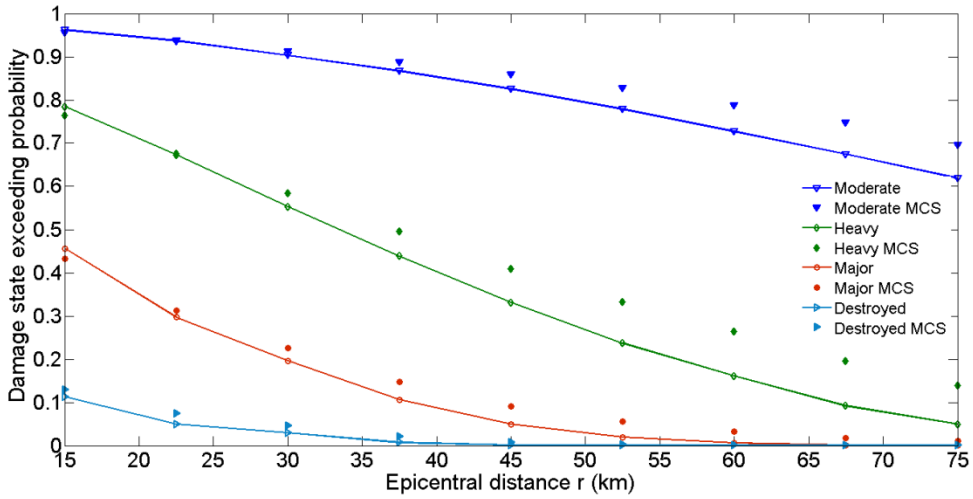

Figure 5.11. Fragility curves of a 3-DOF Bouc-Wen hysteretic system (a = 0.15) for a constant value of moment magnitude $M_m = 8$. Analytical/approximate as well as MCS data (5,000 realizations) are presented for every considered damage state.

5.3.3 Fragility surfaces considering a hysteretic MDOF building structure (case study II)

Seismic fragilities are computed for the case of a hysteretic MDOF structural system characterized by a rigidity ratio a equal to 0.25. Specifically, in Figs.(5.12) and (5.13) the fragility surfaces corresponding to damage state (I) “Moderate” are plotted based on the approximate technique and on MCS, respectively. Similarly, Figs.(5.14-5.15) correspond to damage state (II) “Heavy”, Figs.(5.16-5.17) correspond to damage state (III) “Major”, and Figs.(5.18-5.19) correspond to damage state (IV) “Destroyed”.

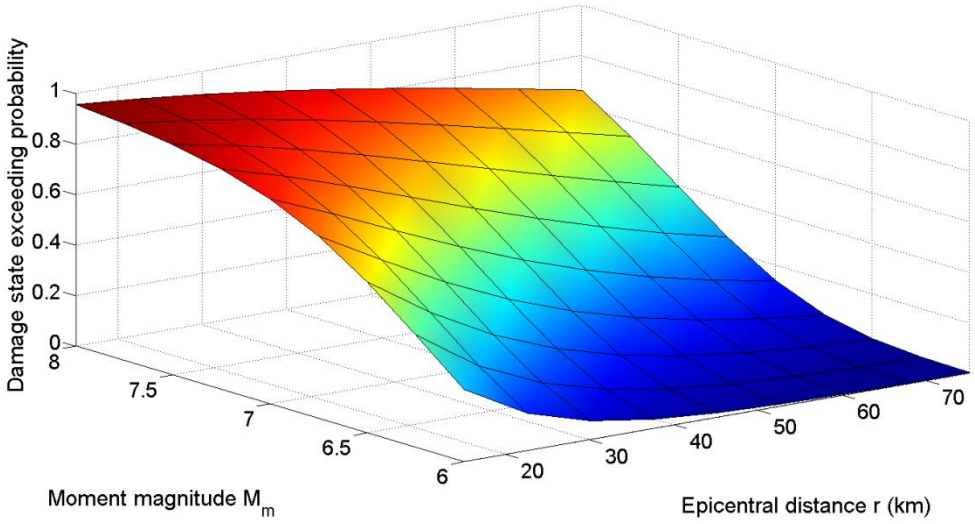

Figure 5.12. Fragility surface of a 3-DOF Bouc-Wen hysteretic system (a = 0.25) via the proposed approximate methodology for damage state (I) "Moderate".

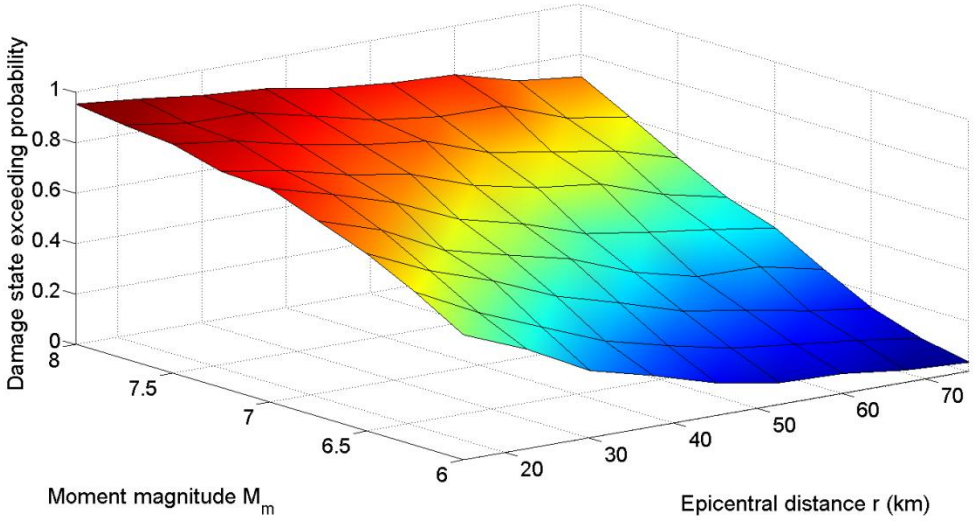

Figure 5.13. Fragility surface of a 3-DOF Bouc-Wen hysteretic system (a = 0.25) via MCS (5,000 realizations) for damage state (I) "Moderate".

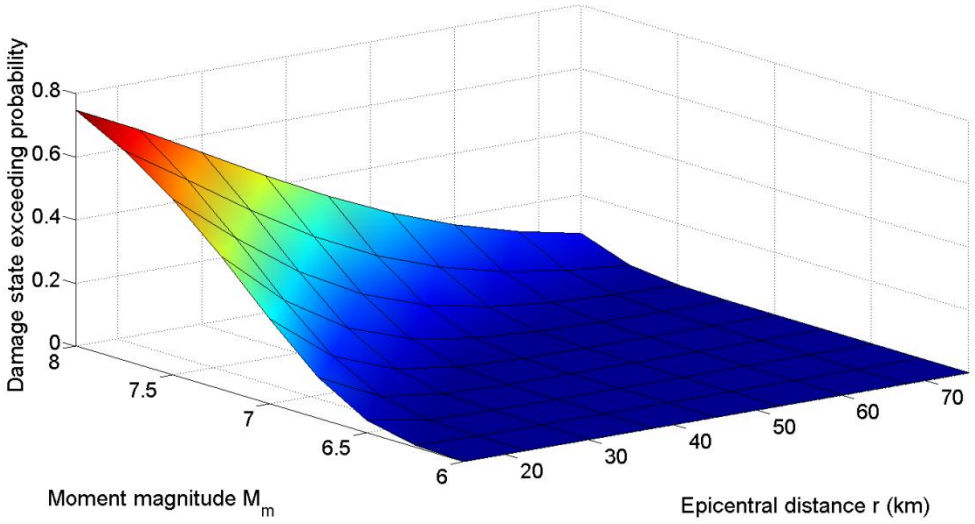

Figure 5.14. Fragility surface of a 3-DOF Bouc-Wen hysteretic system (a = 0.25) via the proposed approximate methodology for damage state (II) "Heavy".

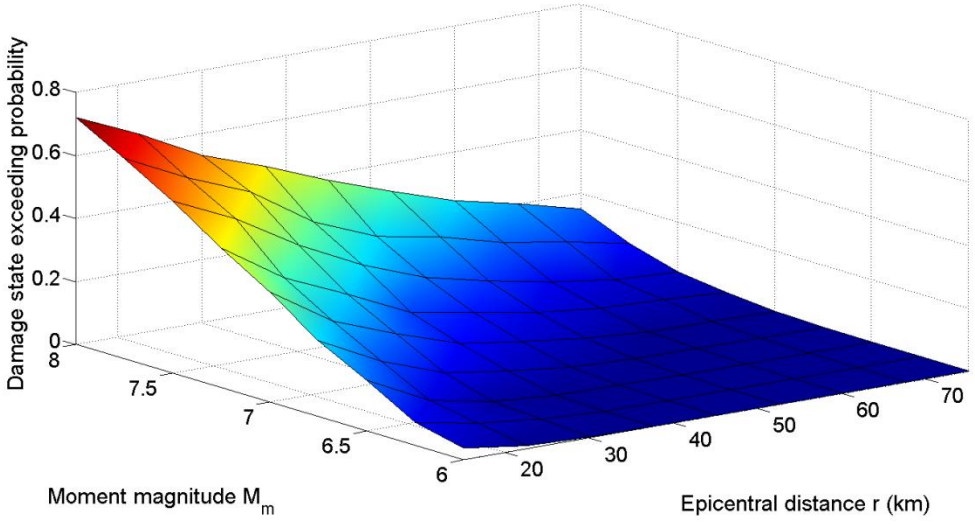

Figure 5.15. Fragility surface of a 3-DOF Bouc-Wen hysteretic system (a = 0.25) via MCS (5,000 realizations) for damage state (II) "Heavy".

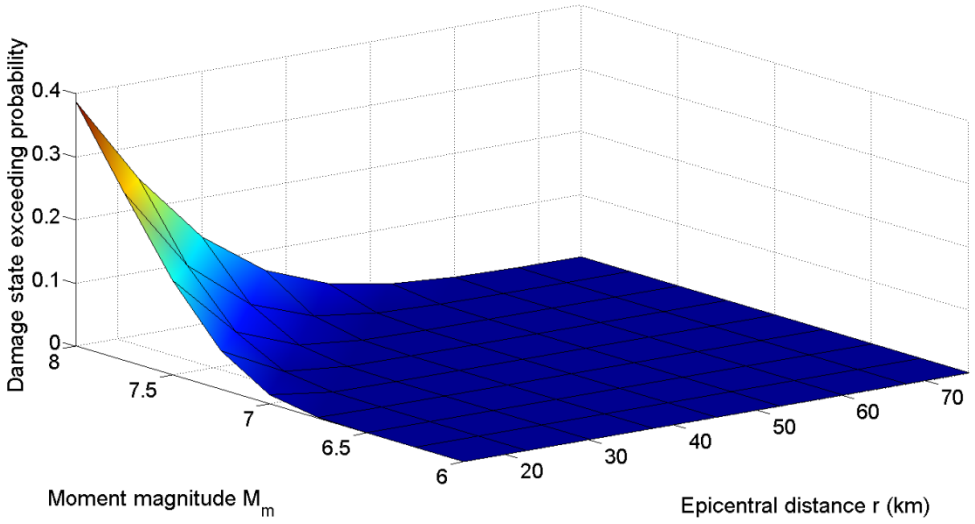

Figure 5.16. Fragility surface of a 3-DOF Bouc-Wen hysteretic system (a = 0.25) via the proposed approximate methodology for damage state (III) "Major".

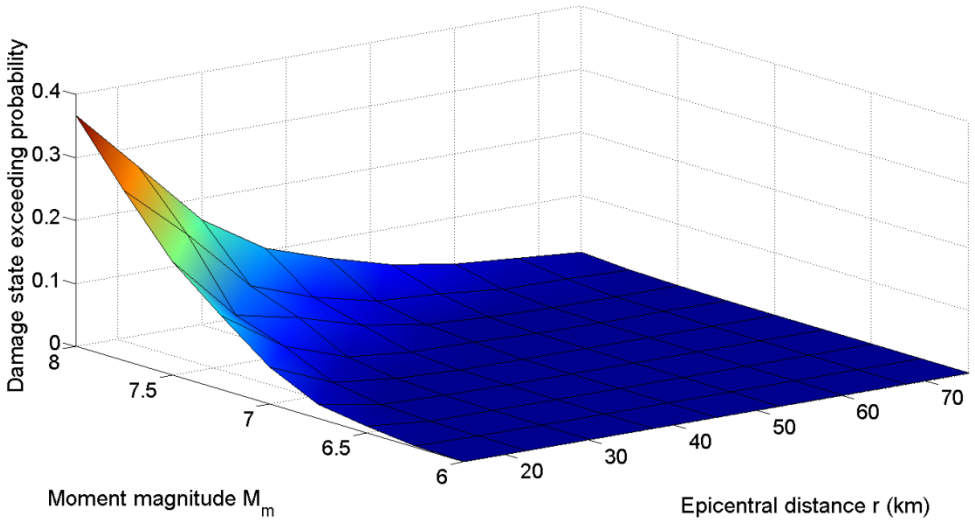

Figure 5.17. Fragility surface of a 3-DOF Bouc-Wen hysteretic system (a = 0.25) via MCS (5,000 realizations) for damage state (III) "Major".

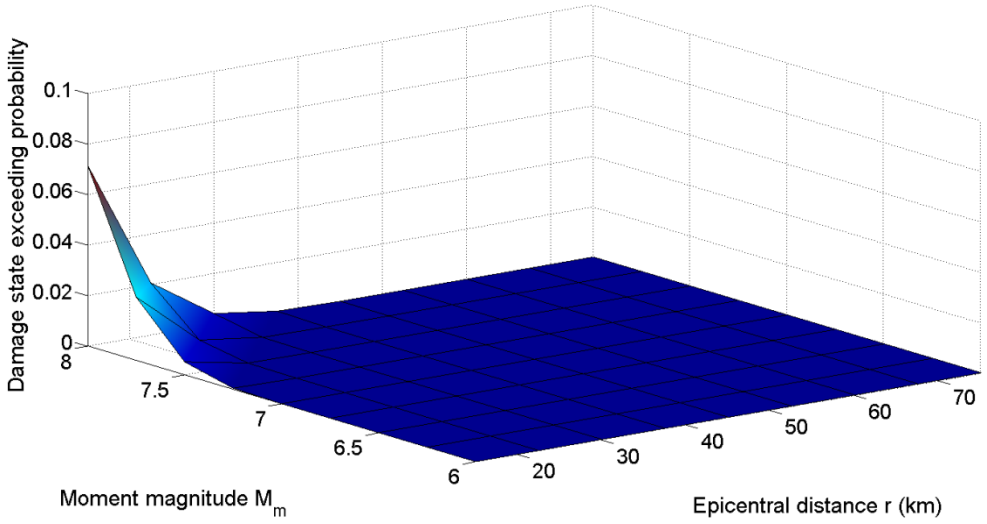

Figure 5.18. Fragility surface of a 3-DOF Bouc-Wen hysteretic system (a = 0.25) via the proposed approximate methodology for damage state (IV) "Destroyed".

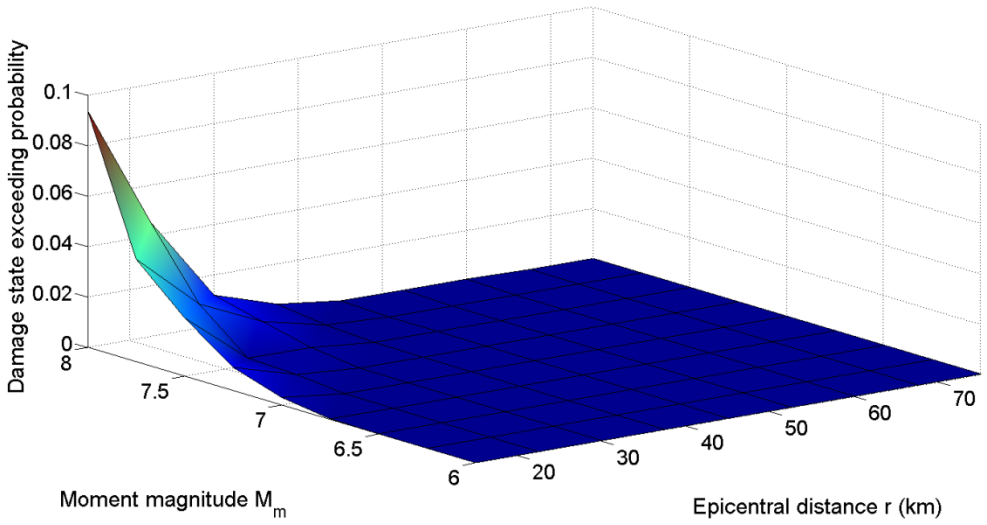

Figure 5.19. Fragility surface of a 3-DOF Bouc-Wen hysteretic system (a = 0.25) via MCS (5,000 realizations) for damage state (IV) "Destroyed".

Further, in Fig.(5.20) computed fragilities of the considered 3-DOF Bouc-Wen hysteretic system for a constant value of epicentral distance $r = 15km$ are presented.

Analytical/approximate as well as MCS data (5,000 realizations) are given for every considered damage state. In this setting, fragilities for the case of treating the moment magnitude as a constant parameter are given as well in Fig.(5.21).

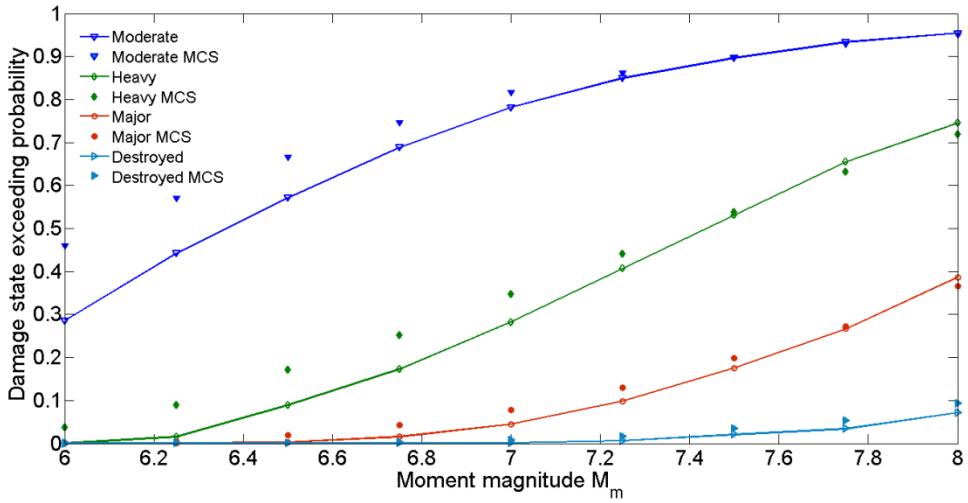

Figure 5.20. Fragility curves of a 3-DOF Bouc-Wen hysteretic system (a = 0.25) for a constant value of epicentral distance $r = 15km$. Analytical/approximate as well as MCS data (5,000 realizations) are presented for every considered damage state.

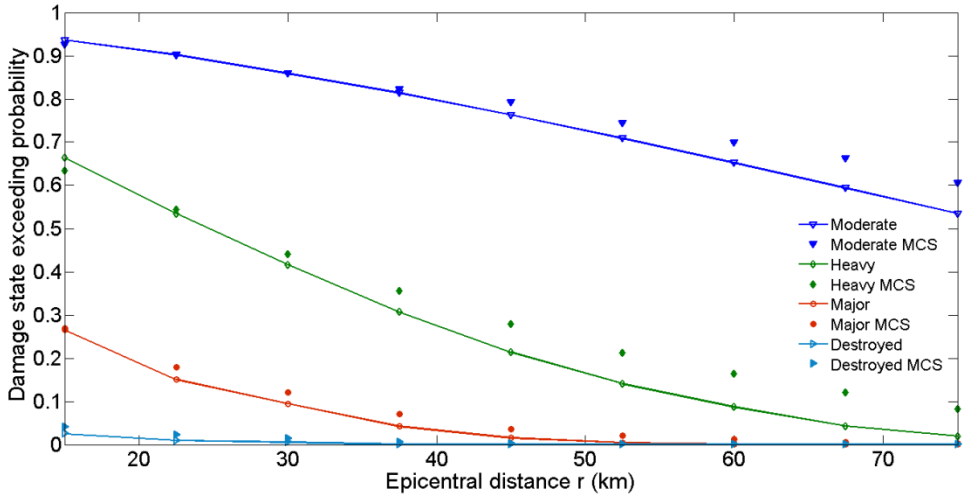

Figure 5.21. Fragility curves of a 3-DOF Bouc-Wen hysteretic system (a = 0.25) for a constant value of moment magnitude $M_m = 8$. Analytical/approximate as well as MCS data (5,000 realizations) are presented for every considered damage state.

It can be readily seen that the proposed seismic fragility methodology demonstrates a satisfactory degree of accuracy regardless the magnitude of the imposed IDR limit (δ_{ds}) and the level of the considered nonlinearity. Further, fragilities are efficiently depicted versus the two basic parameters of the stochastic seismological model rather than a commonly used scalar IM such as the PGA or the spectral acceleration. The achieved accuracy in conjunction with the related low computational cost renders the proposed methodology, hopefully, useful for efficient structural system fragility analysis and design applications, at least at a preliminary level.

Chapter 6

Robust design optimization of linear MDOF structural systems controlling both displacement and acceleration features

6.1 Preliminary remarks

Most often structural systems in seismic prone areas are subject to earthquake excitations that exhibit strong variability in both intensity and frequency content. Therefore, a realistic system analysis and design necessitates the representation of this class of structural loads by non-stationary stochastic processes (e.g., Spanos and Kougioumtzoglou, 2012). Non-stationary stochastic processes are commonly regarded to be filtered stationary stochastic processes according to the concept first proposed by Priestley (1965) and later refined by Dahlhaus (1997), introducing the class of locally stationary processes. Further, the dynamical structural system itself represents another potential source of randomness. In the current state of practice, usually an idealized mathematical/mechanical model of a structural system is adopted. Due to the uncertainty in the system parameters, mechanical/material properties are most generally modeled as non-homogeneous stochastic fields.

In conventional structural optimization, the random nature of a structure's mechanical/material properties and construction imperfections, as well as the inherent stochasticity in the seismic input process are most often neglected. In this regard, only fairly recently, the study of structural optimization problems within a probabilistic framework has attracted the attention of an increasingly large number of researchers. Depending on the model of uncertainty and on the definition of the objective functions

and constraints in the optimization problem, various optimization frameworks have been developed such as reliability-based optimization, fuzzy optimization, and robust optimization (e.g., Gasser and Schüeller, 1997; Au, 2005; Jensen, 2006; Beer and Liebscher, 2008).

Further, optimal structural design strategies require the adoption of appropriate performance measures to characterize the stochastic dynamic response, as well as an efficient probabilistic optimization methodology yielding the most favorable design. Clearly for a more comprehensive treatment of the stochastic structural design attention should be placed in considering and controlling both inter-story drifts and absolute floor accelerations features. In this regard, it is of significant importance for the decision maker to appreciate the tradeoffs between these two performance measures, which often constitute conflicting design requirements.

Note that in the current state of practice, stochastic structural optimization frameworks employ mainly maximum inter-story drift statistics as a single measure for quantifying the performance of a dynamical structural system. Maximum absolute acceleration statistics that represent an additional pertinent measure for evaluating the system performance are usually neglected. In this regard, a commonly employed stochastic structural optimization design approach yielding small values for the inter-story drifts may result in substantial accelerations; thus, yielding potentially significant damage to non-structural building components. Therefore, it can reasonably be argued that performance measures based on system response acceleration should also be embodied in stochastic structural design optimization frameworks.

The importance of considering acceleration as a measure for assessing potential damage of non-structural components and building contents has been demonstrated in a number of research efforts. An interesting contribution in this regard is the work by Viti et al. (2006) where a retrofit strategy based on weakening techniques with supplemental damping was proposed for reducing both relative displacements and absolute accelerations. More recently, Cimellaro (2007) proposed an interesting optimal design

methodology for controlling displacement as well as acceleration features of a multi-story building structure under dynamic actions.

In this chapter, an evolutionary methodology for the efficient solution of structural design optimization problems involving linear systems under non-stationary stochastic excitation is proposed. A Genetic Algorithm-based structural optimization solution procedure is proposed featuring constraints of both inter-story drift and absolute floor acceleration. A MDOF building structure is included as a numerical example to demonstrate the benefits of the proposed stochastic structural design optimization framework.

Following the introductory section, in section 5.2 the mathematical formulation of the evolutionary spectral matrix analysis is presented. In section 5.3 a brief description of the optimal design problem is provided whereas in section 5.4 an illustrative example is considered for demonstrating the efficiency of the proposed approach. Comparisons with pertinent MCS are included as well indicating a satisfactory level of accuracy exhibited by the proposed technique.

6.2 Mathematical formulation

6.2.1 Evolutionary spectral matrix analysis

Consider an n-degree-of-freedom linear structural system governed by the equation

$$\mathbf{M}\ddot{\mathbf{q}} + \mathbf{C}\dot{\mathbf{q}} + \mathbf{K}\mathbf{q} = \mathbf{F}(\mathrm{t}), \tag{6.1}$$

where $\ddot{\mathbf{q}}, \dot{\mathbf{q}}$ and $\mathbf{q}$ denote the response acceleration, velocity and displacement vectors, respectively, defined in absolute coordinates; namely that the vector $\mathbf{q}$ contains the relative floor displacements with respect to the ground motion. $\mathbf{M}$, $\mathbf{C}$ and $\mathbf{K}$ denote the $(\mathrm{n} \times \mathrm{n})$ mass, damping and stiffness matrices, respectively; $\mathbf{F}(\mathrm{t})^{\mathrm{T}} = \left(\mathrm{f}_1(\mathrm{t}), \mathrm{f}_2(\mathrm{t}), \dots, \mathrm{f}_\mathrm{n}(\mathrm{t})\right)$ is a $(\mathrm{n} \times 1)$ zero mean, non-stationary stochastic vector process defined as $\mathbf{F}(\mathrm{t}) = \boldsymbol{\gamma}\boldsymbol{\Gamma}\ddot{\alpha}_\mathrm{g}(\mathrm{t})$, where $\boldsymbol{\Gamma}$ is the unit column vector, $\boldsymbol{\gamma}^{\mathrm{T}} = (\gamma_1, \gamma_2, \dots, \gamma_\mathrm{n})$ is an arbitrary $(\mathrm{n} \times 1)$ vector of constant weighting coefficients, and

$\ddot{\alpha}_g(t)$ is the stochastic non-stationary seismic excitation process; $\mathbf{F}(t)$ possesses an evolutionary power spectrum (EPS) matrix $\mathbf{S_F}(\boldsymbol{\omega}, \mathbf{t})$ of the form of Eq.(3.2).

The non-stationary stochastic process is regarded to be a filtered stationary stochastic process according to studies already cited in chapter 3. Focusing on the joint time-frequency domain , the response determination problem is defined as seeking the system response EPS matrix of the form

$$\mathbf{S_q}(\omega,t)=\begin{bmatrix} S_{q_1q_1}(\omega,t) & S_{q_1q_2}(\omega,t) & \cdots & S_{q_1q_n}(\omega,t) \\ S_{q_2q_1}(\omega,t) & S_{q_2q_2}(\omega,t) & \cdots & \vdots \\ \vdots & \ddots & \cdots & S_{q_{n-1}q_n}(\omega,t) \\ S_{q_nq_1}(\omega,t) & \cdots & S_{q_nq_{n-1}}(\omega,t) & S_{q_nq_n}(\omega,t) \end{bmatrix}. \quad (6.2)$$

In the general case of a linear MDOF system under evolutionary excitation, the quasi-stationary approach delineated in section 3.2 through the Eqs.(3.9-3.11) in conjunction with the expression of the FRF which for the case of a linear structure takes the form

$$\mathbf{H}(\omega)=(-\omega^2\mathbf{M}+i\omega\mathbf{C}+\mathbf{K})^{-1}. \quad (6.3)$$

lead to the following expressions considering the i-th degree-of-freedom,

$$E[q_i^2(t)]=\int_{-\infty}^{\infty}(|H_{i1}(\omega)|^2m_1^2+\cdots+|H_{in}(\omega)|^2m_n^2)\,S_{\ddot{\alpha}_g}(\omega,t)d\omega \quad (6.4)$$

$$E\left[\dot{q}_i^2(t)\right]=\int_{-\infty}^{\infty}\omega^2(|H_{i1}(\omega)|^2m_1^2+\cdots+|H_{in}(\omega)|^2m_n^2)S_{\ddot{\alpha}_g}(\omega,t)\,d\omega \quad (6.5)$$

and

$$E\left[\ddot{q}_i^2(t)\right]=\int_{-\infty}^{\infty}\omega^4(|H_{i1}(\omega)|^2m_1^2+\cdots+|H_{in}(\omega)|^2m_n^2)S_{\ddot{\alpha}_g}(\omega,t)\,d\omega \quad (6.6)$$

Clearly, the approximate frequency domain approach provides an efficient methodology for determining the response of MDOF systems in terms of various performance measures circumventing computationally intensive Monte Carlo simulations (see also Kougioumtzoglou and Spanos, 2013, Mitseas et al., 2014a).

6.3 Formulation of the optimal design problem

6.3.1 Single-objective optimization

Admittedly, uncertainties are ubiquitous in any dynamical structural system of engineering interest. Therefore, there is a necessity for taking uncertainties into consideration during the design process. The continuing tendency to reduce the weight of structures in conjunction with explicit consideration of uncertainties has yielded a variety of stochastic optimization frameworks. In this regard, a general stochastic optimization formulation focusing on the determination of a vector $\mathbf{x}$ of design variables to minimize an objective function takes the form

$$\min_{\mathbf{x}\in D} f^{ind}(\mathbf{x}), \tag{6.7}$$

where

$$\mathbf{x} = [x_z] = [x_1, x_2, \dots x_{n_{dv}}]^T, z = 1, .. n_{dv}, \mathbf{x} \in D, \tag{6.8}$$

subject to system response level constraints of the form

$$\mathbf{G}(\mathbf{x}) = \left[g_j^{ind}(\mathbf{x})\right] = \left[g_1^{ind}(\mathbf{x}), \dots, g_{ncon}^{ind}(\mathbf{x})\right] \leq 0, j = 1, \dots, n_{con}\,. \tag{6.9}$$

In the case of a stochastic objective function $\mu_f^{stoch}(\mathbf{x})$ and $\sigma_f^{stoch}(\mathbf{x})$ are employed. $\mu_f^{stoch}(\mathbf{x})$ and $\sigma_f^{stoch}(\mathbf{x})$ are the maximum over time non-stationary values of the mean and standard deviation of the objective function $f^{stoch}(\mathbf{x})$ respectively, evaluated at the design variables vector $\mathbf{x}$; $f^{det}(\mathbf{x})$ is a deterministic objective function evaluated at the design variables vector $\mathbf{x}$; in case of a stochastic response constraint, $\mu_{g_j}^{stoch}(\mathbf{x})$ and $\sigma_{g_j}^{stoch}(\mathbf{x})$ stand for the maximum over time non-stationary values of the mean and standard deviation of the response function $g_j^{stoch}(\mathbf{x})$ respectively, evaluated at the design variables vector $\mathbf{x}$; $g_j^{det}(\mathbf{x})$ is a deterministic response level constraint evaluated at the design variables vector $\mathbf{x}$; and $\mathbf{G}(\mathbf{x})$ is the vector of the constraint functions of the

optimization problem under consideration. D is a given set that contains the boundary constraints for the vector of design variables **x**.

6.3.2 Genetic algorithms

Genetic algorithms (GAs) belong to the category of Evolutionary algorithms (EAs) which constitute a widely used class of methods for solving optimization problems (Holland, 1975; Goldberg, 1989; Bäck and Schwefel, 1993). The standard GAs imitate the biological evolution in nature and have three significant advantages that make them very efficient: the use of randomized operators, working with population of design points in design variables space as well as the ability to handle continuous, discrete or even mixed optimization problems. In general, GAs appear to be less vulnerable to being trapped in local optima and thus, GAs are considered to be quite robust and reliable in obtaining the global optimum for non-convex constrained optimization problems. Next, the basic GA components are briefly reviewed: (i) initialization component: an initial population of vectors of the design variables **x** is randomly generated; (ii) fitness evaluation component: each member of the population is evaluated by computing the representative penalized objective and the corresponding fitness functions, using an appropriate penalty function; (iii) selection component: a selection operation is applied to the current population, leading to the definition of a "temporary population"; (iv) generation component: crossover and mutation operators are applied to the "temporary population" to create the next population; (v) fitness evaluation component: applied to the "temporary population", and (vi) convergence check component.

6.4 Numerical application

6.4.1 MDOF linear building structure

In this section, the proposed methodology is applied to a linear three-DOF structural system subjected to a non-stationary stochastic excitation. All floors have a constant height equal to 3m, leading to a total height of 9m. The masses of the plates regarded as constant for all floors ($m_{plate} = 10^4$kg). Further, the young modulus E and the mass density ρ are assumed to be equal to 30×10^9Pa and $2{,}5 \times 10^3 kg/m^3$ respectively; the weighting coefficients vector $\boldsymbol{\gamma}$ is assumed to be equal to $[m_i]$. A side view of the structural model can be seen in Fig.(6.1).

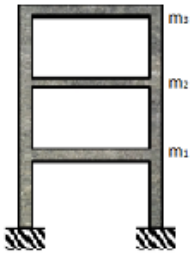

Figure 6.1. Linear 3-DOF structural system.

Considering relative floor displacements with respect to the ground motion, the three-DOF linear structural system is governed by Eq.(6.1) where

$$\mathbf{q}^T = (q_1\ q_2\ q_3), \tag{6.10}$$

$$\mathbf{M} = \begin{bmatrix} m_1 & 0 & 0 \\ 0 & m_2 & 0 \\ 0 & 0 & m_3 \end{bmatrix}, \tag{6.11}$$

and

$$\mathbf{K} = \begin{bmatrix} k_1 + k_2 & -k_2 & 0 \\ -k_2 & k_2 + k_3 & -k_3 \\ 0 & -k_3 & k_3 \end{bmatrix}. \tag{6.12}$$

Next, a Rayleigh damping model is assumed. The damping matrix is expressed as a linear combination of the mass and stiffness matrices according to the expression

$$\mathbf{C} = \alpha_{\mathrm{M}}\mathbf{M} + \beta_K\mathbf{K}, \tag{6.13}$$

where $a_M = 3.5$ and $\beta_K = 1 \times 10^{-4}$. Further, the loading vector takes the form

$$\mathbf{F}(\mathrm{t})^{\mathrm{T}} = \left(\mathrm{f}_1(\mathrm{t})\ \mathrm{f}_2(\mathrm{t})\ \mathrm{f}_3(\mathrm{t})\right). \tag{6.14}$$

Results obtained using the quasi-stationary approach are validated based on comparisons with pertinent Monte Carlo simulation data. In this regard, a set of 5,000 ground motion records compatible with a given EPS are generated according to the spectral representation method (Shinozuka and Deodatis, 1991). The excitation EPS $\mathrm{S}_{\ddot{\alpha}_\mathrm{g}}(\omega, \mathrm{t})$ is assumed to have the separable form given by Eq.(2.5) in which a=0.1 and b=0.3; In Fig.6.2, for amplitude $\mathrm{S_o} = 500\mathrm{m}^2/\mathrm{sec}^3$, the power spectrum (PS) of the embedded stationary process as well as the EPS of the stochastic excitation are plotted. The following values of the parameters are used: $\xi_\mathrm{g} = 0.5, \omega_\mathrm{g} = 1\ \mathrm{rad/s}$, $\xi_\mathrm{f} = 1$, $\omega_\mathrm{f} = 40\ \mathrm{rad/s}$.

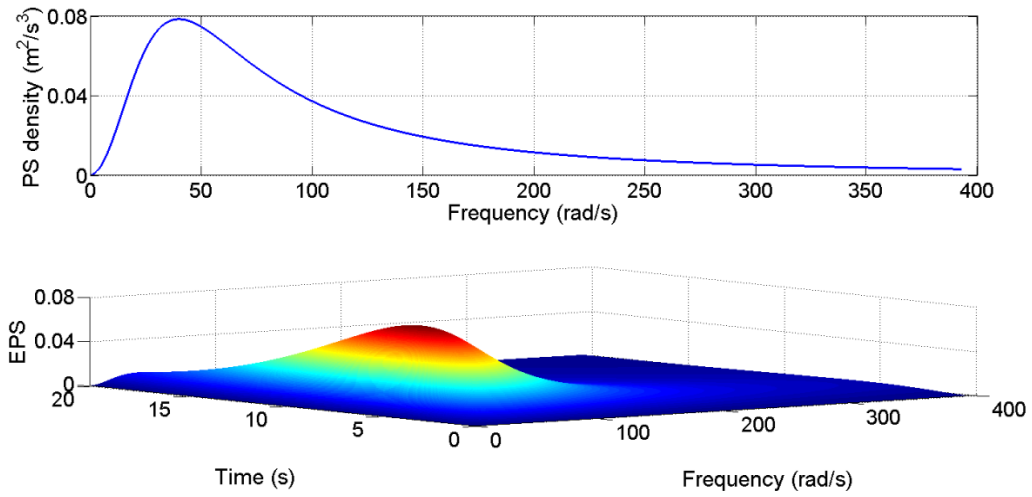

Figure 6.2. PS $\mathrm{S}_{\mathrm{CP}}(\omega)$ and EPS $\mathrm{S}_{\ddot{\alpha}_\mathrm{g}}(\omega, \mathrm{t})$ of the imposed stochastic excitation.

The duration of the considered excitation is taken equal to 20 seconds. Hereinafter, this earthquake excitation model is utilized. In Figs.(6.3-6.4), analytical estimates based on the quasi-stationary approach (see Eqs.(6.4-6.6)) are compared with MCS data demonstrating a high level of accuracy. Further, note that the quasi-stationary approach provides a conservative estimate of the response standard deviation peak values. Next it is deemed appropriate to recall the relation between relative floor displacements with respect to the ground motion and inter-story drifts i.e.,

$$y_{i+1} = q_{i+1} - q_i, \quad i = 1,2,..n_{dof}. \tag{6.15}$$

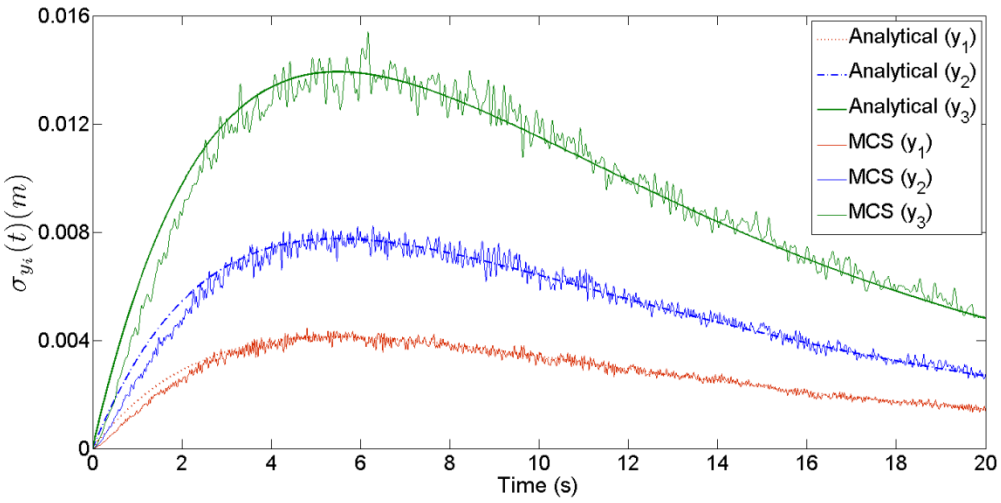

Figure 6.3. Analytical response estimates of the standard deviation of the relative displacements via the quasi-stationary approach compared to MCS data for a set of 5000 realizations ($x^{in} = [0.35m, 0.25m, 0.15m]^T$).

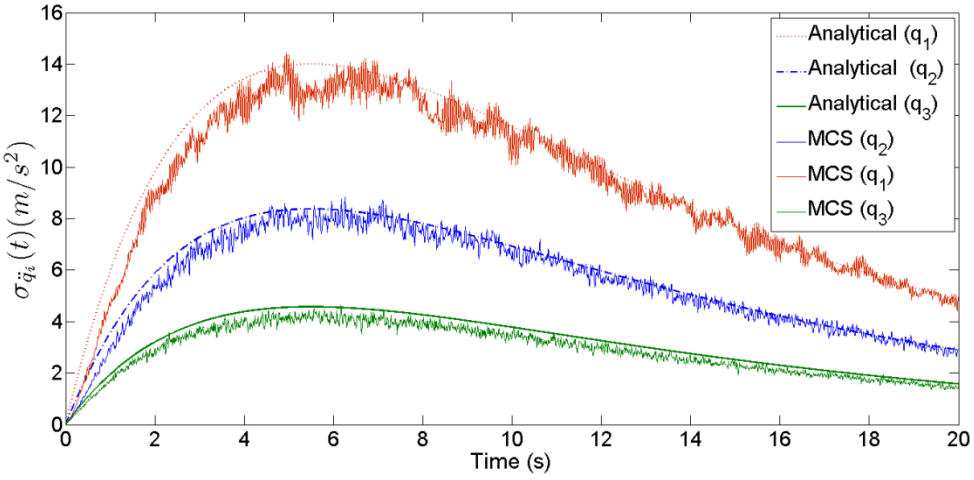

Figure 6.4. Analytical response estimates of the standard deviation of the absolute accelerations via the quasi-stationary approach compared to MCS data for a set of 5000 realizations ($\mathrm{x}^{\mathrm{in}} = [0.35\mathrm{m}, 0.25\mathrm{m}, 0.15\mathrm{m}]^{\mathrm{T}}$).

6.4.2 Performance measures for the determination of the response of a linear MDOF structural system

As discussed earlier, for structural systems under seismic excitation, inter-story drift and absolute floor acceleration become key performance measures for assessing the performance of the structural system. Commonly, structural optimization design approaches yield optimal designs that present very limited inter-story drifts, neglecting the effect of floor acceleration on generating a wide range of failures, mainly related to mechanical, electrical, and hydraulic equipment. Consider next the defined three-degree-of-freedom structural system excited by the evolutionary stochastic seismic excitation. Utilizing the analytical/approximate approach (see Eqs.(6.4), (6.6) and (6.15)), maximum over time non-stationary values of the standard deviation of inter-story drifts as well as absolute floor accelerations are determined specifically for the first floor. In this section, the aim is to demonstrate the interaction and identify potential trade-offs when choosing constraints related to both system response displacement and acceleration. Next, it is assumed that the superstructure (greater than first floor) columns' cross-sections remain

constant over this parametric study. Focus is directed next on the performance measures associated with the first floor.

Considering Fig.(6.5) it can reasonably be argued that increasing the corresponding structural elements stiffness reduces the response displacement drift. However, it results in higher values of the corresponding floor absolute acceleration.

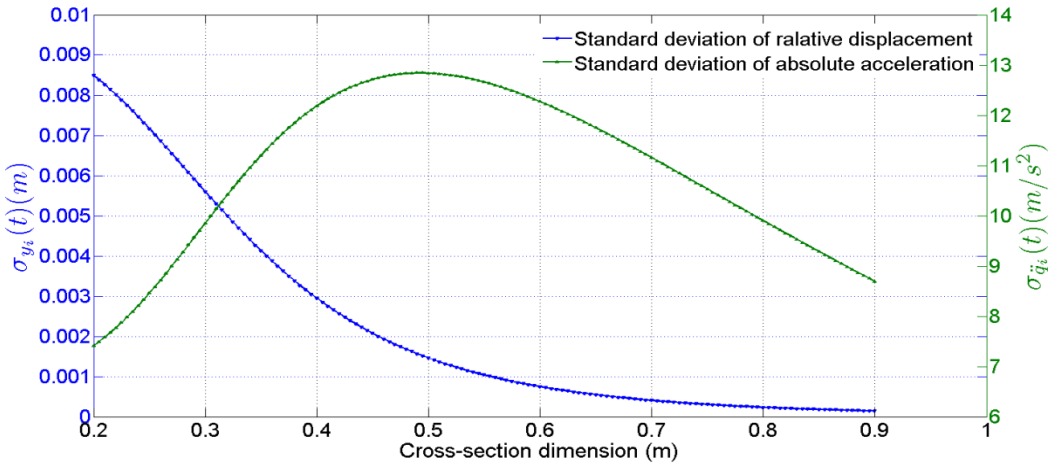

Figure 6.5. Performance measures trade-offs.

To elaborate further, it can be readily seen that although the amplitude of the frequency response function (FRF) Fig.(6.6) close to resonance decreases with increasing the stiffness (larger cross-section dimensions), the response acceleration variance given by Eq.(6.6) increases for a certain range of cross-section dimensions. This is due to the trade-off between the FRF and the term ω^4. For high values of the stiffness the decrease in the FRF dominates over the effect of ω^4 yielding a decreasing trend in the response acceleration.

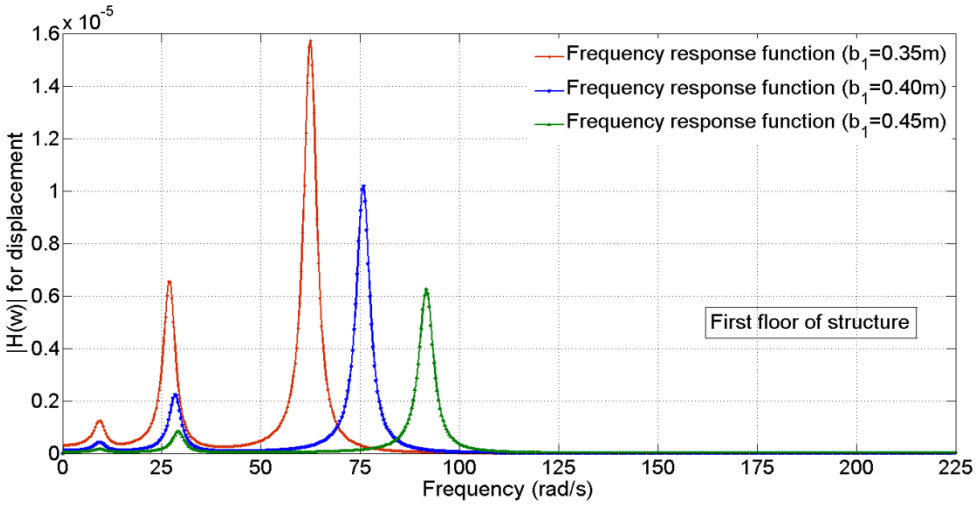

Figure 6.6. Frequency response functions considering the first floor of the structure.

6.4.3 Robust design optimization problem considering various performance measures statistics

A deterministic objective function is chosen for the robust design optimization problem corresponding to the total weight of the column elements plus that of plates. The response of the structural system is constrained in terms of the maximum over time non-stationary values of the standard deviation of inter-story drifts and absolute floor accelerations. The design variables are the dimensions of the square cross-section of the column elements. Columns' cross-section dimensions for a given floor are assumed to be equal, and thus the vector of design variables $\mathbf{x}$ has three components, one for every story. Assume an initial design $\mathrm{x}^{\mathrm{in}} = [0.35, 0.25, 0.15]^{\mathrm{T}}$ and boundary constraints $\mathrm{D} = [0.30, 1.00]$ expressed in (m). The problem under consideration is written as

$$\min_{\mathbf{x}\in \mathrm{D}} \mathrm{w}(\mathbf{x}) \tag{6.16}$$

subject to the following stochastic constraints

$$\boldsymbol{\sigma}_{\mathrm{y}}(\mathrm{t}, \mathbf{x}) = [\sigma_{\mathrm{y_i}}(\mathrm{t}, \mathbf{x})] \leq \sigma_{\mathrm{y}}^{\mathrm{Lim}} \tag{6.17}$$

$$\boldsymbol{\sigma}_{\ddot{\mathrm{q}}}(\mathrm{t}, \mathbf{x}) = [\sigma_{\ddot{\mathrm{q}}_{\mathrm{i}}}(\mathrm{t}, \mathbf{x})] \leq \sigma_{\ddot{\mathrm{q}}}^{\mathrm{Lim}}, \quad \mathrm{i} = 1,2 \ldots \mathrm{n}_{\mathrm{dof}} \tag{6.18}$$

Next, $w(\mathbf{x})$ is defined as the building structure weight which includes the weight of the column elements plus the weight of the plates evaluated at the design variables vector $\mathbf{x}$; $\boldsymbol{\sigma}_{y}(t,\mathbf{x})$ stands for the vector of the maximum over time non-stationary values of the standard deviation of the inter-story drifts while $\boldsymbol{\sigma}_{\ddot{q}}(t,\mathbf{x})$ represents the vector of the maximum over time non-stationary values of the standard deviation of the absolute floor accelerations. Upper bounds for the constraints are imposed as follows: $\sigma_{y}^{Lim} = 6\,x10^{-3}m$ (0,2% of the inter-story height) and $\sigma_{\ddot{q}}^{Lim} = 1.25g = 12.25m/s^2$ where $g = 9.81\,m/s^2$. The selection of the upper bound threshold for the absolute floor accelerations was made based on reasonable conclusions of the work of Elenas and Mescouris (2001).

Cross section's dimensions and response statistics regarding the initial and the proposed optimal design are shown in Table.6.1. Interpreting the results, adjusting properly the dimensions of the columns leads to a design solution that guarantees a quite robust structural performance with respect to both performance measures. Note that the crucial response statistics remain controllable under the design imposed constraints.

Initial design			Proposed optimal design		
x_i (m)	$\sigma_{y_i}^{max}(t,x)$ (10^{-3} m)	$\sigma_{\ddot{q}_i}^{max}(t,x)$ (m/s^2)	x_i (m)	$\sigma_{y_i}^{max}(t,x)$ (10^{-3} m)	$\sigma_{\ddot{q}_i}^{max}(t,x)$ (m/s^2)
0.350	4.13	14.01	0.281	5.9	12.25
0.250	7.81	8.38	0.283	5.9	11.89
0.150	13.91	4.57	0.294	6.0	10.08
Structural weight (kg): $3.311x10^4$			$3.368x10^4$		

Table 6.1. Initial and optimal design solution.

In Figs.(6.7-6.8) the time-varying standard deviations of inter-story drifts and absolute floor accelerations are plotted. It is noteworthy that the proposed optimal design's second order statistics strictly comply with the imposed design constraints for the whole duration of the seismic excitation.

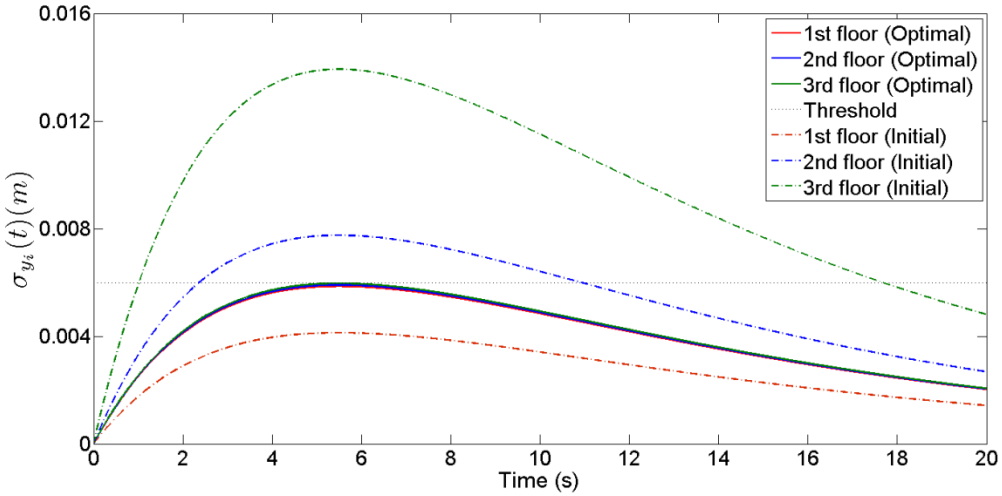

Figure 6.7. Non-stationary values of the standard deviation of inter-story drifts for the initial and optimal design solution.

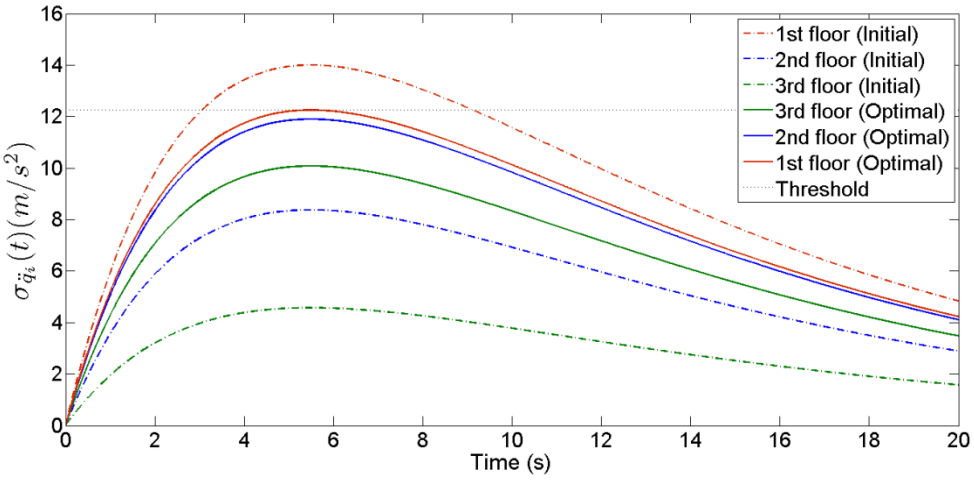

Figure 6.8. Non-stationary values of the standard deviation of the absolute floor acceleration for the initial and optimal design solution.

In general, a framework for the efficient solution of structural robust design optimization problem has been proposed which features controlling both inter-storey drift and absolute floor acceleration non-stationary second order statistics. However,

incorporation of design variables in damping elements as well, via the placement of nonlinear dampers would allow to highlight further the potentials of the proposed framework in the joint time-frequency domain. Notably, the extension of the herein framework for considering structural systems with nonlinearities via a statistical linearization approach and perhaps in conjunction with compatible excitation power spectra to current aseismic code provisions (e.g, Giaralis and Spanos, 2012) is identified as part of future work.

Chapter 7

Structural system performance-based multi-objective optimum design determination considering life-cycle cost

7.1 Preliminary remarks

Most structures and civil infrastructure systems are subject to excitations that exhibit strong variability in both the intensity and the frequency content. Clearly, a realistic system analysis and design necessitates the representation of this class of loads by non-stationary stochastic processes (e.g., Soong and Grigoriu, 1993; Roberts and Spanos, 2003; Li and Chen, 2009; Spanos and Kougioumtzoglou, 2012). Further, structural systems under severe excitations, such as earthquakes, can behave in a nonlinear manner exhibiting a hysteretic restoring force-displacement characteristic. Thus, a sustained challenge in the area of structural dynamics has been the efficient analysis and design of nonlinear/hysteretic systems/structures under evolutionary stochastic excitation.

Further, due to the apparent limitations of a purely deterministic treatment of the structural design optimization problem, several optimization frameworks considering uncertainty have been developed such as robust, reliability-, and risk-based optimization (e.g., Gasser and Schüeller, 1997; Au and Beck, 2003; Jensen, 2009; Beck and Gomes, 2012). In general, a stochastic approach to the structural design optimization problem constitutes a rational framework for providing design configurations that perform in a desirable and consistent manner over the entire design life of the structure. Note, however, that a comprehensive treatment of the stochastic design optimization problem can be a complex task due to inter-related challenges associated with uncertainty treatment. These may include (i) uncertainty modeling, i.e. stochastic representation/modeling of structural system parameters/properties and/or excitation, (ii)

uncertainty propagation, i.e. efficient structural system response statistics determination, and (iii) the solution of an inverse stochastic problem, i.e. an efficient design optimization procedure.

In this regard, the PBE framework aims at providing information for facilitating risk-based decision-making via performance assessment and design methods that properly account for the presence of uncertainties (e.g., Ellingwood, 2001; Porter, 2003). Depending on the hazard kind considered, several PBE-based frameworks have been developed recently in various fields of structural engineering such as earthquake, wind, hurricane, and fire engineering (e.g., Cornell and Krawinkler, 2000; Ellingwood, 2001; Porter, 2003; Ciampoli and Petrini, 2012; Barbato and Petrini, 2013). Although the herein developed PBE framework is tailored specifically for earthquake engineering related applications in general agreement with the PBEE framework proposed by the PEER center (e.g., Cornell and Krawinkler, 2000; Mohle and Deierlein, 2004; Der Kiureghian, 2005), it can be readily modified to account for other hazard kinds as well.

Further, as far as the decision variable (DV) is concerned, the seismic LCC accounting for the structure lifetime expected damage costs is commonly adopted (e.g., Wen and Kang, 2001). Indicatively, Kong and Frangopol (2003) addressed the bridge maintenance schedule optimal design problem and estimated the life-cycle cost performance. Further, adopting a median global Park-Ang damage index, Ang and Lee (2001) considered repair costs for various ground motion intensity levels for the case of reinforced concrete buildings. In Fragiadakis et al. (2006) and Liu et al. (2003) a probabilistic multi-objective optimization framework was applied for the life-cycle cost optimal seismic design of steel structures. Further, Taflanidis and Beck (2009) focused on assessing the performance of passive dissipative devices by utilizing an efficient simulation approach within a performance-based seismic design framework that optimized the expected life cycle cost of structural systems. Next, Takashi et al. (2004) relied on a Monte Carlo simulation approach for assessing the life-cycle cost of a structural system equipped with damping devices.

Regarding the uncertainty associated with the seismic ground motion this is normally described by a probability distribution of a seismic IM such as the spectral acceleration or the PGA. Focusing on the latter case, a mean seismic hazard curve is routinely provided specifying the annual probability of exceeding various levels of PGA. Further, several approaches have been developed for relating the seismic hazard to the system fragility and for producing corresponding fragility curves, i.e. probabilities of exceeding specified damage states given an IM value. These range from the ones that employ a limited number of nonlinear time-history analyses with prescribed IM level compatible scaled real earthquake records (e.g., Vamvatsikos and Cornell, 2002), to the ones that employ standard or efficient Monte Carlo simulation (MCS) based methodologies such as importance/line sampling, and subset simulation (e.g., Rubinstein, 1981; Au and Beck, 2003; Schueller et al., 2004). Nevertheless, note that there are cases where the computational cost of the MCS based techniques can be significantly high; thus, rendering their use computationally cumbersome, or even prohibitive.

Clearly, there is a need for developing approximate analytical and/or numerical techniques for determining efficiently the response and reliability statistics of nonlinear systems subject to stochastic excitation; see (e.g., Soong and Grigoriu, 1993; Roberts and Spanos, 2003; Lutes and Sarkani, 2004; Fujimura and Der Kiureghian, 2007; Kougioumtzoglou and Spanos, 2013) for some recent references. Nevertheless, although there is a considerable body in the literature referring to the development of such techniques there are limited results related to utilizing such techniques. An interesting contribution in this regard is the work by Der Kiureghian and Fujimura (2009) where an efficient tail-equivalent linearization based approach was applied for fragility analysis of a nonlinear building structure.

In this chapter, a PBE multi-objective design optimization framework for nonlinear/hysteretic MDOF structural systems subject to evolutionary stochastic earthquake excitation is formulated. The developed framework is based on an efficient approximate analytical dimension reduction approach for determining the system response EPS matrix based on the concepts of statistical linearization and stochastic

averaging; thus, computationally intensive Monte Carlo simulations are circumvented. Note that the approach can handle readily stochastic excitations of arbitrary EPS forms, even of the non-separable kind. Further, approximate closed-form expressions are derived for the non-stationary response amplitude PDFs of the IDRs corresponding to each and every DOF. In this regard, considering appropriately defined damage measures structural system related fragilities are determined at a low computational cost as well. Further, note that the multi-objective optimization (e.g., Jensen, 2009) allows for objectives that exhibit potentially conflicting requirements to be treated simultaneously. In the present formulation, solving the multi-objective optimization problem typically suggests the determination of a set of Pareto optimal solutions (Pareto front). Each solution of the Pareto front constitutes an acceptable design configuration compromising the potentially conflicting sub-objectives of the problem.

Overall, the proposed framework appears to be highly efficient for performing stochastic design optimization, reducing significantly the computational burden for this task. Further, in the proposed design methodology, for the first time in the literature an efficient approximate nonlinear stochastic dynamics technique, which can handle readily cases of nonlinear/hysteretic systems and of non-stationary stochastic excitations of arbitrary evolutionary power spectrum forms, is incorporated in a robust PBE-based framework for addressing the so called LCC stochastic design optimization problem; thus, circumventing computationally intensive Monte Carlo simulations.

Following this introductory section, in section 7.2 the developed PBEE framework is unfolded. Specifically, the mathematical formulation is provided in sections 7.2.1 and 7.2.2. In section 7.3 the formulation of the stochastic multi-objective optimization problem is delineated. In section 7.4 an illustrative example comprising the versatile Bouc-Wen (hysteretic) model is considered for demonstrating the efficiency of the proposed approach. Comparisons with pertinent Monte Carlo simulations are included as well demonstrating a satisfactory level of accuracy exhibited by the proposed technique.

7.2 Mathematical formulation

7.2.1 Statistical linearization based dimension reduction approach

Consider an n-degree-of-freedom nonlinear structural system governed by the Eq.(3.1) where $\ddot{\mathbf{y}}, \dot{\mathbf{y}}$ and $\mathbf{y}$ denote the response acceleration, velocity and displacement vectors, respectively, defined in relative coordinates; namely that the vector $\mathbf{y}$ contains the inter-story drifts. $\mathbf{M}$, $\mathbf{C}$ and $\mathbf{K}$ denote the $(n \times n)$ mass, damping and stiffness matrices, respectively; $\mathbf{g}(\mathbf{y}, \dot{\mathbf{y}}, t)$ is assumed to be an arbitrary nonlinear $(n \times 1)$ vector function of the variables $\mathbf{y}$, $\dot{\mathbf{y}}$ and t; and $\mathbf{f}(t)^T = (f_1(t), f_2(t), \dots, f_n(t)$ is a $(n \times 1)$ zero mean, non-stationary stochastic vector process defined in Eq.(3.2) where $\boldsymbol{\gamma} = [m_i]$. Regarding the excitation EPS $S_{\ddot{\alpha}_g}(\omega, t)$, it is assumed to have the separable form given in Eq.(2.5). Further, utilizing the statistical linearization approach presented in section 3.2 the following expressions regarding the variances of the response displacement and velocity are defined

$$\sigma_{y_i}^2(t) = \int_{-\infty}^{\infty} (|H_{i1}(\omega)|^2 {m_1}^2 + \cdots + |H_{in}(\omega)|^2 {m_n}^2)\, S_{\ddot{\alpha}_g}(\omega, t) d\omega, \tag{7.1}$$

and

$$\sigma_{\dot{y}_i}^2(t) = \int_{-\infty}^{\infty} \omega^2 (|H_{i1}(\omega)|^2 {m_1}^2 + \cdots + |H_{in}(\omega)|^2 {m_n}^2)\, S_{\ddot{\alpha}_g}(\omega, t) d\omega. \tag{7.2}$$

Next, following the dimension reduction/decoupling approach in conjunction with the stochastic averaging treatment delineated analytically in section 3.3 and 3.4 respectively, the efficient determination of the time-dependent response amplitude PDF is achieved through the Eqs.(3.25-3.26). Note in passing that the computational cost is kept at a minimum level. Further, it can be readily seen that the approximate analytical nonlinear stochastic dynamics technique presented in chapter 3 not only determines the original MDOF system response amplitude PDF $p(\alpha_i, t)$ for each and every DOF in an efficient manner by circumventing computationally demanding MC simulations, but also

decouples the original system providing with effective time-varying stiffness and damping elements corresponding to the i-th DOF. The latter feature is especially important for a number of reasons such as determining peak system response estimates based on design spectrum compatible excitation power spectra (e.g., Giaralis and Spanos, 2010; Spanos and Giaralis 2013), tracking and avoiding moving resonance phenomena (e.g., Tubaldi and Kougioumtzoglou, 2014), and developing efficient approximate techniques for determining nonlinear system survival probabilities and first-passage PDFs (e.g., Solomos and Spanos, 1983; Spanos and Kougioumtzoglou, 2014; Mitseas et al., 2014b).

Furthermore, the herein considered damage states (DS) are expressed in terms of the IDR that is defined as the difference of the horizontal displacements between two successive stories, normalized by the inter-story height h. Considering in the ensuing analysis the IDR amplitude $A_i(t)$, a direct transformation (e.g. Ang and Tang, 2007) of the response amplitude PDF $p(\alpha_i, t)$ (see Eq.(3.25)) yields the non-stationary IDR amplitude PDF in the form

$$p(A_i, t) = h^2 \frac{A_i}{c_i(t)} \exp\left(-\frac{h^2 {A_i}^2}{2c_i(t)}\right). \tag{7.3}$$

Further, of particular interest from a reliability assessment perspective is the time instant where the IDR amplitude reaches its most critical value, i.e. $p_{cr}(A_i) = p(A_i, t = t_{cr})$. In the following, this is assumed to be the time where $c_i(t)$ reaches its peak value, and thus, the PDF of Eq.(7.3) takes its most broad-band form yielding higher failure probabilities. Specifically, the failure probability P_i defined as the probability of exceeding various levels of damage δ_{ds} conditioned upon the peak ground acceleration (PGA), is expressed as

$$P_i[A_i(t) \geq \delta_{ds} = \delta \big| \mathrm{PGA} = \alpha_{pga}] = 1 - \int_0^{\delta} p_{cr}\left(A_i \big| \mathrm{PGA} = \alpha_{pga}\right) dA \tag{7.4}$$

Considering Eq.(7.3), and integrating analytically Eq.(7.4) yields

$$P_i[A_i(t) \geq \delta_{ds} = \delta \big| PGA = \alpha_{pga}] = \exp\left(-\frac{h^2\delta^2}{2c_i(t)}\right). \quad (7.5)$$

It is deemed appropriate to note that the above determined failure probability of Eq.(7.5) should not be confused with the first-passage kind failure probability. The former does not pose any restriction to the number of times failure can occur, whereas the latter is uniquely defined by satisfying a failure criterion for the first time, or in other words the interest lies in the first time that failure occurs. It can be argued that the failure definition of Eq.(7.5) is more relevant to the herein considered applications since the drift ratio amplitude may cross a prescribed damage level several times during an earthquake event without leading to total collapse of the structure.

7.2.2 Life-cycle cost PBE framework

The PBE methodology serves as a potent stochastic framework for assessing the performance of engineering structural systems subject to various hazards via an appropriately defined DV. For the specific case of PBEE (e.g., Cornell and Krawinkler, 2000; Mohle and Deierlein, 2004; Der Kiureghian 2005), the evaluation of a DV typically depends on a number of analysis components such as (i) stochastic hazard analysis treating the uncertainty in the seismic input IMs; the seismic hazard is usually described by the annual probabilities of exceeding various levels of IMs, (ii) stochastic structural analysis associated with the uncertainty of the engineering demand parameter (EDP) used to monitor the structural response conditional on the IMs; the IDR is a commonly selected EDP for building structures, (iii) stochastic damage analysis relating the EDPs to DS, which in turn describe the generated damage, and (iv) stochastic loss analysis reflecting the effect of the underlying uncertainties on a quantifiable DV.

The uncertainty in seismic ground motions is normally described in terms of the probability distribution of a seismic intensity measure, such as the PGA. In this regard, the seismic hazard is presented as a mean seismic hazard curve $H(\alpha_{pga})$, which provides the annual probability of exceeding specified levels of PGA (e.g., Cornell et al., 2002; Tubaldi et al., 2014); that is,

$$H(\alpha_{pga}) = P[PGA \geq \alpha_{pga}]. \quad (7.6)$$

In various PBEE studies (e.g. Liu et al., 2003; Fragiadakis et al., 2006) as well as in the ensuing analysis, discrete DS are considered. The non-stationary IDR amplitudes $A_i(t)$ serve as global EDPs while the employed relationship between the EDP and the DS is based on the work by Ghobarah (2004) related to ductile reinforced concrete (RC) moment resisting frames (see Table. 7.1). Note that IDR constitutes one of the most reliable measures of structural damage due to its close relationship to plastic rotation demands for individual beam-column connection assemblies. Typically, the damage states for reliability analysis purposes are defined in terms of the overall inelastic deformation or the maximum inter-story drift of the structural system (Ellingwood, 2001).

Damage State	Inter-Story Drift (%)	Cost (% C_{in})
(I)-None	$0.0 \leq \delta_{ds} < 0.1$	0
(II)-Slight	$0.1 \leq \delta_{ds} < 0.2$	0.5
(III)-Light	$0.2 \leq \delta_{ds} < 0.4$	5
(IV)-Moderate	$0.4 \leq \delta_{ds} < 1.0$	20
(V)-Heavy	$1.0 \leq \delta_{ds} < 1.8$	45
(VI)-Major	$1.8 \leq \delta_{ds} < 3.0$	80
(VII)-Destroyed	$3.0 \leq \delta_{ds}$	100

Table 7.1. Damage states (DS), Inter-story drift ratio limits δ_{ds} and associated costs.

Further, the seismic fragility curves serving as a quantitative tool of the structure vulnerability are evaluated for various damage levels. Specifically, based on the approximate nonlinear stochastic dynamics technique briefly outlined in section 7.2.1, the seismic fragility curves are efficiently determined by simply integrating the critical non-stationary response IDR amplitude PDF $p_{cr}(A_i)$ for the time instant t_{cr}; see Eqs.(7.3-7.4). In this regard, the probability of the i–th DOF exceeding various levels of damage given a specified PGA value, i.e. $P_i[A_i(t) \geq \delta_{ds} = \delta | PGA = \alpha_{pga}]$, can be efficiently computed via Eq.(7.5).

Notably, the fragility curves corresponding to each and every DOF for various damage levels are determined at a minimum computational cost via Eq.(7.5). Next, considering the i-th DOF of the MDOF system, the annual probability of exceeding a given state of damage can be defined as

$$\mathrm{P_{i,a}} = \int \mathrm{P_i}\left[\mathrm{A_i(t)} \geq \delta_{ds} = \delta \middle| \mathrm{PGA} = \alpha_{\mathrm{pga}}\right] \left|\frac{\mathrm{dH}(\alpha_{\mathrm{pga}})}{\mathrm{d}\alpha_{\mathrm{pga}}}\right| \mathrm{d}\alpha_{\mathrm{pga}}. \tag{7.7}$$

In the herein study, the earthquake occurrence is assumed to follow a Poisson process (e.g., Ellingwood and Wen, 2005). Further, the expected value of the life-cycle cost (LCC) due to seismic hazard can be expressed in the form

$$\mathrm{E}\left[\mathrm{LCC}\left(\mathrm{A_i}(\mathbf{x},\mathbf{t})\right)\right] = \frac{1}{\lambda T_d}(1 - \exp\left(-\lambda T_d\right)) \times \ldots$$

$$\sum_{\mathrm{i=1}}^{\mathrm{n_{dof}}} \sum_{\mathrm{m=1}}^{\mathrm{n_{ds}}} \left(-\mathrm{C_m}\left[\ln\left(1 - \mathrm{P_{i,T_d}}(\mathrm{A_i(t)} > \delta_{\mathrm{m}})\right) - \ln\left(1 - \mathrm{P_{i,T_d}}(\mathrm{A_i(t)} > \delta_{\mathrm{m+1}})\right)\right]\right), \tag{7.8}$$

where $\mathrm{n_{ds}}$ is the total number of damage states considered; $\mathrm{n_{dof}}$ is the number of degrees of freedom of the MDOF system, λ is a constant discount rate/year, T_d is the design life of the structure, $\mathrm{C_m}$ is the cost associated with the m-th damage state, given in Table 7.1 as a percentage of the initial cost; $\mathrm{P_{i,T_d}}$ refers to the i-th DOF and represents the T_d-year probability of exceeding the m-th damage state given by the expression

$$\mathrm{P_{i,T_d}} = 1 - \exp\left(-\mathrm{P_{i,a}} T_d\right). \tag{7.9}$$

Furthermore, it is assumed that the structure is restored to its initial undamaged state after each earthquake occurrence, whereas losses due to fatalities and building downtime are ignored in this study.

Note that in the herein proposed LCC model the contribution of each and every DOF is considered resulting in a better account of the system overall performance; this is not the case with commonly used LCC models in PBEE studies where the system performance is associated with the most critical component only (e.g., Ellingwood, 2001; Liu et al., 2003; Fragiadakis et al., 2006). Considering cases where the roof drift is

employed as an EDP, the corresponding damage analysis cannot account for the distribution of damage along the height of the structure, or take into account soft stories phenomena (e.g., Ghobarah, 2004). Further, the adoption of the maximum value of the induced inter-story drifts as an EDP leads to a stochastic damage analysis based on information corresponding to a specific story only. Thus, information regarding the response behavior of the rest of the stories and their contribution to damage is disregarded.

Overall, in the herein novel proposed LCC formulation the expected value of the seismic losses given by Eq.(7.8) serves as the DV, whereas the attribute of considering n_{dof} EDPs is expected to better account for the system overall performance in the formulation of the multi-objective optimization problem in the following section.

7.3 Formulation of the optimal design problem

7.3.1 Multi-objective optimization

In the field of structural system optimization, most often several conflicting objectives need to be treated simultaneously. In this regard, a multi-objective optimization problem is formulated yielding a compromise between various objective functions. A general stochastic multi-objective optimization formulation for the determination of a vector $\mathbf{x}$ of design variables to minimize a vector of objective functions takes the form

$$\min_{\mathbf{x}\in D} \mathbf{F}(\mathbf{x}), \tag{7.10}$$

where

$$\mathbf{F}(\mathbf{x}) = \left[f_z^{ind}(\mathbf{x})\right] = \left[f_1^{ind}(\mathbf{x}), \dots, f_{nobj}^{ind}(\mathbf{x})\right], z = 1, \dots, n_{obj}$$

$$\mathbf{x} = \left[x_j\right] = [x_1, x_2, \dots x_{n_{dv}}]^T, j = 1, .. n_{dv}, \mathbf{x} \in D, \tag{7.11}$$

subject to system response level constraints of the form

$$\mathbf{G}(\mathbf{x}) = \left[g_p^{ind}(\mathbf{x})\right] = \left[g_1^{ind}(\mathbf{x}), \dots, g_{ncon}^{ind}(\mathbf{x})\right] \leq 0, p = 1, \dots, n_{con}\,. \tag{7.12}$$

In the case of a stochastic objective function $\mu_{f_z}^{stoch}(\mathbf{x})$ and $\sigma_{f_z}^{stoch}(\mathbf{x})$ are employed. $\mu_{f_z}^{stoch}(\mathbf{x})$ and $\sigma_{f_z}^{stoch}(\mathbf{x})$ are the maximum over time non-stationary values of the mean and standard deviation of the objective function $f_z^{stoch}(\mathbf{x})$ respectively, evaluated at the design variables vector $\mathbf{x}$; $f_z^{det}(\mathbf{x})$ is a deterministic objective function evaluated at the design variables vector $\mathbf{x}$; in case of a stochastic response constraint, $\mu_{g_p}^{stoch}(\mathbf{x})$ and $\sigma_{g_p}^{stoch}(\mathbf{x})$ stand for the maximum over time non-stationary values of the mean and standard deviation of the response function $g_p^{stoch}(\mathbf{x})$ respectively, evaluated at the design variables vector $\mathbf{x}$; $g_p^{det}(\mathbf{x})$ is a deterministic response level constraint evaluated at the design variables vector $\mathbf{x}$; and $\mathbf{G}(\mathbf{x})$ is the vector of the constraint functions of the optimization problem under consideration. D is a given set that contains the boundary constraints for the vector of design variables $\mathbf{x}$.

Further, a linear combination of the aforementioned quantities, which is the case in most practical applications (e.g., Jensen, 2009), is considered in the herein work as well. In this regard, a single parameterized objective function under several optimization runs with different parameter settings is responsible for the generation of the Pareto optimal set (e.g., Deb et al., 2002).

Considering next a combination of stochastic and deterministic objective functions $\mathbf{F}(\mathbf{x})$ is defined as a weighted linear combination of the individual objective components, i.e.

$$\mathbf{F}(\mathbf{x}) = \sum_{k=1}^{n_{obj}^{stoch}} \left(\frac{w_{\mu,\kappa}}{s_{\mu,\kappa}} \mu_{f_k}^{stoch}(\mathbf{x}) + \frac{w_{\sigma,\kappa}}{s_{\sigma,\kappa}} \sigma_{f_k}^{stoch}(\mathbf{x}) \right) + \sum_{n=1}^{n_{obj}^{det}} \left(\frac{w_n}{s_n} f_n^{det}(\mathbf{x}) \right), \qquad (7.13)$$

where $w_{\mu,\kappa}$, $w_{\sigma,\kappa}$ are weights and $s_{\mu,\kappa}$, $s_{\sigma,\kappa}$ are scale factors for the mean and standard deviation of the stochastic objective components $f_k^{stoch}(\mathbf{x})$, $k = 1, \dots, n_{obj}^{stoch}$; w_n and s_n are the weight and scale factor of the deterministic objective components $f_n^{det}(\mathbf{x}), n = 1,...,$nobjdet. Regarding the weighting factors w the following normalization is employed; that is,

$$\sum_{z=1}^{n_{obj}} w_z = 1. \tag{7.14}$$

The weighting factors can be adjusted appropriately, according to the importance of each objective and therefore the trade-off between the objectives can be readily studied. Any combination of the weighting factors corresponds to a single Pareto optimal solution (e.g., Liu et al., 2003; Fragiadakis et al., 2006; Jensen, 2009). Thus, by performing a set of optimization processes utilizing various weighting factors combinations it is possible to generate the full set of the Pareto optimal solutions.

Since the generation of the Pareto optimal set involves performing a number of optimization procedures, the selection of an optimization algorithm with considerable advantages specifically tailored to meet the characteristics of the herein problem formulation is of particular importance. Specifically, an outer loop that systematically varies the weighting factors of the parameterized objective function and an inner loop that features a standard genetic algorithm (GA) based optimization process are utilized for solving the multi-objective optimization problem. Regarding GAs, they belong to the class of Evolutionary algorithms (EAs) and they appear to be quite robust in the sense that they are less vulnerable to being trapped in local optima; and thus, more likely to obtain the global optimum for a non-convex constrained optimization problem (e.g., Bäck T., Schwefel, 1993).

7.4 Numerical application

In this section, the proposed methodology is applied to a 3-story reinforced concrete building which is modeled as a nonlinear/hysteretic 3-DOF structural system subject to evolutionary stochastic earthquake excitation. All floors are assumed to be rigid and have a constant height equal to 3m, whereas the masses of the plates are considered to be constant for all floors with a value $m_{plate} = 3.5 \times 10^4 \text{kg}$. A Young's modulus of $E = 30 \times 10^9 \text{Pa}$ and mass density of $\rho = 2{,}5 \times 10^3 \text{kg/m}^3$ are considered herein. The

nonlinearity is assumed to be in the form of the Bouc-Wen hysteretic model (e.g., Wen, 1980; Ikhouane and Rodellar, 2007). Columns' square cross-section dimensions for a given floor are assumed to be equal, and thus, the vector of design variables **x** has one component for every story, i.e. the width of the cross-section.

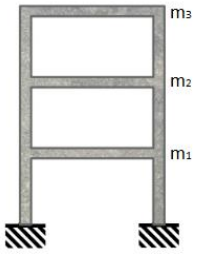

Figure 7.1. Nonlinear 3-DOF building structure.

7.4.1 Three-story Bouc-Wen hysteretic building structure

Considering displacements defined in relative coordinates, the 3-DOF nonlinear structural system is governed by Eq.(3.1) where

$$\mathbf{y}^{\mathrm{T}} = (\mathrm{y}_1\ \mathrm{y}_2\ \mathrm{y}_3\ \mathrm{z}_1\ \mathrm{z}_2\ \mathrm{z}_3). \tag{7.15}$$

The Bouc-Wen formulation related to MDOF systems which is unfolded in Eqs.(4.26-4.48) is also adopted herein. Considering the parameters of the model the following values are employed: $\mathrm{a} = 0.15$, $\beta = \gamma = 0.5$, $\mathrm{n} = 1$, $\mathrm{c_o} = 2 \times 10^{-2}$, and $\mathrm{A} = 1$. Regarding the excitation EPS $S_{\ddot{\alpha}_g}(\omega, \mathrm{t})$, it is assumed to have the separable form given in Eq.(2.5) where $\mathrm{b}_1 = 0.1$ and $\mathrm{b}_2 = 0.3$; the weighting coefficients vector $\boldsymbol{\gamma}$ is assumed to be equal to $[\mathrm{m_i}]$. The parameters values chosen are $\xi_g = 0.7, \omega_g = 2\ \mathrm{rad/s}$, $\xi_f = 0.6$, $\omega f = 12.5\ \mathrm{rad/s}$. The duration of the earthquake excitation *to* is assumed to be equal to 20 seconds. Note in passing that in the ensuing analysis the following definition for the α_{pga} is adopted; i.e.,

$$\alpha_{\mathrm{pga}} = \mathrm{E}\left[\max\left(\left|\ddot{\alpha}_{\mathrm{g}}(\mathrm{t})\right|\right)\right], \quad 0 \le t \le t_o \tag{7.16}$$

Thus, to provide with a mapping between the α_{pga} and the modulated C-P excitation spectrum intensity factor S_0, several MCS are conducted for various S_0 values via the

spectral representation approach of Shinozuka and Deodatis (1991). For each ensemble of excitation realizations Eq.(7.16) is applied for determining the value α_{pga} that corresponds to the given S_0. In this manner, repeating this process for various values of S_0 the relationship $S_0(\alpha_{pga})$ depicted in Fig.(7.2) is obtained.

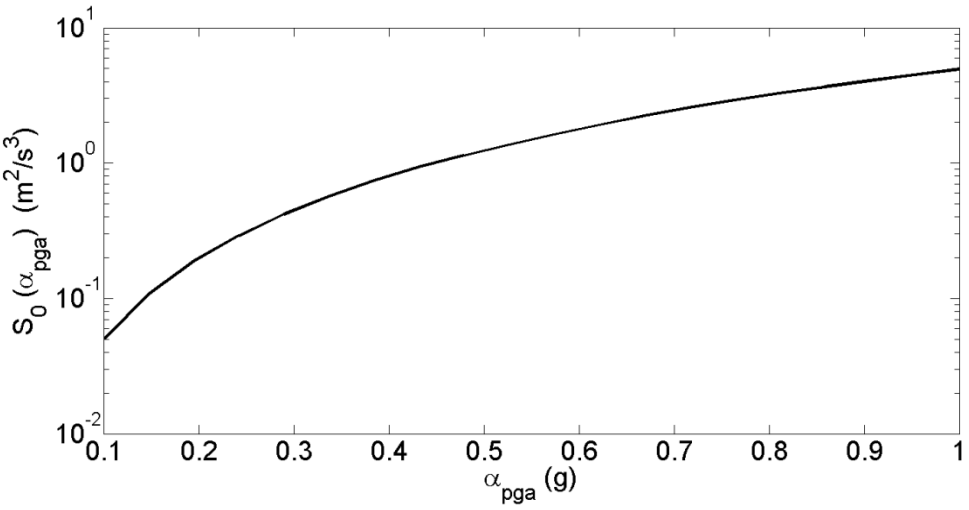

Figure 7.2. Mapping between the amplitude $S_0(\alpha_{pga})$ of the excitation spectrum and α_{pga}.

In Fig.(7.3), the EPS of $S_{\ddot{\alpha}_g}(\omega, t)$ is plotted for $S_0 = 0.5692\ m^2/s^3$ which corresponds to an acceleration of the earthquake input α_{pga} equal to $0.34g$ according to the definition of Eq.(7.16).

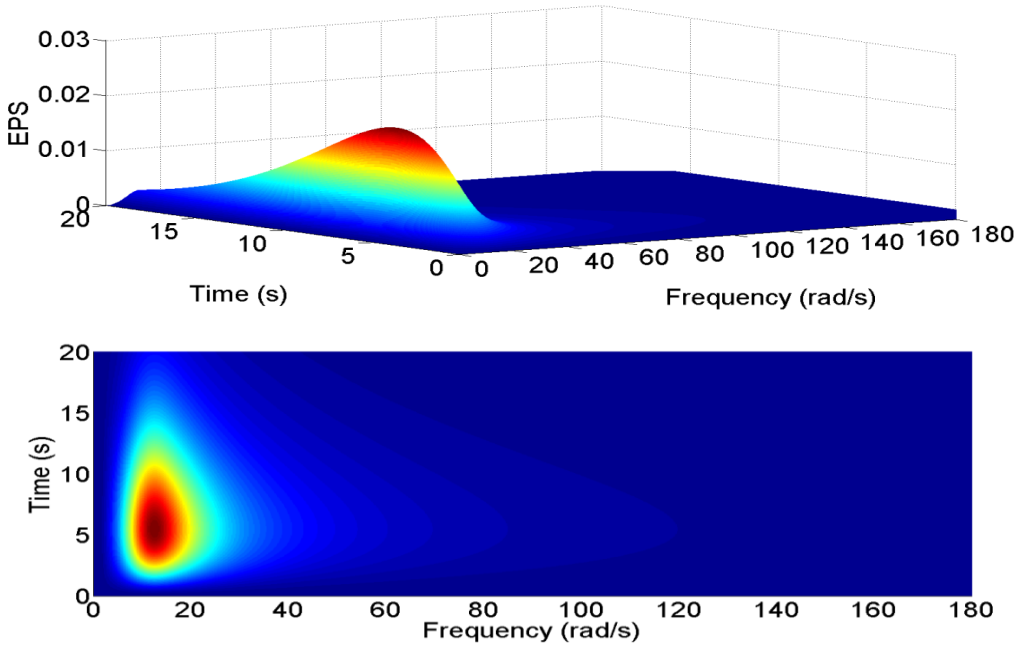

Figure 7.3. Clough-Penzien Evolutionary Power Spectrum $S_{\ddot{\alpha}_g}(\omega, t)$.

Note that the herein utilized C-P spectrum has been widely used in earthquake engineering applications, also as an excitation power spectrum model compatible with the seismic design spectrum (e.g., Giaralis and Spanos, 2010). Of course, more sophisticated than the C-P earthquake excitation models can be used if deemed necessary such as the ones in Boore (2003) or Rezaeian and Der Kiureghian (2008).

Next, the seismic hazard curve of Eq.(7.6) is expressed in the approximate form used in Cornell et al. (2002) and Tubaldi et al. (2014), i.e.,

$$H(\alpha_{pga}) = P[PGA \geq \alpha_{pga}] = k_0 \times {\alpha_{pga}}^{-k_1}, \tag{7.17}$$

where for $k_0 = 6.734 \times 10^{-5}$ and $k_1 = 2.857$ the site hazard curve takes the form shown in Fig.(7.4).

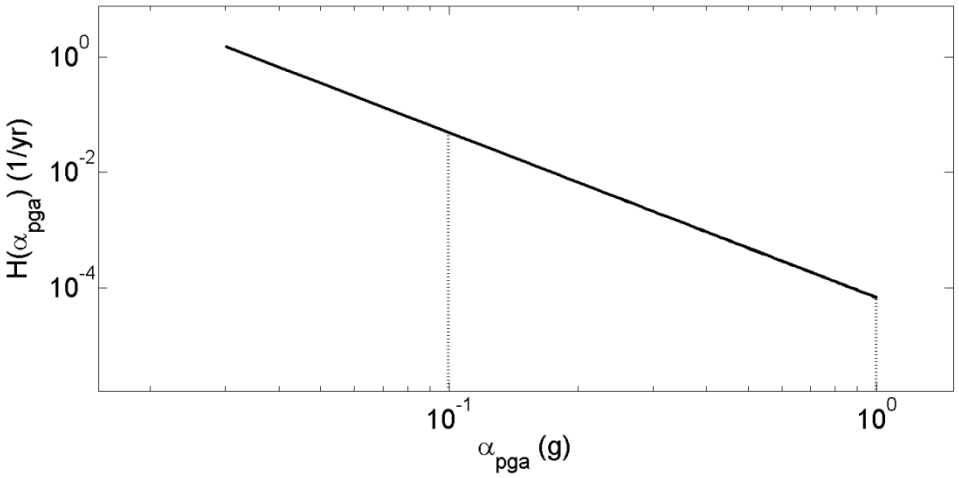

Figure 7.4. Site hazard curve $H(\alpha_{pga})$.

Note that when dealing with the evaluation of the expected value of LCC (see Eq.(7.8)), and for the purpose of taking into account all possible earthquake scenarios a structure is anticipated to encounter during its lifetime, all seismic events with acceleration input α_{pga} values between 0.1 and 1g are considered. In this setting, a wide range of imposed seismic inputs α_{pga} is regarded while neglecting those with ground acceleration less than 0.1g that are not expected to cause significant damage to the structure.

Approximate technique based data are compared in this regard with pertinent Monte Carlo simulation data utilizing 10,000 realizations. Specifically, excitation realizations compatible with the EPS of Eq.(2.2) are generated based on the spectral representation technique of Shinozuka and Deodatis (1991). Next, the nonlinear equation of motion (Eq.(3.1)) is numerically integrated via a standard fourth order Runge-Kutta scheme, and finally, system response statistics are obtained based on the ensemble of the response realizations. In Figs.(7.5-7.7), the non-stationary response IDR amplitude PDFs determined via the technique presented in section 7.2 are compared with corresponding MCS data for a design variables vector x^{in}. The seismic excitation intensity level S_0 is selected to yield a α_{pga}value equal to 0.34g; see Fig.(7.3). It can be readily seen that the

proposed approximate stochastic dynamics technique demonstrates a satisfactory degree of accuracy.

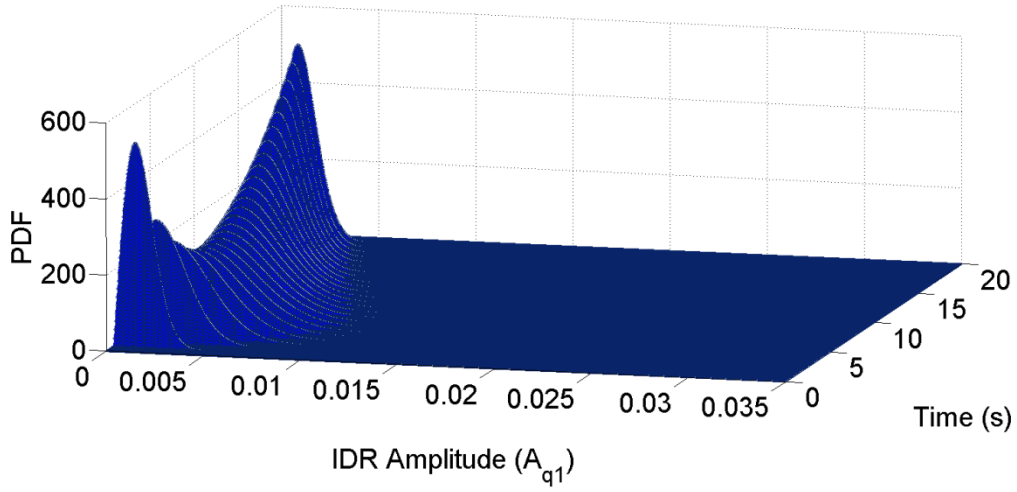

Figure 7.5a. Non-stationary response IDR amplitude PDF of the first DOF of the hysteretic MDOF system ($x^{in} = [0.30m, 0.25m, 0.20m]^T, \alpha_{pga} = 0.34g$) via the analytical approach.

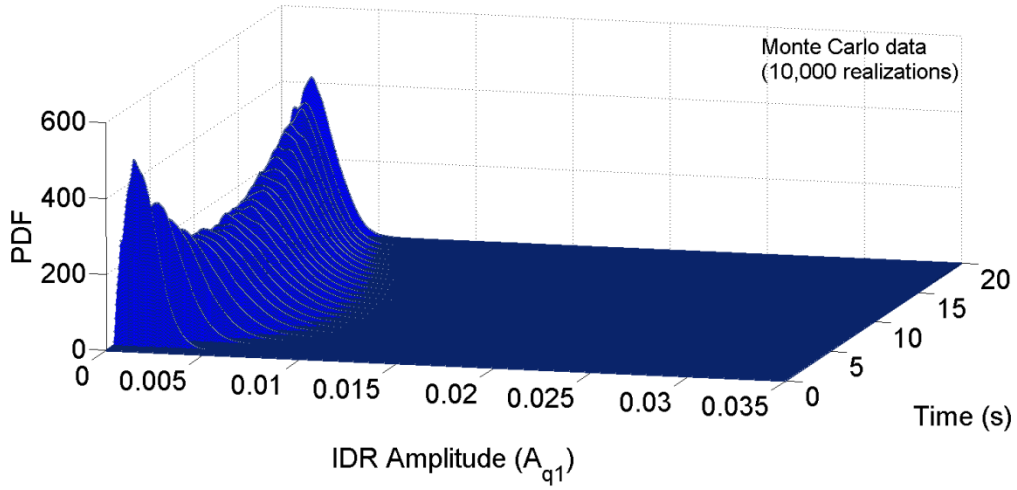

Figure 7.5b. Non-stationary response IDR amplitude PDF of the first DOF of the hysteretic MDOF system ($x^{in} = [0.30m, 0.25m, 0.20m]^T, \alpha_{pga} = 0.34g$) via Monte Carlo data (10,000 realizations).

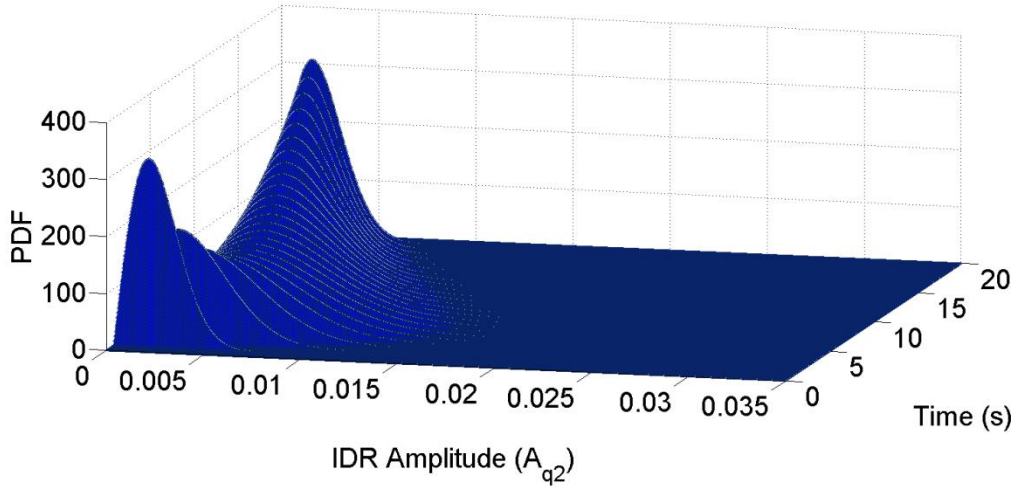

Figure 7.6a. Non-stationary response IDR amplitude PDF of the second DOF of the hysteretic MDOF system ($x^{in} = [0.30m, 0.25m, 0.20m]^T, \alpha_{pga} = 0.34g$) via the analytical approach.

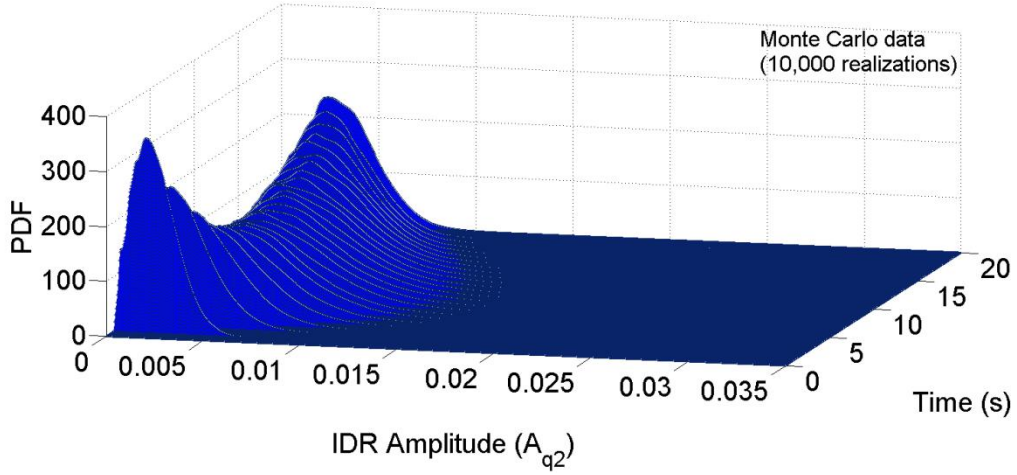

Figure 7.6b. Non-stationary response IDR amplitude PDF of the second DOF of the hysteretic MDOF system ($x^{in} = [0.30m, 0.25m, 0.20m]^T, \alpha_{pga} = 0.34g$) via Monte Carlo data (10,000 realizations).

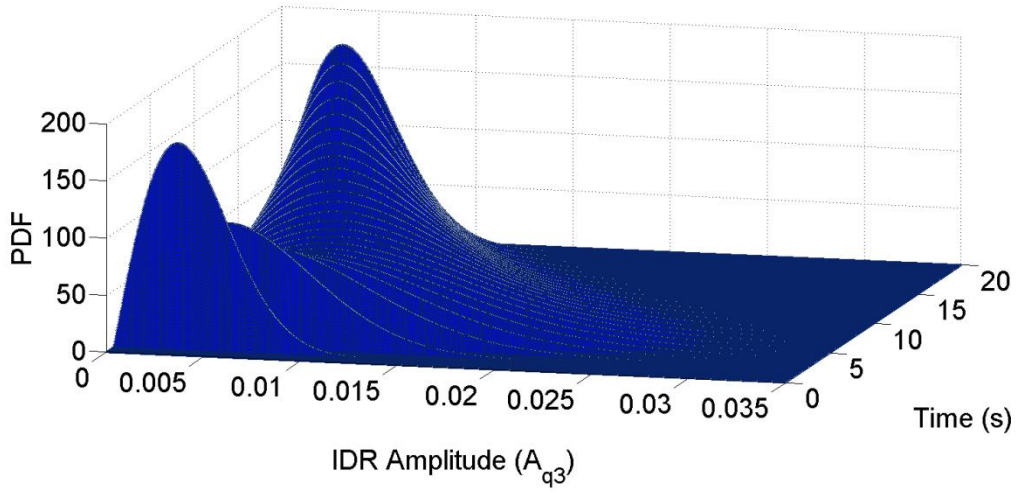

Figure 7.7a. Non-stationary response IDR amplitude PDF of the third DOF of the hysteretic MDOF system ($x^{in} = [0.30m, 0.25m, 0.20m]^T, \alpha_{pga} = 0.34g$) via the analytical approach.

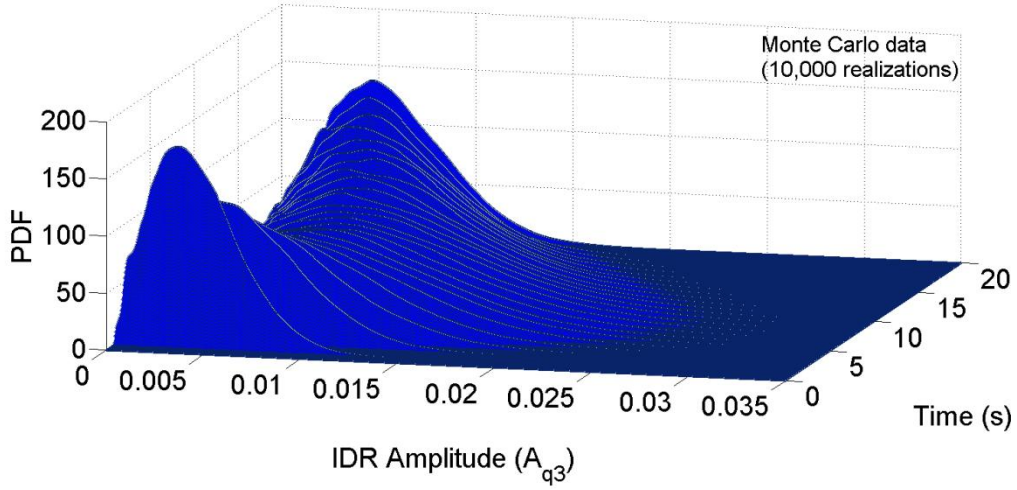

Figure 7.7b. Non-stationary response IDR amplitude PDF of the third DOF of the hysteretic MDOF system ($x^{in} = [0.30m, 0.25m, 0.20m]^T, \alpha_{pga} = 0.34g$) via Monte Carlo data (10,000 realizations).

Further, in Figs. (7.8a) and (7.8b) the most critical (as defined in section 7.2.1) response IDR amplitude PDFs $p_{cr}(A_i) = p(A_i, t = t_{cr})$ are plotted for two distinct **x** design variables values and compared with MCS data demonstrating a reasonable degree of accuracy.

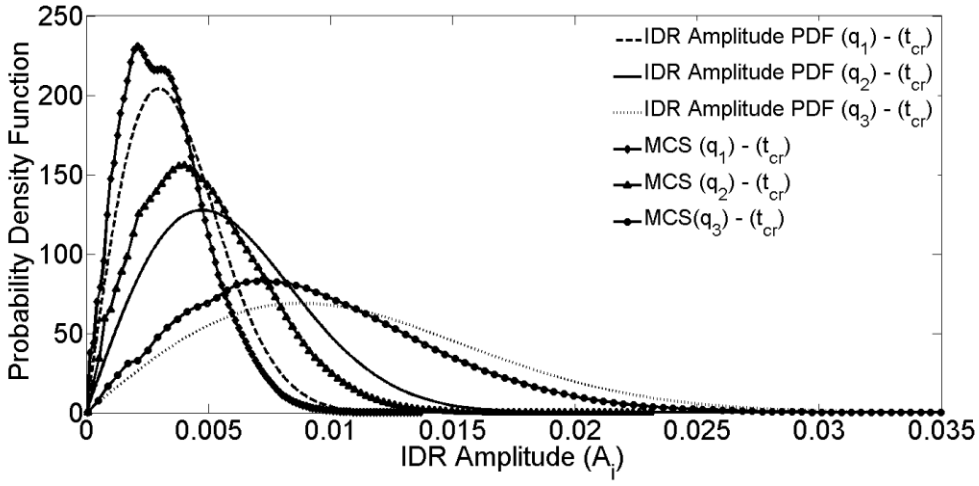

Figure 7.8a. Non-stationary response IDR amplitude PDF of every DOF of the hysteretic MDOF system; comparison with MCS for $x^{in} = [0.30m, 0.25m, 0.20m]^T$.

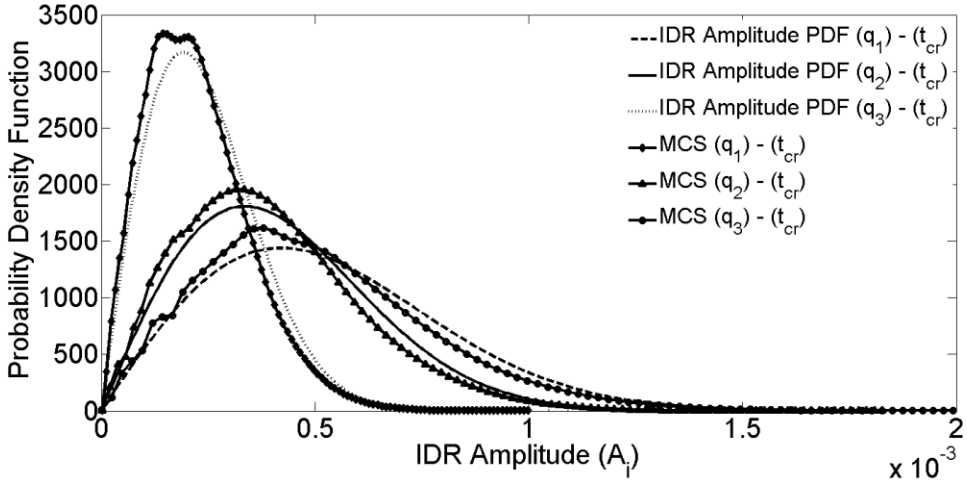

Figure 7.8b. Non-stationary response IDR amplitude PDF of every DOF of the hysteretic MDOF system; comparison with MCS for $x^{ub} = [0.55m, 0.55m, 0.55m]^T$.

Comparing Figs.(7.8a) and (7.8b) it can be readily seen that a slightly higher level of accuracy is observed in Fig.(7.8b). To explain this, note that in Fig.(7.8b) the chosen value $\mathbf{x}^{\mathrm{ub}} = [0.55\mathrm{m}, 0.55\mathrm{m}, 0.55\mathrm{m}]^{\mathrm{T}}$ yields a relatively stiffer structure than the one depicted in Fig.(7.8a), where $\mathbf{x}^{\mathrm{in}} = [0.30\mathrm{m}, 0.25\mathrm{m}, 0.20\mathrm{m}]^{\mathrm{T}}$. As pointed out in chapter 3 and explained in detail in Hammond (1973), Jangid and Datta (1999) and Kougioumtzoglou and Spanos (2013) the approximation induced by considering Eq.(3.14) instead of Eq.(3.9) implies a relatively lower level of accuracy for softer systems. Nevertheless, as shown in Fig.(7.8a), even in cases where the technique deviates slightly from the exact value, it still provides with conservative estimates; thus, rendering itself well-suited for structure design applications.

Next, in Figs. (7.9-7.11) the fragility curves for each damage state are plotted for the first, the second and the third DOF of the MDOF system, respectively; see also Table 7.1.

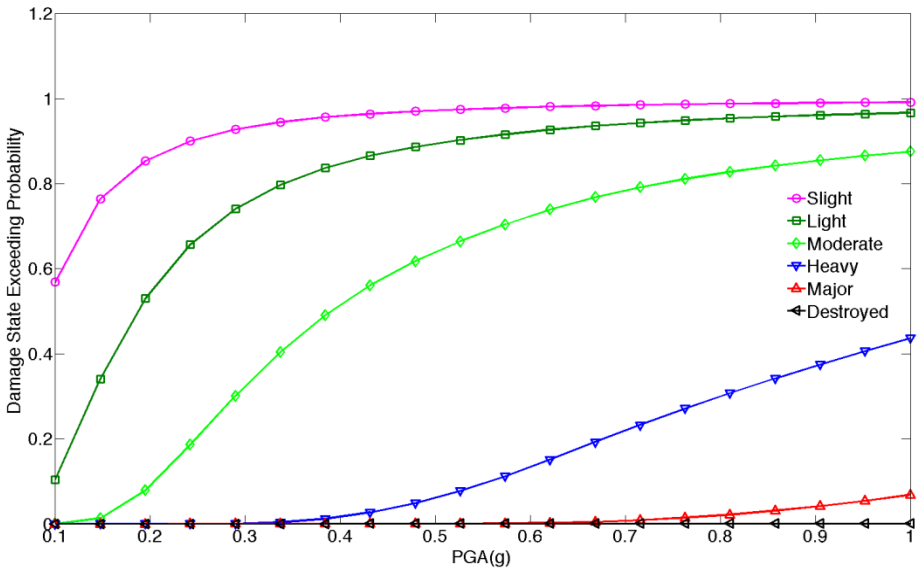

Figure 7.9. Fragility curves for the first DOF of the hysteretic MDOF system considering each damage state ($\mathrm{x}^{\mathrm{in}} = [0.30\mathrm{m}, 0.25\mathrm{m}, 0.20\mathrm{m}]^{\mathrm{T}}$).

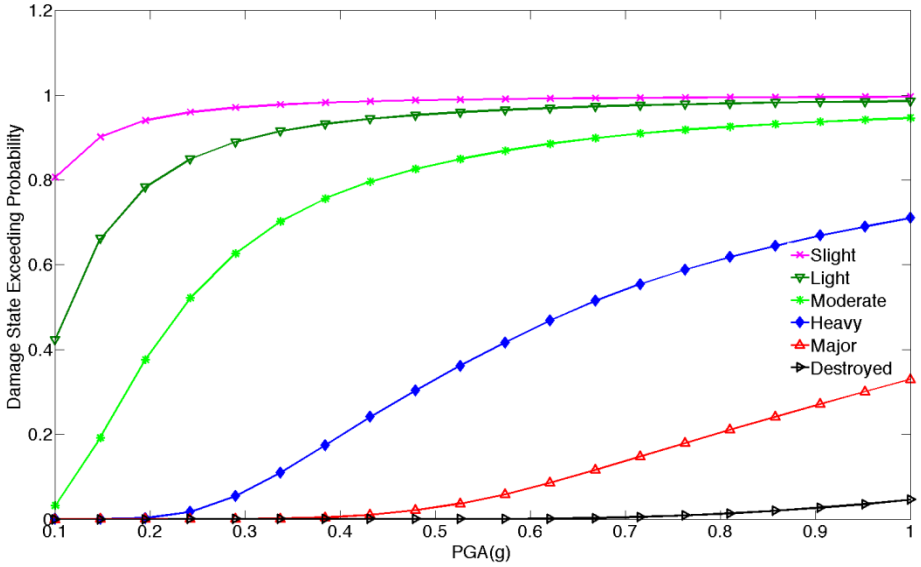

Figure 7.10. Fragility curves for the second DOF of the hysteretic MDOF system considering each damage state ($x^{in} = [0.30m, 0.25m, 0.20m]^T$).

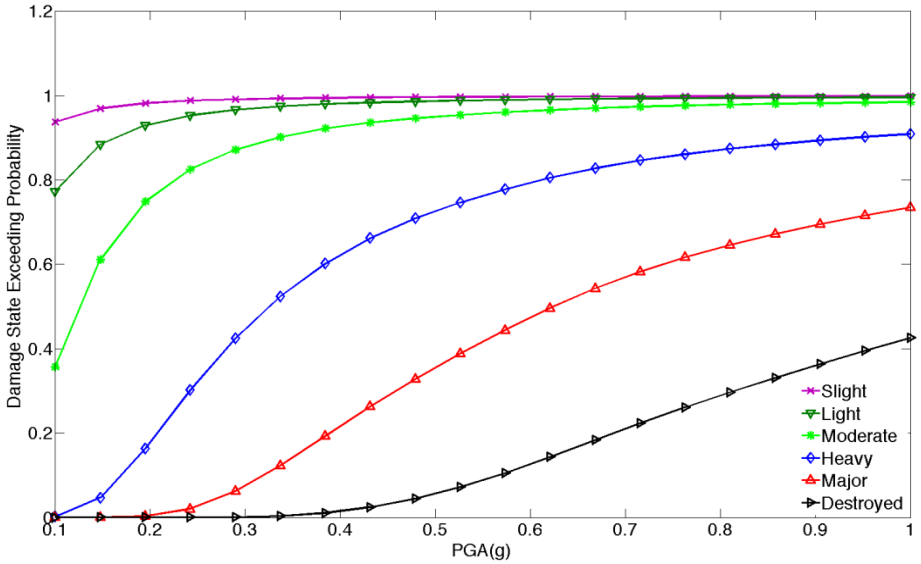

Figure 7.11. Fragility curves for the third DOF of the hysteretic MDOF system considering each damage state ($x^{in} = [0.30m, 0.25m, 0.20m]^T$).

7.4.2 Multi-objective optimal designs - Pareto optimal set

The objective function is defined as a weighted linear combination of the initial cost function and of the expected value of the LCC. Further, the response of the structural system is constrained in terms of the modes (i.e. most probable values) of the non-stationary response IDR amplitude PDFs of every DOF of the hysteretic MDOF system. The design variables are the dimensions of the square cross-section of the column elements. Columns' cross-section dimensions for a given floor are assumed to be equal, and thus the vector of design variables **x** has three components, one for every story. Next, assuming an initial design $\mathbf{x}^{\mathrm{in}} = [0.30\mathrm{m}, 0.25\mathrm{m}, 0.20\mathrm{m}]^{\mathrm{T}}$ and boundary constraints $\mathrm{x_i}^{\mathrm{in}} \leq \mathrm{x_i} \leq \mathrm{x_i}^{\mathrm{ub}},\ \mathrm{i} = 1, \dots, \mathrm{n_{dof}}$, where $\mathbf{x}^{\mathrm{ub}} = [0.55\mathrm{m}, 0.55\mathrm{m}, 0.55\mathrm{m}]^{\mathrm{T}}$ the optimization problem takes the form

$$\min_{\mathrm{x}\in\mathrm{D}}(\mathrm{C_{in}}, \mathrm{E}[\mathrm{LCC}(\mathrm{A_i}(\mathbf{x}, \mathbf{t}))]) = \min_{\mathrm{x}\in\mathrm{D}}(\mathbf{F}(\mathbf{x})), \tag{7.18}$$

where the conflicting sub-objectives are normalized as

$$\tilde{\mathrm{f}}_{\mathrm{z}}^{\mathrm{ind}}(\mathbf{x}) = \frac{\mathrm{f}_{\mathrm{z}}^{\mathrm{ind}}(\mathbf{x}) - \mathrm{f}_{\mathrm{z}}^{\mathrm{ind}}(\mathbf{x})_{,\min}}{\mathrm{f}_{\mathrm{z}}^{\mathrm{ind}}(\mathbf{x})_{,\max} - \mathrm{f}_{\mathrm{z}}^{\mathrm{ind}}(\mathbf{x})_{,\min}}, \mathrm{z} = 1, \dots, \mathrm{n_{obj}}. \tag{7.19}$$

In this regard, $\mathbf{F}(\mathbf{x})$ takes the form

$$\mathbf{F}(\mathbf{x}) = \mathrm{w_z}\frac{\mathrm{C_{in}}(\mathbf{x}) - \mathrm{C_{in}}(\mathbf{x})_{,\min}}{\mathrm{C_{in}}(\mathbf{x})_{,\max} - \mathrm{C_{in}}(\mathbf{x})_{,\min}} + (1 - \mathrm{w_z}) \times \dots$$
$$\frac{\mathrm{E}[\mathrm{LCC}(\mathrm{A_i}(\mathbf{x}, \mathbf{t}))] - \mathrm{E}[\mathrm{LCC}(\mathrm{A_i}(\mathbf{x}, \mathbf{t}))]_{,\min}}{\mathrm{E}[\mathrm{LCC}(\mathrm{A_i}(\mathbf{x}, \mathbf{t}))]_{,\max} - \mathrm{E}[\mathrm{LCC}(\mathrm{A_i}(\mathbf{x}, \mathbf{t}))]_{,\min}}, \tag{7.20}$$

under the stochastic constraints

$$\boldsymbol{\mu}_{\mathbf{o,i}}(\mathrm{S_o^*}, \mathbf{x}, \mathbf{t}) = \frac{\sqrt{\mathbf{c_i}(\mathrm{t})}}{\mathrm{h}} \leq \boldsymbol{\delta}_{\mathrm{ds}}^{\mathrm{Limit}} \tag{7.21}$$

and

$$\boldsymbol{\omega}_{aux,i}(\mathrm{S_o^*}, \mathbf{x}, \mathbf{t})_{,\max} \leq \boldsymbol{\omega}_{cr,L} \quad \text{or} \quad \boldsymbol{\omega}_{aux,i}(\mathrm{S_o^*}, \mathbf{x}, \mathbf{t})_{,\min} \geq \boldsymbol{\omega}_{cr,R} \tag{7.22}$$

and the deterministic constraint

$$x_i \geq x_{i+1}\,, \quad i = 1, \ldots, n_{dof}\,. \tag{7.23}$$

In Eq.(7.20) $C_{in}(\mathbf{x})$ stands for the initial cost which is assumed to be directly proportional to the building structure weight; this includes the weight of the column elements plus the weight of the plates evaluated at the design variables vector $\mathbf{x}$; $E[LCC(A_i(\mathbf{x}, \mathbf{t}))]$ is the expected value of the LCC, evaluated at the design variables vector $\mathbf{x}$. In Eq.(7.21) $\boldsymbol{\mu}_{\mathbf{o},\mathbf{i}}(S_o^*, \mathbf{x}, \mathbf{t})$ is a vector of the modes (i.e. most probable values) of the non-stationary response IDR amplitude PDFs of every DOF of the hysteretic MDOF system for the whole duration t_o of the seismic excitation with intensity factor S_o^*, evaluated at the design variables vector $\mathbf{x}$. The structure design service life T_d is considered to be equal to fifty years while the discount ratio, λ, is taken to be equal to 3%. Regarding the stochastic constraints of Eqs.(7.21) and (7.22) the critical excitation was selected to be the one with intensity factor S_o^* yielding an earthquake input α_{pga} equal to $0.34g$; see Fig(7.3). The rationale behind this choice lies in the fact that the above chosen value for α_{pga} represents a relatively severe earthquake event which is characterized by a low annual probability of occurrence according to the hazard curve depicted in Fig.(7.4); thus, highly appropriate for applying constraints considering safety issues (e.g., Porter, 2003; Fragiadakis et al. 2006). In this setting, the imposed stochastic constraint of Eq.(7.21) ensures that the vector of the modes of the non-stationary response IDR amplitude PDFs of every DOF of the hysteretic MDOF system for the whole duration t_o of the seismic excitation with intensity factor S_o^* will not exceed a preselected limit $\boldsymbol{\delta}_{ds}^{Limit}$ which is taken equal to 0.2% and corresponds to a specific damage state according to the defined IDR limits of Table 7.1.

Further, regarding the constraint of Eq.(7.22), it efficiently exploits one of the significant features of the approximate technique. Specifically, the technique not only provides with the system response amplitude PDF for each and every DOF, but also decouples the original n-DOF system of Eq.(3.1) into n SDOF LTV oscillators of the form given in Eq.(3.17) yielding time-varying effective stiffness $\omega_{aux,i}^2(t)$ and damping $\beta_{aux,i}(t)$ elements. This important additional output of the technique is exploited in the

constraint of Eq.(7.22) for avoiding "moving resonance" phenomena (e.g., Tubaldi and Kougioumtzoglou, 2014). In this regard, it facilitates the optimization process to avoid unnecessary optimal design searching in areas where surely optimal designs do not exist. Specifically, considering the quasi-stationary treatment of the LTV oscillator expressed by the following form

$$\sigma_{y_i}^2(\mathrm{t}) = \int_{-\infty}^{\infty} \left(\frac{1}{(\omega_{\mathrm{aux,i}}^2(\mathrm{t}) - \omega^2)^2 + (\beta_{\mathrm{aux,i}}(\mathrm{t})\omega)^2} \right) \mathrm{m_i}^2 \mathrm{S}_{\ddot{\alpha}_\mathrm{g}}(\omega, \mathrm{t}) \mathrm{d}\omega, \qquad (7.24)$$

it can be reasonably argued that the maximum response variance of the original MDOF system occurs when the excitation EPS $\mathrm{S}_{\ddot{\alpha}_\mathrm{g}}(\omega, \mathrm{t})$ resonates with the LTV oscillator equivalent natural frequency $\omega_{\mathrm{aux,i}}(\mathrm{t})$. Thus, to avoid this resonance phenomenon, the constraint of Eq.(7.22) is formulated so that $\omega_{\mathrm{aux,i}}(\mathrm{t})$ is kept outside a critical range in the frequency domain $[\omega_{cr,L}\,, \omega_{cr,R}]$ where the excitation EPS $\mathrm{S}_{\ddot{\alpha}_\mathrm{g}}(\omega, \mathrm{t})$ takes its largest values. In this regard, the expression

$$\mathrm{S}_{\ddot{\alpha}_{\mathrm{g,L}}}(\boldsymbol{\omega}, \mathrm{t}) \leq \varepsilon \times \mathrm{S}^*_{\ddot{\alpha}_{\mathrm{g,P}}}(\boldsymbol{\omega}, \mathrm{t}) \qquad (7.25)$$

is adopted, where $\mathrm{S}_{\ddot{\alpha}_{\mathrm{g,L}}}(\boldsymbol{\omega}, \mathrm{t})$ is a selected EPS value given as a percentage ε of the peak EPS value $\mathrm{S}^*_{\ddot{\alpha}_{\mathrm{g,P}}}(\boldsymbol{\omega}, \mathrm{t})$ corresponding to the time instant where $|\mathrm{g}(\mathrm{t})|^2$ takes its peak value; see Figs.(7.3) and (7.12). In the herein considered application, ε was taken equal to 75%.

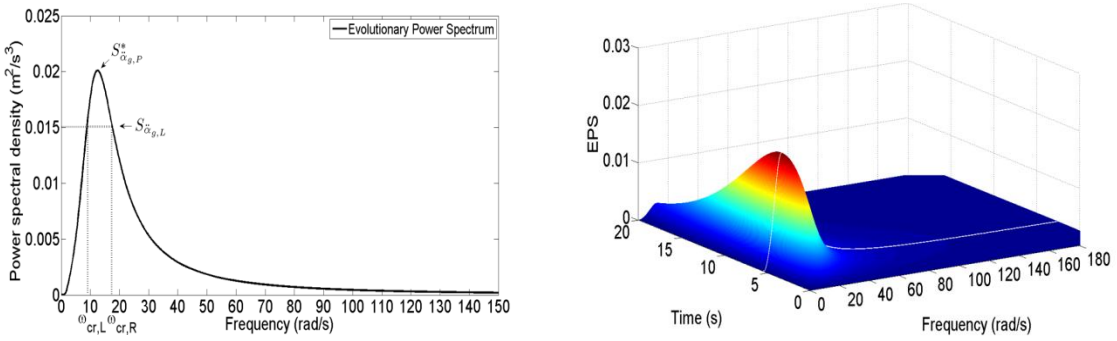

Figure 7.12. Depiction of the imposed stochastic constraint (two and three dimensions).

Note that the deterministic constraints of Eq.(7.23) ensure that the optimization procedure will provide applicable design solutions from a practical viewpoint. Further, the expected value of the total cost, the initial cost and the expected value of the LCC are related according to the following expression (e.g., Wen and Kang, 2001)

$$\mathrm{E}\left[\mathrm{C}_{\mathrm{Total}}\left(\mathrm{A}_{\mathrm{i}}(\mathbf{x},\mathbf{t})\right)\right] = \mathrm{C}_{\mathrm{in}}(\mathbf{x}) + \mathrm{E}\left[\mathrm{LCC}\left(\mathrm{A}_{\mathrm{i}}(\mathbf{x},\mathbf{t})\right)\right] \times \mathrm{C}_{\mathrm{in}}(\mathbf{x}). \qquad (7.26)$$

The Pareto front curves for both the expected value of the LCC and the expected value of the total cost with respect to the initial cost are presented in Fig.(7.13).

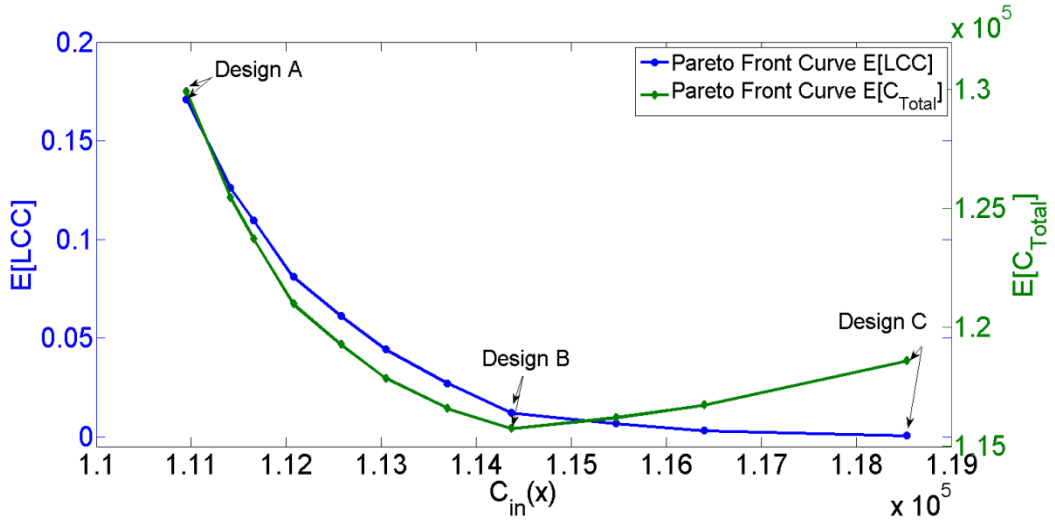

Figure 7.13. Pareto front curves for the expected values of LCC and total cost against the initial cost.

Next, to highlight the flexibility of the proposed methodology, the compromise design solution from the Pareto front curve exhibiting the lowest expected value of the total cost, as well as the ones corresponding to the two tails (see Fig.(7.13)) are presented in Table 7.2.

Designs		$\mathbf{x}$(m)	$C_{in}(\mathbf{x})$	$E[LCC(A_i(\mathbf{x},\mathbf{t}))]$	$E\left[C_{Total}\left(A_i(\mathbf{x},\mathbf{t})\right)\right]$
Design A	1st	0.3892	1.1095×10^5	17.1103×10^{-2}	1.2993×10^5
	2nd	0.3701			
	3rd	0.3294			
Design B	1st	0.4750	1.1415×10^5	1.1302×10^{-2}	1.1544×10^5
	2nd	0.4749			
	3rd	0.3981			
Design C	1st	0.5492	1.1853×10^5	5.5901×10^{-4}	1.1860×10^5
	2nd	0.5489			
	3rd	0.5471			

Table 7.2. Synoptically presented results regarding three different design solution configurations from the Pareto front curves (Designs A, B and C).

Moreover it was deemed appropriate to present also the non-stationary response IDR amplitude PDFs determined by the analytical technique regarding the design variables vector **x** that corresponds to the compromise solution named "Design B"; see Figs.(7.14-7.16). The presented results corresponds to the case where the imposed intensity factor is taken equal to S_o^*.

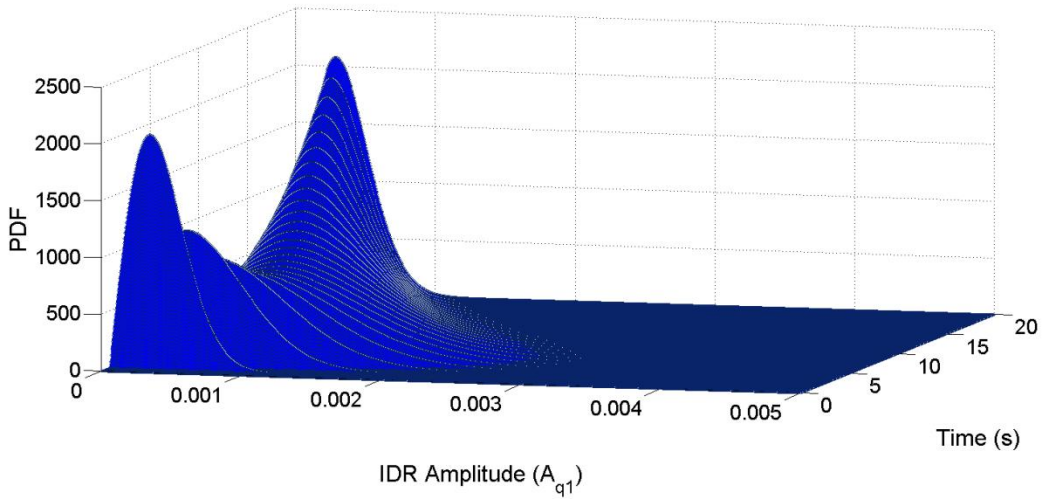

Figure 7.14. Non-stationary response IDR amplitude PDF of the first DOF of the hysteretic MDOF system via the analytical approach (compromise solution-Design B).

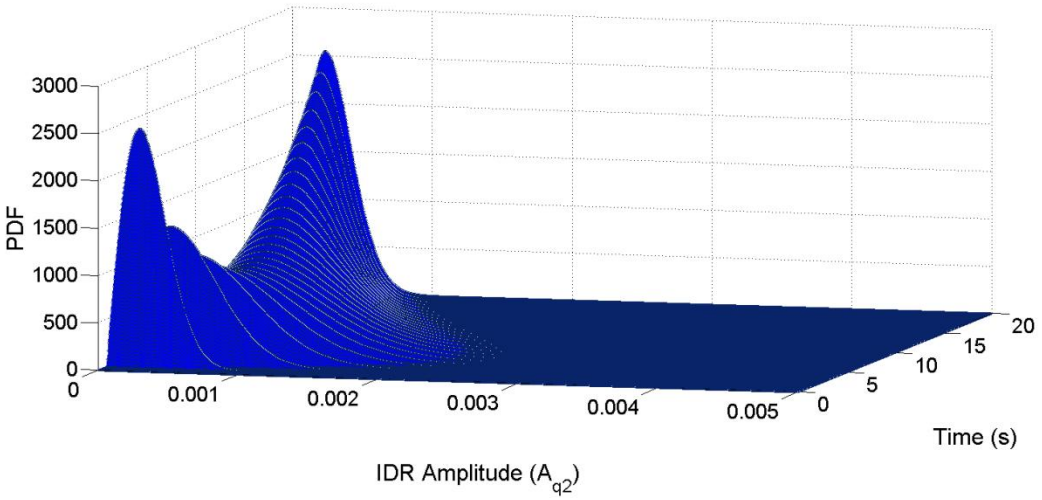

Figure 7.15. Non-stationary response IDR amplitude PDF of the second DOF of the hysteretic MDOF system via the analytical approach (compromise solution-Design B).

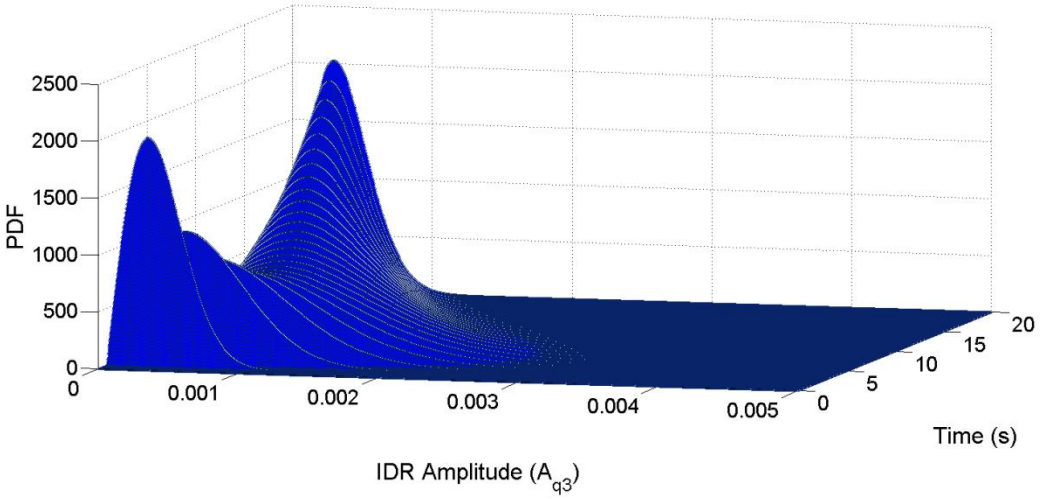

Figure 7.16. Non-stationary response IDR amplitude PDF of the third DOF of the hysteretic MDOF system via the analytical approach (compromise solution-Design B).

In this setting, the designer/analyst possesses a considerable amount of information for every compromise solution configuration regarding the initial cost as well as the expected values of both the LCC and the total cost. This is of particular importance for an educated decision-making analysis where the final optimal design will be the compromise solution that best balances the initial cost, the LCC cost, and the total cost according to the project stakeholders' perspective.

Chapter 8

Concluding remarks

In this chapter, the main conclusions along with pertinent remarks associated with the analytical formulations and the numerical results considered in this thesis are presented and discussed. Also, potential directions for future research work are outlined.

In chapter 1 a conspectus of the objectives and tools of this thesis is provided as well as a brief review of methods for nonlinear stochastic dynamic analysis.

In chapter 2, various stochastic models for the representation of the seismic action are provided. These include phenomenological seismic stationary as well as non-stationary stochastic models of both the separable and non-separable form. Further, a seismological model (Boore, 2003) of the more sophisticated kind that is based on two basic parameters, namely the earthquake moment magnitude and the epicentral distance is also presented.

In chapter 3, a review of an alternative analytical/approximate method to the type of nonlinear stochastic dynamic analysis, recently proposed by Kougioumtzoglou and Spanos (2013) is given. The analytical approach based on the concepts of statistical linearization and of stochastic averaging has been developed for determining the evolutionary stochastic response of MDOF nonlinear systems.

In chapter 4 an approximate analytical technique for determining the time-varying survival probability and associated first-passage PDF of nonlinear/hysteretic MDOF structural systems subject to evolutionary stochastic excitation has been developed. Specifically, based on an efficient dimension reduction approach and relying on the concepts of stochastic averaging and statistical linearization, the original nonlinear n-degree-of-freedom system has been decoupled and cast into (n) effective SDOF LTV oscillators corresponding to each and every DOF. In this regard, time-varying effective

stiffness $\omega_{eq,i}^2(t)$ and damping $\beta_{eq,i}(t)$ elements corresponding to each and every DOF have been defined and computed, while the non-stationary marginal, transition and joint response amplitude PDFs have been efficiently determined in closed-form expressions. Finally, the MDOF system survival probability and first-passage PDF have been determined approximately in a computationally efficient manner. Overall, the developed technique exhibits enhanced versatility since it can handle readily a wide range of nonlinear behaviors as well as various stochastic excitations with arbitrary non-separable EPS forms that exhibit strong variability in both the intensity and the frequency content. A 3-DOF structural system exhibiting hysteresis following the Bouc-Wen model subject to evolutionary stochastic excitation of both separable and non-separble kind has been included in the numerical examples. Comparisons with pertinent Monte Carlo simulations have demonstrated the reliability of the technique. Future work may include adaptation of the proposed theoretical framework to count for reliability assessment of sensitive complex systems of engineering interest.

In chapter 5 a novel methodology for determining the seismic fragility of nonlinear MDOF structural systems has been presented that can be potentially used in conjunction with a PBEE analysis framework. Specifically, fragility surfaces are determined for nonlinear/hysteretic MDOF structural systems subject to earthquake excitations compatible with a prescribed stochastic seismological model. Note that the employed vector-valued IM comprises two parameters, namely the earthquake moment magnitude (M_m) and the epicentral distance (r). The developed framework relies on an efficient approximate dimension reduction/decoupling technique for determining the non-stationary system response amplitude PDFs based on the concepts of statistical linearization and of stochastic averaging; thus, computationally intensive Monte Carlo simulations are circumvented. Further, considering the inter-story drift ratio as the selected damage measure and appropriately defined damage states structural system related fragility surfaces are determined at a low computational cost as well.

This attribute renders the proposed methodology, hopefully, useful for efficient structural system fragility analysis and design applications, at least at a preliminary level.

A building structure comprising the versatile Bouc-Wen (hysteretic) model has served as a numerical example for demonstrating the reliability of the proposed fragility analysis methodology. Future work may stem from the combination of the chapters 4 and 5 by proposing an efficient fragility analysis framework regarding fragilities of the first-passage kind. The first-passage kind failure definition may, perhaps, be appropriate for the most severe damage state. The choice of this bound as a threshold for considering the first-passage problem is absolutely justified since the first violation of this barrier leads to a collapse. Considering hysteretic multi-story building structures and relying on the proposed theoretical developments, fragility surfaces regarding first-passage kind fragilities could be obtained in a straightforward manner and at considerable low computational cost.

In chapter 6 a framework for the efficient solution of structural robust optimization problems has been proposed which features controlling both inter-story drift and absolute floor acceleration non-stationary second order statistics. It can be viewed as a systematic and efficient methodology for providing optimal robust design solutions. Due to the joint consideration of displacement and acceleration constraints, the framework provides robust design solutions even in cases where potentially incurred damages are associated with non-structural components. An important feature of the proposed framework relates to the utilization of an efficient approximate frequency domain approach for determining the system response non-stationary second-order statistics; thus, circumventing computationally intensive MCS. The proposed stochastic structural design methodology can be used in a straightforward manner in structural design problems involving systems with a large number of DOFs and subject to stochastic earthquake excitation even of the non-separable kind.

Future work may include the extension of the herein stochastic design methodology to structural systems equipped with nonlinear energy dissipation devices. A potential direction for future work could include as well stochastic earthquake excitations of the non-separable kind which comprise some of the main characteristics of seismic shaking,

such as decreasing of the dominant frequency with respect to time (Liu, 1970; Spanos and Solomos, 1983).

In chapter 7 a performance-based multi-objective design optimization framework considering LCC has been developed for nonlinear/hysteretic MDOF structural systems subject to evolutionary stochastic excitations. Although the developments herein have been tailored specifically for earthquake engineering related applications, they can be readily modified to account for other hazard kinds as well. The developed framework relies on an efficient approximate dimension reduction technique for determining the non-stationary system response amplitude PDFs based on the concepts of statistical linearization and of stochastic averaging; thus, computationally intensive Monte Carlo simulations are circumvented. Note that the technique not only provides with the system response amplitude PDF for each and every DOF, but also decouples the original n-DOF system into n SDOF LTV oscillators yielding time-varying effective stiffness $\omega_{aux,i}^2(t)$ and damping $\beta_{aux,i}(t)$ elements corresponding to each and every DOF. This important additional output has been exploited in the formulation of the optimization problem for avoiding "moving resonance" phenomena. Further, the framework can readily account for excitations with arbitrary non-separable EPS forms that exhibit strong variability in both the intensity and the frequency content.

In this regard, considering appropriately defined damage measures structural system related fragility curves for each story are determined at a low computational cost as well. Finally, the structural system design optimization problem is formulated as a multi-objective one to be solved by a Genetic Algorithm based approach; thus, various compromise solutions are obtained providing the designer with enhanced flexibility regarding decision-making analysis. A building structure comprising the versatile Bouc-Wen (hysteretic) model serves as a numerical example for demonstrating the efficiency of the proposed methodology. Future work may include the adaptation of the developed framework for the study of the advantageous contribution of passive vibration control devices such as tuned-mass-dampers, base isolators and viscous dampers on a realistic hysteretic multi-story building structure.

The proposed development contributes substantially to promoting well-established random vibration theory techniques in current problems related to the challenging area of nonlinear structural dynamics. Hopefully, such approaches will further contribute to familiarizing the structural engineering community with well-established and theoretically solid concepts from the random vibration field.

Appendix A

Spectral representation method for simulating time-histories as samples of a stochastic process with a given power spectrum

Consider an one-dimensional, uni-variate, stationary, Gaussian stochastic process $f_0(t)$ with mean value equal to zero, autocorrelation function $R_{f_0 f_0}(\tau)$ and two-sided power spectrum $S_{f_0 f_0}(\omega)$. The stochastic process $f_0(t)$ can be simulated by the following series as $N \to \infty$

$$f(t) = \sqrt{2} \sum_{n=0}^{N-1} A_n \cos(\omega_n t + \varphi_n) \tag{A.1}$$

where

$$A_n = \sqrt{2 S_{f_0 f_0}(\omega_n) \Delta\omega}\,, \quad n = 0, 1, 2 \ldots, N-1 \tag{A.2}$$

$$\omega_n = n\Delta\omega \tag{A.3}$$

and

$$\Delta\omega = \frac{\omega_u}{N} \tag{A.4}$$

with

$$S_{f_0 f_0}(\omega_0 = 0) = 0 \tag{A.5}$$

In Eq.(A.4) ω_u represents an upper cut-off frequency beyond which the power spectrum $S_{f_0 f_0}(\omega)$ may be reasonably assumed to be zero for either mathematical or physical reasons.

References

Abramowitz M., Stegun I. A., 1970. *Handbook of Mathematical Functions*, Dover Publications, New York.

Amin M., Ang A. H.-S., 1968. Nonstationary stochastic model of earthquake motions, *Journal of Engineering Mechanics Division, ASCE, 94 (EM2), 559-583.*

Ang A. H-S., Lee J-C., 2001. Cost optimal design of R/C buildings. *Reliability Engineering and System Safety, 73:233–8.*

Ang A. H-S., Tang W.H., 2007. *Probability concepts in engineering,* 2nd edition Wiley.

Atkinson G. M., Silva W., 2000. Stochastic modeling of California ground motions, *Bulletin of the Seismological Society of America, 90(2):255-74.*

Au S. K., Beck J. L., 2001. First excursion probabilities for linear systems by very efficient importance sampling, *Probabilistic Engineering Mechanics 16, pp. 193-207.*

Au, S. K., Beck, J. L., 2001b. Estimation of small failure probabilities in high dimensions by subset simulation, *Probabilistic Engineering Mechanics*, 16(4), 263-277.

Au S. K., Beck J. L., 2003. Subset simulation and its application to seismic risk based on dynamic analysis, *Journal of Engineering Mechanics (ASCE), 129:901–917.*

Au, S. K., 2005. Reliability-based design sensitivity by efficient simulation, *Computers and Structures, 83:1048–61.*

Bäck, T., Schwefel, H.-P., 1993. An overview of evolutionary algorithms for parameter optimization, *Evoutionary Computation, 1(1), 1-23.*

Baker J. W., Cornell C. A., 2005, A vector-valued ground motion intensity measure consisting of spectral acceleration and epsilon, *Earthquake Engineering and Structural Dynamics, 34:1193–1217.*

Barbato, M., Conte, J. P., 2001. Structural Reliability Applications of Non-Stationary Spectral Characteristics, *ASCE Journal of Engineering Mechanics, 137, pp. 371–382.*

Barbato M., Conte J. P., 2006. Finite element structural response sensitivity and reliability analyses using smooth versus non-smooth material constitutive models. *International Journal of Reliability and Safety, 1:3–39.*

Barbato M., Petrini F., Unnikrishnan V.U., Ciampoli M., 2013. Probabilistic performance-based hurricane engineering (PBHE) framework, *Structural Safety, 45, pp. 24–35*.

Beck A. T., Gomes W. J. S., 2012. A comparison of deterministic, reliability-based and risk-based structural optimization under uncertainty, *Probabilistic Engineering Mechanics, 28: 18–29.*

Beck J.L., Papadimitriou C., 1993. Moving resonance in nonlinear response to fully non-stationary stochastic ground motion, *Probabilistic Engineering Mechanics, 8(3-4):157–167.*

Beer, M., Liebscher, M., 2008. Designing robust structures – A nonlinear simulation based approach, *Computers and Structures, 86, 10: 1102–1122*.

Boore D. M., 1983. Stochastic simulation of high-frequency ground motions based on seismological models of the radiated spectra, *Bulletin of the Seismological Society of America, 73(6), 1865-1894*.

Boore, D. M., Joyner, W. B., 1997. Site amplifications for generic rock sites, *Bulletin of the Seismological Society of America, 87(2) 327–341*.

Boore D. M., 2003. Simulation of ground motion using the stochastic method, *Journal of Pure and Applied Geophysics, 160 635-676.*

Bucher, C. G., 1988. Adaptive sampling - an iterative fast Monte Carlo procedure, *Structural Safety, 5, 119-126.*

Caughey T. K., 1960. Random excitation of a system with bilinear hysteresis, *Journal of Applied Mechanics, ASME, 27, 649-652.*

Ciampoli M., Petrini F., 2012. Performance-based aeolian risk assessment and reduction for tall buildings, *Probabilistic Engineering Mechanics, 28: 75–84*.

Cimellaro G. P., 2007. Simultaneous stifness-damping optimization of structures with respect to Acceleration, Displacement and Base shear, *Engineering Structures, 29, 2853-2870.*

Clough R. W., Penzien J., 1993. *Dynamics of structures*, McGraw-Hill.

Conte J. P., Peng B. F., 1997, Fully Nonstationary Analytical Earthquake Ground-Motion Model, *Journal of Engineering Mechanics, 123(1), 15–24.*

Cornell C. A., Jalayer F., Hamburger R., Foutch D., 2002. Probabilistic basis for 2000 SAC federal emergency management agency steel moment frame guidelines, *ASCE Journal of Structural Engineering, 128: 526–32.*

Cornell C. A., Krawinkler H., 2000. Progress and challenges in seismic performance assessment, *PEER Center News, Spring 2000. http://peer.berkeley.edu/news/2000 spring/index.html*.

Corotis R., Vanmarcke E. H. and Cornell, C. A., 1972. First passage of nonstationary random processes. *Journal of the Engineering Mechanics Division, Proc. ASCE, 98 (EM2): 401-414.*

Crandall S. H., ed., 1958. *Random vibration*, vol. I. Cambridge, MA: MIT Press.

Crandall S. H., ed., 1963. *Random vibration*, vol. II. Cambridge, MA: MIT Press.

Crandall S. H., Mark W. D., 1963. *Random vibration in mechanical systems*. New York: Academic Press.

Crandall S. H., 2001. Is stochastic equivalent linearization a subtly flawed procedure, *Probabilistic Engineering Mechanics, 16: 169-176.*

Dahlhaus, R., 1997. Fitting time series models to non-stationary processes, *The Annals of Statistics, 25: 1–37.*

Deb K., Pratap A., Agarwal S., Meyarivan T., 2002. A fast and elitist multiobjective genetic algorithm: NSGA-II. *IEEE Transactions on Evolutionary Computation, 6(2):182–197*.

Der Kiureghian A., 2000. The geometry of random vibrations and solutions by FORM and SORM, *Probabilistic Engineering Mechanics, 15:81–90*.

Der Kiureghian A., 2005. Non-ergodicity and PEER's framework formula, *Earthquake Engineering and Structural Dynamics, 34(13):1643-52*.

Der Kiureghian A., Fujimura K., 2009. Nonlinear stochastic dynamic analysis for performance-based earthquake engineering, *Earthquake Engineering and Structural Dynamics, 38:719–738*.

Ditlevsen O., Madsen H. O., 1996. Structural Reliability Methods. Wiley: New York.

Elenas, A., Meskouris, K., 2001. Correlation study between seismic acceleration parameters and damage indices of structures, *Engineering Structures, 23: 698–704*.

Elishakoff I. E., 1999. *Probabilistic theory of structures*. New York: Dover Publications.

Ellingwood BR., 2001. Earthquake risk assessment of building structures, *Reliability Engineering and System Safety, 74: 251–62*.

Ellingwood BR., Wen Y. K., 2005. Risk-benefit-based design decisions for low probability/high consequence earthquake events in Mid-America. *Progress in Structural Engineering and Materials, (7):56–70*.

Fishman, G. S., and Huang, B. D., 1983. Antithetic variates revisited, *Communications of the ACM, 26(11), 964-971*.

Florian, A., 1992. An efficient sampling scheme: Updated Latin Hypercube Sampling, *Probabilistic Engineering Mechanics, 7(2), 123-130*.

Fragiadakis M., Lagaros N. D, Papadrakakis M., 2006. Performance-based multiobjective optimum design of steel structures considering life-cycle cost, *Structural and Multidisciplinary Optimization, 32:1-11*.

Franchin P., 2004. Reliability of uncertain inelastic structures under earthquake excitation. *Journal of Engineering Mechanics (ASCE), 130:180–191*.

Fujimura K., Der Kiureghian A., 2007. Tail-equivalent linearization method for nonlinear random vibration, *Probabilistic Engineering Mechanics, 22:63–76*.

Gajic Z., Qureshi M., 1995. *Lyapunov Matrix Equation in System Stability and Control*, Academic Press, New York.

Gamerman D., 2006. *Markov Chain Monte Carlo: a stochastic simulation for Bayesian interference*, Taylor and Francis.

Gasser, M., and Schüeller, G.I., 1997. Reliability-based optimization of structural systems, *Mathematical Methods of Operation Research, 46: 287–307*.

Ghobarah A., 2004. On drift limits associated with different damage levels. In: Fajfar P., Krawinkler H. (eds) *International workshop on performance-based seismic design. Bled, Slovenia*.

Giaralis, A., Spanos, P. D., 2010. Effective linear damping and stiffness coefficients of nonlinear systems for design spectrum based analysis, *Soil Dynamics and Earthquake Engineering, 30: 9 798-810*.

Giaralis, A., Spanos, P. D., 2012. Derivation of response spectrum compatible non-stationary stochastic processes relying on Monte Carlo-based peak factor estimation, Earthquake and Structures, 3 (3-4), 581-609.

Giaralis, A., Vamvatsikos, D., 2014. Local Wavelet-Based Spectral "Epsilon" Modification of Ground Motions in Support of Incremental Dynamic Analysis, *Proceedings of the 2nd ICVRAM 2014 & ISUMA 2014, Liverpool, UK, July 13 – 16, 2014, M. Beer, S.-K. Au, J. W. Hall, (Eds.), (ASCE), pp. 1706-1715. doi:10.1061/978078 4413609.171*

Goldberg D. E., 1989. *Genetic algorithms in search, optimization and machine learning*, Addison-Wesley Longman Publishing Co., Boston, Massachusetts.

Grigoriu M., 2011. To Scale or Not to Scale Seismic Ground-Acceleration Records, *Journal of Engineering Mechanics, 137:284-293*.

Hammersley, J. M., Handscomb, D. C., 1964. *Monte-Carlo methods*, Methuen, London.

Hammond J. K., 1973. Evolutionary spectra in random vibration, *Journal of the Royal Statistical Society, 35: 167–188.*

Hanks T. C., Kanamori H., 1979. A moment magnitude scale, *Journal of Geophysical Research, B, 84, 2348-2350*.

Holland, J., 1975. *Adaptation in natural and artificial systems*, University of Michigan Press, Ann Arbor.

Hwang H. H. M., Huo J-R., 1994. Generation of hazard-consistent fragility curves. *Soil dynamics and Earthquake Engineering, 13:345–354.*

Hwang H. H. M., Jaw J-W., 1990. Probabilistic damage analysis of structures, *Journal of Structural Engineering, 116:1992-2007.*

Ikhouane F., Rodellar J., 2007. *Systems with hysteresis: analysis, identification and control using the Bouc-Wen model*, John Wiley and Sons.

Iourtchenko D. V., Mo E., Naess A. 2006. Response probability density functions of strongly non-linear systems by the path integration method, *International Journal of Non-Linear Mechanics*, vol. 41: 693-705.

Iwan W. D., 1974. Application of Nonlinear Analysis Techniques, *Applied Mechanics in Earthquake Engineering, W. D. Iwan, ed., ASME Symposium, AMD vol. 8*.

Jangid R. S., Datta T. K., 1999. Evaluation of the methods for response analysis under non-stationary excitation, *Shock and Vibration, 6: 285–297.*

Jensen, H. A., 2006. Structural optimization of non-linear systems under stochastic excitation, *Probabilistic Engineering Mechanics, 21: 397-409.*

Jensen H. A., 2009. Tradeoff analysis of non-linear dynamical systems under stochastic excitation, *Probabilistic Engineering Mechanics, 24: 585-599.*

Jensen J. J., Capul J., 2006. Extreme response predictions for jack-up units in second order stochastic waves by FORM. *Probabilistic Engineering Mechanics, 21:330–337.*

Kafali C., Grigoriu M., 2007. Seismic fragility analysis: Application to simple linear and nonlinear systems, *Journal of Earthquake Engineering and Structural Dynamics, 36: 1885-1900.*

Kanai K., 1957. Semi-empirical formula for the seismic characteristics of the ground, *University of Tokyo, Bulletin of Earthquake Research Institute*.

Kanamori H., 1977. The energy release in great earthquakes, *Journal of Geophysical Research, 82, 2981-2987*.

Kijewski-Correa T., Kareem A., 2006. Efficacy of Hilbert and wavelet transforms for time-frequency analysis, *Journal of Engineering Mechanics, 132(10):1037–1049.*

Kong J. S., Frangopol D. M., 2003. Life-cycle reliability-based maintenance cost optimization of deteriorating structures with emphasis on bridges, *Journal of Structural Engineering, 129(6):818–28.*

Koo H, Der Kiureghian A, Fujimura K., 2005. Design point excitation for nonlinear random vibration, *Probabilistic Engineering Mechanics, 20:136–147.*

Kougioumtzoglou I. A., 2013. Stochastic joint time-frequency response analysis of nonlinear structural systems, *Journal of Sound and Vibration, vol. 332: 7153-7173.*

Kougioumtzoglou I. A., Spanos P. D., 2009. An approximate approach for nonlinear system response determination under evolutionary stochastic excitation, *Current Science, Indian Academy of Sciences, vol. 97: 1203-1211*.

Kougioumtzoglou I. A., Spanos P. D., 2009. An approximate approach for nonlinear system response determination under evolutionary stochastic excitation, *Current Science, Indian Academy of Sciences, vol. 97: 1203-1211*.

Kougioumtzoglou I. A., Spanos P. D., 2013. Nonlinear MDOF system stochastic response determination via a dimension reduction approach, *Computers and Structures, 126: 135-148.*

Kougioumtzoglou, I. A., and Spanos, P. D., 2013b. Response and First-Passage Statistics of Nonlinear Oscillators Via a Numerical Path Integral Approach, *ASCE Journal of Engineering Mechanics, 139, pp. 1207–1217*.

Kougioumtzoglou, I. A., and Spanos, P. D., 2014. Stochastic Response Analysis of the Softening Duffing Oscillator and Ship Capsizing Probability Determination Via Numerical Path Integral Approach, *Probabilistic Engineering Mechanics 35, pp 67–74*.

Koutsourelakis P. S., 2010. Assessing structural vulnerability against earthquakes using multi-dimensional fragility surfaces: A Bayesian framework, *Probabilistic Engineering Mechanics, vol. 25 (1): 49-60.*

Koutsourelakis, P. S., Pradlwarter, H. J., and Schuëller, G. I., 2004. Reliability of structures in high dimensions, part I: Algorithms and applications, *Probabilistic Engineering Mechanics, 19(4), 409-417.*

Kovaleva A., 2009. An exact solution of the first-exit time problem for a class of structural systems, *Probabilistic Engineering Mechanics*, 24(3), 463-466.

Li C-C, Der Kiureghian A., 1995. Mean out-crossing rate of nonlinear response to stochastic input. *In Proceedings of the Seventh International Conference on Applications of Statistics and Probability (ICASP) in Civil Engineering Reliability and Risk Analysis, Lemaire M., Favre J.-L., Mebarki A. (eds). Paris, France; 295–302*.

Li J., Chen J., 2009. *Stochastic dynamics of structures*, John Wiley and Sons.

Lin Y. K., Cai G. Q., 1995. *Probabilistic Structural Dynamics*, McGraw-Hill.

Liu S. C., 1970. Evolutionary power spectral density of strong-motion earthquakes, *Bulletin of the Seismological Society of America, vol. 60: 891-900*.

Liu M., Burns S. A., Wen Y. K., 2003. Optimal seismic design of steel frame buildings based on life cycle cost considerations, *Earthquake Engineering and Structural Dynamics, 32:1313–32*.

Luco N., Bazzuro P., 2007. Does amplitude scaling of ground motion records result in biased nonlinear structural drift responses? *Earthquake Engineering and Structural Dynamics, 36:1813–1835*

Lungu and Giaralis, 2013. A non-separable stochastic model for pulse-like ground motions, *Safety, Reliability, Risk and Life-Cycle Performance of Structures & Infrastructures – Deodatis, Ellingwood & Frangopol (Eds) © 2013 Taylor & Francis Group, London, ISBN 978-1-138-00086-5*.

Lutes L. D., Sarkani S., 2004. *Random Vibrations: Analysis of Structural and Mechanical Systems.* Elsevier Butterworth-Heinemann: Burlington, MA.

Mayergoyz I.D., 2003. *Mathematical Models of Hysteresis and Their Applications*, Elsevier, New York, USA.

McKay, M. D., Beckman, R. J., and Conover, W. J., 1979. Comparison of three methods for selecting values of input variables in the analysis of output from a computer code, *Technometrics, 21(2), 239-245*.

Melchers, R. E., 1989. Importance sampling in structural systems, *Structural Safety, 6, 3-10.*

Mitseas I. P., Kougioumtzoglou I. A., Beer M., 2014a. Optimal design of nonlinear structures under evolutionary stochastic earthquake excitations, *Proceedings of the (OPT-i), Kos, Greece, June 4 - 6, 2014, M. G. Karlaftis, N. D. Lagaros, M. Papadrakakis, (Eds.),p. 2213-2233, ISBN: 978-960-99994-5-8*.

Mitseas I. P., Kougioumtzoglou I. A., Spanos P. D., Beer M., 2014b. Reliability assessment of nonlinear MDOF systems subject to evolutionary stochastic excitation, *Proceedings of the 7th International Conference on Computational Stochastic Mechanics (CSM 7), Santorini, Greece, 15-18 June*.

Mitseas I. P., Kougioumtzoglou I. A., Beer M., Patelli E., Mottershead J. E., 2014c. Robust design optimization of dynamical systems under evolutionary stochastic seismic excitation, *Proceedings of the 2nd ICVRAM 2014 & ISUMA 2014, Liverpool, UK, July 13 – 16, 2014, M. Beer, S.-K. Au, J. W. Hall, (Eds.), (ASCE), pp. 215-224, doi: 10.1061/9780784413609.022*.

Mohle J., Deierlein G. G., 2004. A framework methodology for performance-based earthquake engineering, *Proceedings13th World Conference on Earthquake Engineering, Paper No 679, Vancouver, B,C., Canada*.

Mori, Y., Ellingwood, BR., 1993. Time-dependent system reliability analysis by adaptive importance sampling, *Structural Safety, 12(1), 59-73*.

Naess, A., Iourtchenko, D., and Batsevych, O., 2011. Reliability of Systems With Randomly Varying Parameters by the Path Integration Method, *Probabilistic Engineering Mechanics, 26, pp. 5–9.*

Nason G. P., von Sachs R., Kroisand G., 2000. Wavelet processes and adaptive estimation of evolutionary wavelet spectra, J*ournal of the Royal Statistical Society, vol. 62: 271-292.*

Newland D. E., 1993. *An introduction to random vibrations, spectral and wavelet analysis*, 3rd Edition, Dover, New York.

Nie, J., Ellingwood, BR., 2004. A new directional simulation method for system reliability. Part II: Application of neural networks, *Probabilistic Engineering Mechanics, 19(4), 437-447.*

Nie, J., Ellingwood, BR. 2005. Finite Element-Based Structural Reliability Assessment Using Efficient Directional Simulation, *Journal of Engineering Mechanics, 131(3), 259-267.*

Nigam N. C., 1983. *Introduction to Random Vibrations*, The MIT Press, Cambridge, Massachusetts.

Porter K. A., 2003. An overview of PEER's performance-based earthquake engineering methodology. *Proceedings of the ninth international conference on applications of statistics and probability in civil engineering (ICASP9), 2003 July6–9, San Francisco, USA. Rotterdam: Millpress, pp.973–80.*

Porter, K. A., Kennedy, R. P., Bachman, R. E., 2007. Creating fragility functions for performance-based earthquake engineering, *Earthquake Spectra, 23 (2), 471-489.*

Preumont A., 1994. *Random vibration and spectral analysis*, Kluwer Academic.

Priestley M. B., 1965. Evolutionary spectra and non-stationary processes, *Journal of the Royal Statistical Society, vol. 27: 204-237.*

Proppe C., Pradlwarter H.J., Schueller G. I., 2003. Equivalent linearization and Monte Carlo simulation in stochastic dynamics, *Probabilistic Engineering Mechanics, vol. 18: 1-15.*

Qian S., 2002. *Introduction to Time-frequency and Wavelet Transforms,* Prentice Hall, New Jersey.

Rezaeian S., Der Kiureghian A., 2008. A stochastic ground motion model with separable temporal and spectral nonstationarities, *Earthquake Engineering and Strucural Dynamics, 37:1565–1584.*

Roberts J. B., Spanos P. D., 2003. *Random vibration and statistical linearization*, New York: Dover Publications.

Rubino G., Tuffin B. (eds), 2009. *Rare event simulation using Monte Carlo methods*, John Wiley and Sons.

Rubinstein R. Y., 1981. *Simulation and the Monte Carlo Method*, Wiley.

Rubinstein R. Y., Kroese D. P., 2008. *Simulation and the Monte Carlo method*, Wiley.

Saliby, E., 1990. Descriptive Sampling: A Better Approach to Monte Carlo Simulation, *Journal of the Operational Research Society, 41(12), 1133-1142*.

Schueller, G. I., Pradlwarter, H. J., and Koutsourelakis, P. S., 2004. A Critical Appraisal of Reliability Estimation Procedures for High Dimensions, *Probabilistic Engineering Mechanics, 19, pp. 463–474.*

Schueller G. I., Spanos P. D. (eds), 2000. Monte Carlo simulation: *proceedings of the International Conference on Monte Carlo simulation, Principality of Monaco*.

Shinozuka M., Deodatis G., 1991. Simulation of stochastic processes by spectral representation, *Applied Mechanics Reviews, vol. 44, no. 4, pp. 191-204.*

Song, B. F., 1997. A technique for computing failure probability of a structure using importance sampling, *Computers and Structures, 62(4), 659-665*.

Song J., Der Kiureghian A. D., 2006. Generalized Bouc–Wen Model for Highly Asymmetric Hysteresis, *Journal of Engeering Mechanics ASCE,* 132(6), 610–618.

Soong T. T., 1973. *Random Differential Equations in Science and Engineering*, Academic Press New York and London

Soong T. T., Grigoriu M., 1993. *Random vibrations of mechanical and structural systems*, Prentice-Hall, New Jersey.

Solomos G. P., and Spanos P. D., 1983. Structural reliability under evolutionary seismic excitation, *Soil Dynamics and Earthquake Engineering, 2: 110-16*.

Spanos P. D., 1976. Linearization techniques for non-linear dynamical systems, *PhD thesis, California Institute of Technology*.

Spanos P. D., 1978. Non-stationary random vibration of a linear structure, *International Journal of Solids and Structures, vol 14: 861-867*.

Spanos P. D., Giaralis A., 2013. Third-order statistical linearization-based approach to derive equivalent linear properties of bilinear hysteretic systems for seismic response spectrum analysis, *Structural Safety 44 (2013) 59–69.*

Spanos P. D., Giaralis A., Politis N. P., Roesset J. M., 2007. Numerical treatment of seismic accelerograms and of inelastic seismic structural responses using harmonic wavelets, *Computer-Aided Civil and Infrastructure Engineering, 22(4):254–264*.

Spanos P. D., Kougioumtzoglou I. A., 2012. Harmonic wavelets based statistical linearization for response evolutionary power spectrum determination, *Probabilictic Engeering Mechanics, 27: 57-68.*

Spanos P. D., Kougioumtzoglou I. A., 2014. Survival probability determination of nonlinear oscillators subject to evolutionary stochastic excitation, *ASME Journal of Applied Mechanics, 81(5),051016 1–9.*

Spanos P. D., Lutes L. D., 1980. Probability of response to evolutionary process, *Journal of Engineering Mechanics (ASCE), 106, 213-224.*

Spanos P. D., Solomos G. P., 1983. Markov approximation to transient vibration, *Journal of Engineering Mechanics, 109: 1134–50.*

Spanos P. D., Zeldin B. A., 1998. Monte Carlo treatment of random fields: A broad perspective, *Applied Mechanics Reviews, vol. 51, no3: 219-237.*

Taflanidis A. A., Beck J. L., 2009. Life-cycle cost optimal design of passive dissipative devices, *Structural Safety, 31: 508-22*.

Tajimi H., A statistical method for determining the maximum response of a building structure during an earthquake, *Proceedings of the second World conference on earthquake engineering, Tokyo and Kyoto, Japan, 1960*.

Takahashi Y., Der Kiureghian A., Ang A. H-S., 2004. Life-cycle cost analysis based on a renewal model of earthquake occurrences, *Earthquake Engineering and Structural Dynamics, 33(7): 859–80*.

Tubaldi E., Barbato M., Dall' Asta A., 2014. Performance-based seismic risk assessment for buildings equipped with linear and nonlinear viscous dampers, *Engineering Structures, 78: 90-99*.

Tubaldi E., Kougioumtzoglou I. A., 2014. Nonstationary stochastic response of structural systems equipped with nonlinear viscous dampers under seismic excitation, *Earthquake Engineering and Structural Dynamics, 44:121-138*.

Vamvatsikos D, Cornell CA., 2002. Incremental dynamic analysis, *Earthquake Engineering and Structural Dynamics, 31:491–514.*

Vanmarcke, E. H., 1975. On the Distribution of the First-Passage Time for Normal Stationary Random Processes, *ASME Journal of Applied Mechanics, 42: 215–220*.

Viti S., Cimellaro G., Reinhorn A. M., 2006. Retrofit of a hospital through strength reduction and enhanced damping, *Smart Structures and Systems, 2(4), 339-355.*

Wen Y. K., 1980. Equivalent linearization for hysteretic systems under random excitation, *Journal of Applied Mechanics, vol. 47: 150-154*.

Wen Y. K., Kang Y. J., 2001. Minimum building life-cycle cost design criteria. I: methodology, *Journal of Structural Engineering, 127(3): 330-7.*

Zhang Y., Der Kiureghian A., 1997. Finite element reliability methods for inelastic structures. *Report No. UCB/SEMM-97/05, Department of Civil and Environmental Engineering, University of California, Berkeley, CA.*

List of publications

A. Conference proceedings

A1. **Mitseas I. P.**, Kougioumtzoglou I. A., Beer M., 2014. Optimal design of nonlinear structures under evolutionary stochastic earthquake excitations, *Proceedings of the International Conference on Engineering and Applied Sciences Optimization (OPT-i), Kos, Greece, June 4 - 6, 2014, M. G. Karlaftis, N. D. Lagaros, M. Papadrakakis, (Eds.),p. 2213-2233, ISBN: 978-960-99994-5-8*.

A2. **Mitseas I. P.**, Kougioumtzoglou I. A., Spanos P. D., Beer M., 2014. Reliability assessment of nonlinear MDOF systems subject to evolutionary stochastic excitation, *Proceedings of the 7th International Conference on Computational Stochastic Mechanics (CSM 7), Santorini, Greece, 15-18 June*.

A3. **Mitseas I. P.**, Kougioumtzoglou I. A., Beer M., Patelli E., Mottershead J. E., 2014. Robust design optimization of dynamical systems under evolutionary stochastic seismic excitation, *Proceedings of the 2nd International Conference on Vulnerability and Risk Analysis and Management (ICVRAM 2014) & 6th International Symposium on Uncertainty Modelling and Analysis (ISUMA 2014), University of Liverpool, Liverpool, UK, July 13 – 16, 2014, M. Beer, S.-K. Au, J. W. Hall, (Eds.), American Society of Civil Engineers (ASCE), pp. 215-224, doi: 10.1061/9780784413609.022*.

A4. **Mitseas I. P.**, Kougioumtzoglou I. A., Beer M., 2015. Nonlinear stochastic dynamic analysis for performance based multi-objective optimum design considering life cycle seismic loss estimation, *Proceedings of the 12th International Conference on Applications of Statistics and Probability in Civil Engineering (ICASP 12), Vancouver, Canada, 12-15 July, 2015, (Accepted)*.

A5. **Mitseas I. P.**, Kougioumtzoglou I. A., Beer M., 2015. Fragility analysis of hysteretic MDOF structural systems subject to evolutionary stochastic excitations, *Proceedings of the 8th GRACM International Congress on Computational Mechanics (GRACM 15), Volos, Greece, 12-15 July, 2015, (Accepted).*

A6. **Mitseas I. P.**, Kougioumtzoglou I. A., Beer M. 2015. An approximate stochastic dynamics approach for efficient performance-based earthquake engineering, *Proceedings of the International Engineering Mechanics Institute Conference (EMI 2015), Stanford, USA, 16-19 June, 2015 (Accepted).*

A7. **Mitseas I. P.**, Kougioumtzoglou I. A., Beer M., 2015. Seismic fragility analysis of nonlinear MDOF structural systems subject to evolutionary stochastic excitation, *Proceedings of the 5th International Conference on Computational Methods in Structural Dynamics and Earthquake Engineering (COMPDYN 15), Crete Island, Greece, 25-27 May, 2015 (Accepted).*

B. International journals

B1. **Mitseas I. P.**, Kougioumtzoglou I. A., Beer M., 2014. An approximate stochastic dynamics approach for nonlinear structural system performance-based multi-objective optimum design considering life-cycle cost, *Structural Safety* (Under Review).

B2. **Mitseas I. P.**, Kougioumtzoglou I. A., Spanos P. D., Beer M., 2015. Nonlinear MDOF structural system survival probability determination subject to evolutionary stochastic excitation, *Probabilistic Engineering Mechanics* (To be submitted).

B3. **Mitseas I. P.**, Kougioumtzoglou I. A., Deodatis G., Beer M., 2015. Efficient fragility analysis of nonlinear MDOF structural systems subject to evolutionary stochastic earthquake excitations, *Earthquake Engineering and Structural Dynamics* (To be submitted).